GEO-ARCHAEOLOGY AND VISUAL CONCEPT

A SCIENTIFIC SYNTHESIS

Methods, Visual Technologies and Artificial Intelligence
for the Study of Past Human-Environment Interactions

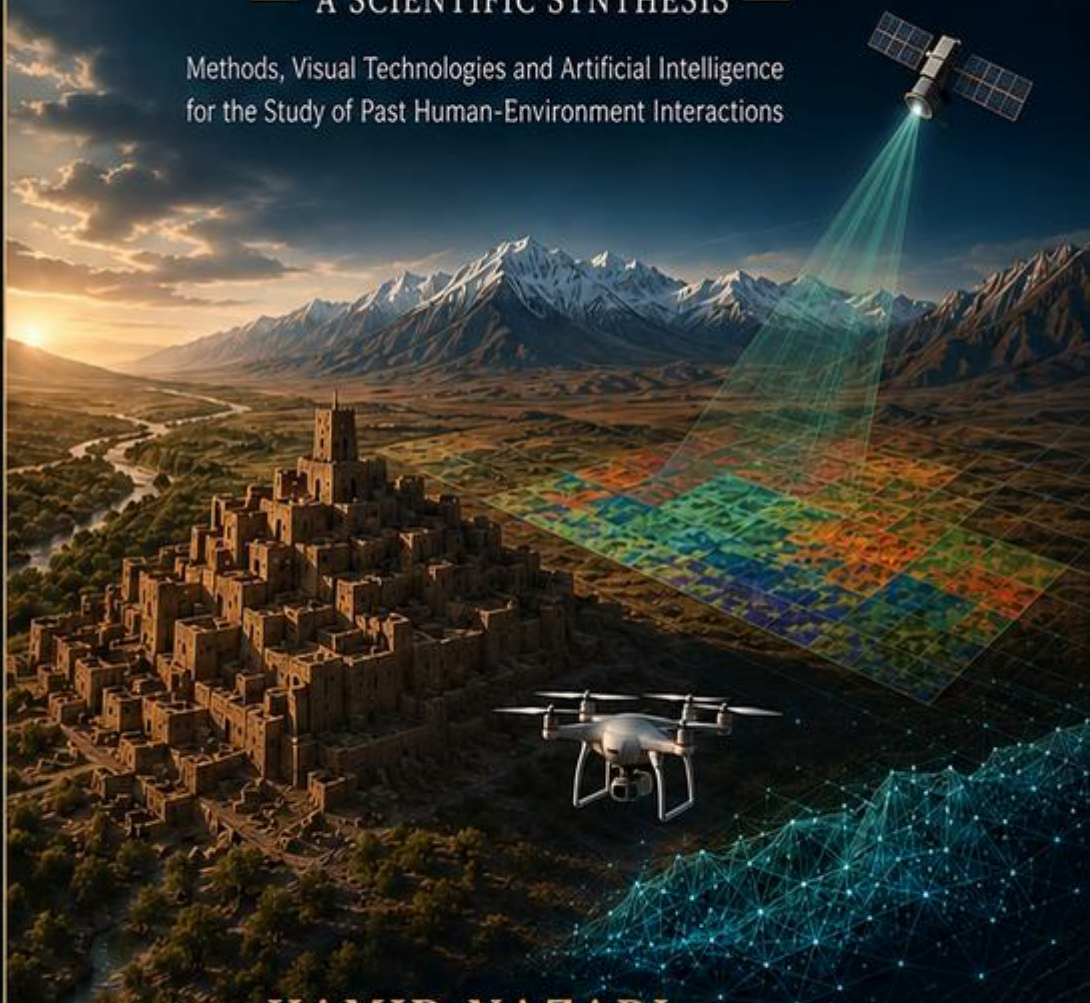

HAMID NAZARI

UNESCO Chair on Coastal Geo-Hazard Analysis
Research Institute for Earth Sciences
Geological Survey of Iran

GEO-ARCHAEOLOGY
AND VISUAL CONCEPT

— A Scientific Synthesis —

Methods, Visual Technologies and Artificial Intelligence
for the Study of Past Human-Environment Interactions

سرشناسه	:	نظری، حمید، ۱۳۴۶- -Nazari, Hamid, 1968
عنوان و نام پدیدآور	:	Geo-archaeology and visual concept: a scientific synthesis[Book]: methods, visual technologies and artificial intelligence for the study of past human-environment interactions/ Hamid Nazari; employer Research Institute for Earth Sciences; affiliation UNESCO Chair on Coastal Geohazard Analysis.
مشخصات نشر	:	تهران: نشر خزه، ۱۴۰۵= ۲۰۲۶م.
مشخصات ظاهری	:	کتاب. دو جلد، جلد اول انگلیسی (۱۶۴ ص)، جلد دوم فارسی (۳۸ ص).: مصور؛ ۱۴×۲۱س‌م.
شابک	:	۹۷۸-622-1582-14-3
وضعیت فهرست نویسی	:	فیپا
یادداشت	:	زبان: انگلیسی. فارسی.
یادداشت	:	عنوان به فارسی زمین باستانشناسی و مفهوم دیداری- یک واکاوی علمی.
عنوان دیگر	:	Methods, visual technologies and artificial intelligence for the study of past human-environment interactions
آوانویسی عنوان	:	جئو آرکائولاجی...
موضوع	:	زمین باستان‌شناسی
موضوع	:	Archaeological geology
شناسه افزوده	:	یونسکو. کرسی مخاطرات زمین شناختی ساحلی
شناسه افزوده	:	UNESCO Chair on Coastal Geo-Hazard Analysis
شناسه افزوده	:	سازمان زمین‌شناسی و اکتشافات معدنی کشور. پژوهشکده علوم زمین
شناسه افزوده	:	Geological Survey and Mineral Exploration of Iran. Research Institute for Earth Sciences
رده بندی کنگره	:	۵/CCV۵
رده بندی دیویی	:	۶/۵۵۱
شماره کتابشناسی ملی	:	۱۰۵۳۱۲۳۲

GEO-ARCHAEOLOGY
AND VISUAL CONCEPT

— A Scientific Synthesis —

Methods, Visual Technologies and Artificial Intelligence
for the Study of Past Human-Environment Interactions

Hamid Nazari
UNESCO Chair on Coastal Geo-Hazard Analysis
Research Institute for Earth Sciences
Geological Survey of Iran

2026

نشر خزه

Geo-archaeology and Visual Concept
A Scientific Synthesis

Author and Principal Investigator: Hamid Nazari

Affiliation: *UNESCO Chair on Coastal Geo-Hazard Analysis* – *Research Institute for Earth Sciences – Geological Survey of Iran*

2026

Type: Office-based documentary synthesis

This report is a documentary synthesis prepared as part of the six-month research proposal “Geo-archaeology and Visual Concepts: A Documentary and Office-Based Approach”. It compiles, organizes and reformulates existing scientific knowledge on geo-archaeological methods, remote-sensing technologies and artificial-intelligence pipelines, with the aim of producing a coherent reference document for researchers, students and heritage managers.

All bibliographic references are listed in the consolidated bibliography that accompanies the second volume of this report. Figures and tables prepared specifically for this volume are original and may be reused under the standard academic fair-use convention with appropriate citation.

Suggested citation:
Nazari, H. (2026). Geo-archaeology and Visual Concept — A Scientific Synthesis. Volume I, Chapters 1–7. UNESCO Chair on Coastal Geo-Hazard Analysis, Research Institute for Earth Sciences, Geological Survey of Iran, Tehran.

اطلاعات گزارش

عنوان: زمین‌باستان‌شناسی و مفهوم دیداری- یک واکاوی علمی

مجری: پژوهشکده علوم زمین

زبان مرجع: انگلیسی

خروجی: کتاب

نویسنده: حمید نظری

رییس کرسی یونسکو در مخاطرات زمین شناختی ساحلی: حمید نظری

ناشر: نشر خزه

با همکاری کرسی یونسکو در مخاطرات زمین شناختی ساحلی و شرکت دانش‌بنیان هوش زمین کانسار

چاپ اول: ۱۴۰۵

شمارگان: ۵۰ نسخه

صفحات: ۱۶۴

شابک: ۹۷۸-۶۲۲-۱۵۸۲-۱۴-۳

khazepub@gmail.com

Report Information

Title: Geo-Archaeology and Visual Concept — A Scientific Synthesis

Employer: Research Institute for Earth Sciences

Original language: English

Output: Book

Author: Hamid Nazari

Chairholder in the UNESCO Chair on Coastal Geo-Hazard Analysis: Hamid Nazari

Publisher: Khazeh Publication

With Cooperation UNESCO Chair on Coastal Geo-Hazard Analysis and Intelligent Geo-Mine Company

First Edition: 2026

Edition number: 50

Page: 164

Shabak: 978-622-1582-14-3

khazepub@gmail.com

TABLE OF CONTENTS

LIST OF FIGURES

LIST OF TABLES

ABSTRACT

Geo-archaeology is the interdisciplinary application of Earth-science and geographical methods to the study of prehistory, archaeology and history. It is concerned with the interactions between past human societies and the physical environments in which they lived: the sediments and soils that record their activities, the climates that shaped their decisions, and the landscapes that bear the imprint of their occupation. Over the past two centuries the discipline has evolved from an informal collaboration between nineteenth-century geologists and antiquarians into a fully recognized field of research, with its own journals, methods and theoretical frameworks.

This work — prepared as a documentary synthesis at the UNESCO Chair on Coastal Geo-Hazard Analysis, Research Institute for Earth Sciences, Geological Survey of Iran — surveys the fundamental methods of modern geo-archaeology and explores how recent advances in remote sensing, light detection and ranging (LiDAR), unmanned aerial vehicles (UAVs), geographic information systems (GIS) and artificial intelligence (AI) are reshaping the discipline. The work is exclusively office-based and draws upon the published literature, openly available datasets and established processing pipelines. It does not include any new fieldwork or laboratory analyses. In compiling this book, the author has used artificial intelligence as a drafting, structuring and editorial aid; all scientific judgements, citations and final formulations remain those of the author.

The report is organized in twelve chapters. After an introductory chapter that defines the discipline and traces its historical development (Chapter 1), the report reviews the Earth-science principles on which geo-archaeology is built (Chapter 2), the field and laboratory techniques routinely deployed at archaeological sites (Chapter 3), the main families of absolute and relative dating methods (Chapter 4), and the geochemical analyses that allow the chemical fingerprint of past activity to be retrieved from sediments and artefacts (Chapter 5). The middle chapters then introduce the visual concepts that distinguish contemporary practice: satellite-based remote sensing and spectral indices (Chapter 6), airborne LiDAR with vegetation removal (Chapter 7), and UAV photogrammetry combined with GIS-based spatial analysis (Chapter 8).

The final chapters address the methodological frontier of the discipline. Chapter 9 introduces artificial intelligence and machine learning, with particular attention to convolutional neural networks and object-detection architectures and to the methodological and ethical concerns that their use raises. Chapter 10 returns to first principles with a systematic treatment of cultural and natural site-formation processes, which condition every interpretation drawn from the

archaeological record. Chapter 11 examines two recent case studies in detail — airborne LiDAR over the Maya lowlands and AI-assisted detection of Roman roads — and Chapter 12 closes the report with a discussion of stewardship, community engagement, site protection, open science, responsible AI, and likely future directions for the discipline.

Throughout, the report emphasizes the complementarity between traditional methods rooted in the careful observation of sediments and the new visual technologies that allow whole landscapes to be examined non-invasively. It is hoped that the synthesis will be useful both to graduate students entering the field and to professional archaeologists wishing to assess where modern Earth-observation and computational tools can be productively integrated into their own research programs.

Keywords: geo-archaeology, stratigraphy, sedimentology, radiocarbon dating, OSL, XRF, stable isotopes, remote sensing, Landsat, Sentinel-2, LiDAR, UAV, GIS, machine learning, convolutional neural networks, cultural heritage

Chapter 1 — Introduction to Geo-archaeology

1.1 Definition and scope of the discipline

Geo-archaeology is most usefully defined as the application of Earth-science and geographical methods to prehistory, archaeology and history. The definition is deliberately broad. Some practitioners adopt a narrower view in which geo-archaeology consists primarily of sedimentological and stratigraphic analyses applied to archaeological deposits; others stress the off-site dimension, in which geomorphology and paleoenvironmental reconstruction are mobilized to understand the regional context within which sites are embedded. A third position — and the one adopted here — regards geo-archaeology as an integrative synthetic approach that combines in-site and off-site analyses, draws equally on biotic and abiotic evidence, and operates simultaneously across several spatial and temporal scales.

This synthetic view is captured well in the definition proposed by Fouache in 2010, who described geo-archaeology as a synthetic approach that combines in-site and off-site analyses and brings together biotic and abiotic elements within a transversal, interdisciplinary perspective. Three implications follow from this definition. First, the geo-archaeologist cannot be a specialist in a single sub-discipline: training in geology, geomorphology, soil science, palynology, geochemistry and archaeological method are all required at some level. Second, the discipline is by its nature collaborative, since no single individual can plausibly master every relevant technique. Third, geo-archaeology occupies an intermediate position between the natural and the human sciences, with a methodological identity that distinguishes it from either parent discipline.

A working definition. For the remainder of this report, the geo-archaeologist will be understood as a specialist in Earth and life sciences who can evaluate the specific problems posed by an archaeological site and its surrounding region and propose a holistic, streamlined approach to addressing them. This definition emphasizes both the breadth of the geo-archaeologist's competence and the practical, problem-oriented nature of the discipline.

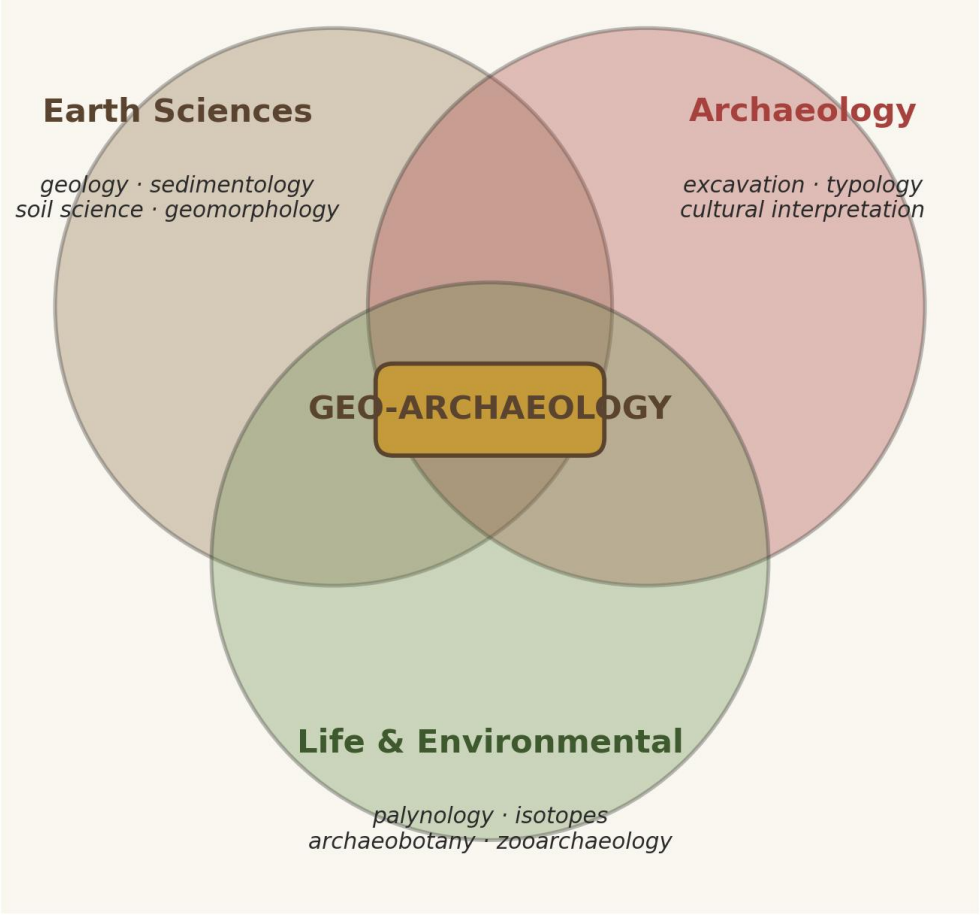

Figure 1.1 · Geo-archaeology occupies the intersection between Earth sciences, archaeology and the life/environmental sciences, drawing methods and concepts from all three.

The scope of geo-archaeology can be appreciated by enumerating its principal sub-fields. Six broad themes recur in the literature: (i) occupation and territorial patterns; (ii) site exploitation and natural-resource management; (iii) palaeoclimatic, palaeoenvironmental and palaeogeographic change and its impact on the landscape's potential for occupation; (iv) anthropogenic impacts and the response of natural systems to them; (v) the identification of anthropogenic influence in micro-remains, including taphonomy and stratigraphic analysis; and (vi) the management of natural hazards as they affect archaeological sites. Table 1.1 summarizes each of these themes together with the kinds of evidence on which it draws.

Table 1.1 — Key sub-fields and contributions of geo-archaeology

Sub-field	Typical questions	Principal methods
Occupation & territorial patterns	Where did people settle? Why there?	GIS, predictive modelling, surveys
Site exploitation & resources	How were stones, soils and water used?	Petrography, sourcing, XRF, mineralogy
Palaeoenvironmental change	What was the climate and vegetation like?	Pollen, isotopes, sediment cores
Anthropogenic impact	How did people modify the landscape?	Geomorphology, soil chemistry, erosion records
Site formation & taphonomy	How did the deposit come to look the way it does?	Micromorphology, stratigraphy, sedimentology
Hazards & site management	What threatens the preservation of the site?	Geomorphic mapping, GIS, monitoring

Table 1.1 — Six recurring themes in geo-archaeological research and the principal methods used to address them.

1.2 Historical development

The history of geo-archaeology is essentially the history of a productive collaboration between geologists and archaeologists. The earliest documented example dates from 1837, when Jacques Boucher de Crèvecoeur de Perthes began his investigations of the gravel terraces of the Somme valley in northern France. Working at a time when the antiquity of the human species was still a matter of intense debate, Boucher de Perthes recognized that the chipped-stone tools he was recovering were embedded together with the bones of extinct animals in geologically ancient deposits. He could not have argued the antiquity of these tools without a stratigraphic context, and he could not have established that context without the help of geologists.

The British geologist Sir Charles Lyell — sometimes referred to as the father of geo-archaeology — codified the approach in his benchmark 1863 work Geological Evidence of the Antiquity of Man. Lyell systematically reviewed the geological evidence then available for the great antiquity of humanity and effectively legitimized the use of geological reasoning in archaeological enquiry. The result was the gradual emergence of a school of thought sometimes called Quaternary Science, in which prehistoric archaeology and the Earth sciences were treated as complementary rather than separate disciplines.

For roughly a century the integration of geology and archaeology was concerned mainly with very ancient periods — the Palaeolithic and the Pleistocene — for which an independent chronology and a clear stratigraphic context were essential. It was only in the second half of the twentieth century that the same approach was extended to protohistoric and historic periods. The pioneering work in this regard was carried out in the Mediterranean basin by Claudio Vita-Finzi, whose 1969 book The Mediterranean Valleys analyzed the alluvial history of more than two dozen catchments and demonstrated that landscape evolution had been entirely intertwined with the human history of the region.

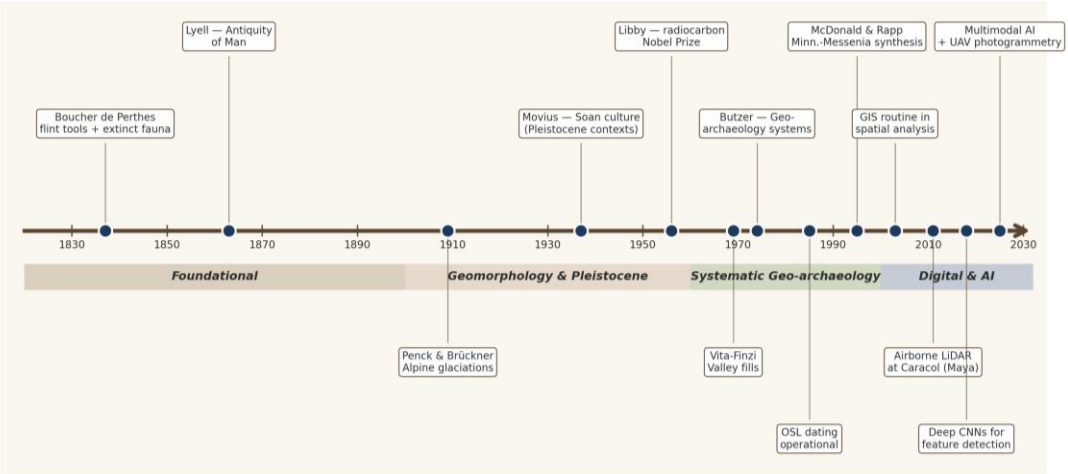

Figure 1.2 · Selected milestones in the development of geo-archaeology, from the first archaeologist–geologist collaborations of the 1830s to today's routine integration of unmanned aerial vehicles and machine-learning pipelines.

Three years after Vita-Finzi's book, William McDonald and George Rapp published the Minnesota Messenia Expedition: Reconstructing a Bronze Age Regional Environment, in which a team of specialists reconstructed the physical setting of Mycenaean Greece by combining soil science, palaeobotany and detailed survey. The volume is often cited as the founding text of Mediterranean geo-archaeology. Two years later again, in 1974, Karl Butzer published a paper in the Journal of Archaeological Science titled Geo-archaeological interpretation of Acheulian calc-pan sites at Doornlaagte and Rooidam (Kimberley, South Africa). It is in this paper that the specific term geo-archaeology — hyphenated at that stage — first appeared in print.

After 1974 the discipline gained ground rapidly. Its status was formally recognised in 1986 with the foundation of the dedicated journal Geoarchaeology by Wiley. From the 1990s onwards, the growing awareness of the impact of climate change and anthropogenic activity on the environment introduced geographers and geomorphologists into the field in larger numbers, and

a strong tradition of palaeoenvironmental reconstruction in conjunction with human–environment interaction studies emerged.

The most recent phase in the history of geo-archaeology is essentially digital. It began around the year 2000 with the routine use of geographic information systems for spatial analysis and the first widespread applications of airborne LiDAR to archaeological landscapes. It has accelerated dramatically since 2015 with the application of deep-learning algorithms — particularly convolutional neural networks — to the automatic detection of archaeological features in satellite and aerial imagery, and with the widespread deployment of consumer-grade UAVs for high-resolution photogrammetric survey. This digital turn is the subject of much of the present report.

1.3 Significance in contemporary research

Why does geo-archaeology matter today? Three answers can be given. The first is historical: many archaeological problems simply cannot be solved without geo-archaeological input. The chronology of a stratified Palaeolithic cave site, the relationship between a tell and the river that once watered it, the question of whether a buried Roman road follows a pre-existing track — none of these can be addressed without combining archaeological observation with the methods of the Earth sciences. As fieldwork becomes increasingly destructive and excavation increasingly expensive, the prior characterization of sites and landscapes by geo-archaeological means has become more important, not less.

The second answer is environmental. The Anthropocene — the era characterised by the planet-wide imprint of human activity on biotic and abiotic systems — has placed human–environment interactions at the center of scientific and political attention. Geo-archaeology offers an unrivalled deep-time perspective on these interactions. The decisions made by past societies to deforest a watershed, to terrace a hillside or to abandon a region in the face of drought all left traces in the sedimentological record. Reading those traces helps to calibrate predictions about the future.

The third answer is technological. The rapid expansion of remote-sensing data — Landsat, Sentinel-2, commercial high-resolution platforms, airborne LiDAR, UAV photogrammetry — has produced an avalanche of geospatial information that is increasingly impossible to process by hand. Artificial-intelligence methods are now indispensable for sifting this material, and geo-

archaeologists are well placed to apply them, since the discipline has long combined a quantitative orientation with a sensitivity to spatial context.

1.4 Aims and structure of this report

This report has three principal aims. The first is to synthesize the fundamental methods of geo-archaeology — Earth-science principles, field techniques, dating methods and geochemical analysis — into a coherent reference for graduate students and early-career researchers. The second is to survey the visual concepts and technologies that have become central to the discipline in recent decades, with particular attention to satellite remote sensing, LiDAR, UAV photogrammetry and the integration of these tools with GIS. The third is to assess the contribution of artificial intelligence to geo-archaeological research, both through pattern-recognition in imagery and through the broader integration of heterogeneous datasets.

The report is divided into two volumes. The present Volume I covers the fundamental methods and the imaging technologies (Chapters 1–7). The companion Volume II will treat artificial intelligence in detail, present extended case studies (including the well-known applications of LiDAR-plus-AI in the Maya lowlands and machine-learning detection of Roman roads in Britain), and conclude with a chapter on ethics, cultural heritage and the future of the discipline.

Throughout the report, an effort has been made to integrate textual exposition, illustrative figures and synoptic tables. Each chapter is self-contained but is cross-referenced to the others so that the reader can navigate the material in whatever sequence is most useful. A consolidated bibliography is provided at the end of Volume II.

A note on methodology is also in order. In compiling this book, the author has used artificial intelligence as a drafting, structuring and editorial aid — for organizing the literature, for cross-checking references, for harmonizing the exposition across chapters, and for the language editing of an English text written by a non-native speaker. All scientific judgements, the selection of case studies, the interpretation of the cited literature, and the final formulations of every section remain those of the author. The use of artificial intelligence is itself an illustration of the methodological theme that runs through the later chapters of this volume: machine-learning tools are now routinely integrated into the working practice of Earth scientists and geo-archaeologists, both for the analysis of imagery and for the synthesis of the published literature, and the responsible disclosure of their use is part of the contemporary scholarly contract.

Chapter 2 — Earth Science Principles

Geo-archaeology is built upon a small number of fundamental principles drawn from the Earth sciences. Of these, four are of overriding importance: the geological understanding of how rocks and sediments are formed and altered; the sedimentological understanding of how individual deposits accumulate and become organized in space; the pedological understanding of how soils develop in time; and the broader palaeoenvironmental framework within which past climates, vegetation regimes and ecosystems are reconstructed. The present chapter introduces each of these in turn and explains how they bear on the archaeological problem.

2.1 Geology and sedimentology

Geology — the science of the solid Earth — provides geo-archaeology with two indispensable resources. The first is a stratigraphic framework: the principle, first articulated by Nicolas Steno in the seventeenth century, that in an undisturbed sequence of sedimentary layers the older lie below the younger. This law of superposition is the bedrock (literally) of all archaeological reasoning about chronology. The second resource is a catalogue of the materials of which the Earth's surface is composed — the bedrocks and the loose sediments that overlie them — together with the processes by which those materials are produced, transported and modified.

Sedimentology, narrowly construed, is the study of how sediments are deposited, what they consist of, and what their internal organization reveals about the conditions of deposition. For the geo-archaeologist three classes of sediment are of particular importance: clastic sediments composed of mineral grains derived from the weathering of older rocks; chemical sediments precipitated from solution; and biogenic sediments produced by living organisms. In archaeological contexts a fourth class is often added: anthropogenic sediments produced by human activity, including ash, midden material, mud-brick collapse and the like.

Grain size as a diagnostic tool: Among the simplest and most powerful sedimentological observations is grain size. The Wentworth scale — introduced in 1922 and still standard today — divides clastic sediments into a logarithmic series from clays at one end (less than 4 μm) to boulders at the other (more than 256 mm). Each grain-size class is associated with a characteristic mode of transport: clays settle out of still water; silts are transported in suspension; sands are moved by traction and saltation; gravels and boulders are moved by strong currents or by mass movement. By logging grain size carefully along a vertical profile, the sedimentologist can therefore reconstruct the energy of the depositional environment through time.

Table 2.1 — Sediment classification by grain size (Wentworth scale, simplified)

Class	Size range	Typical depositional setting	Archaeological relevance
Clay	< 0.004 mm	Standing water; floodplain backswamps	Sealing of features; pottery raw material
Silt	0.004 – 0.0625 mm	Slow rivers; lake margins; loess	Loess plateaus often rich in sites; alluvial sequences
Sand	0.0625 – 2 mm	Rivers; beaches; dunes	Sand quarries; building sand; OSL targets
Gravel	2 – 64 mm	High-energy rivers; raised beaches	Clast support for stratigraphic markers
Cobbles & boulders	> 64 mm	Torrents; mass movement; glaciers	Raw material for stone tools; debris-flow hazards

Table 2.1 — Simplified sediment classification adapted from the Wentworth scale; archaeological relevance highlights how each class enters the geo-archaeological record.

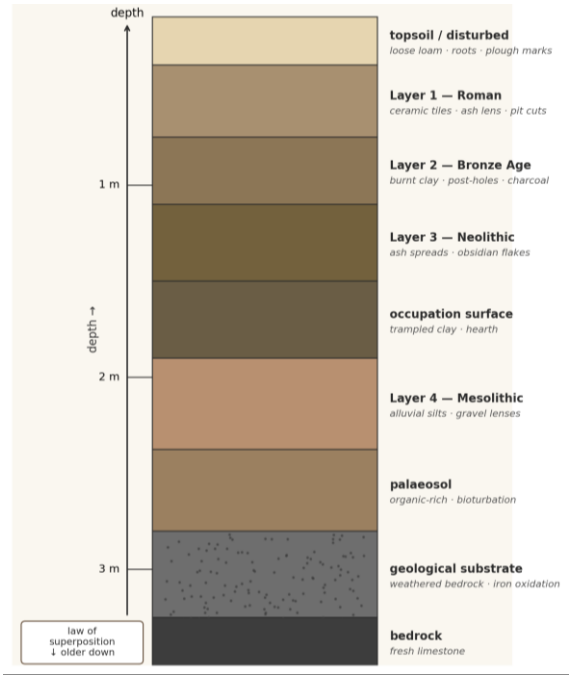

Figure 2.1 · Idealized stratigraphic column at a multi-period archaeological site. From bottom to top, the sequence records Pleistocene periglacial gravels, a buried Mid-Holocene palaeosol, an alluvial flood deposit, a Late Bronze Age floor, a Roman destruction horizon, a Medieval occupation layer and modern ploughsoil. Such sequences are routinely encountered at long-lived sites in the Mediterranean and the Near East.

Beyond grain size, sedimentological logging records color (often using a Munsell soil-color chart), sorting (the homogeneity of the grain population), rounding (an index of transport distance), composition (the mineralogy and lithology of the grains), and primary sedimentary structures (laminations, cross-bedding, graded beds and the like). Each of these has its own diagnostic value. Well-sorted, rounded grains generally indicate prolonged transport by water or wind; poorly sorted, angular grains suggest short-distance transport by mass movement; horizontal laminations imply quiet-water deposition; cross-bedding implies traction transport by currents or wind. A geo-archaeologist reading a section is, in effect, reconstructing an entire depositional history from these clues.

2.2 Soil science

Sediments turn into soils through the slow process of pedogenesis. Pedogenesis is driven by five state factors, originally enumerated by Hans Jenny in 1941: climate, organisms, relief, parent material and time. Given enough time and a stable land surface, the action of these factors produces a vertically zoned profile within the original sediment — a soil. The horizons of the soil profile are conventionally labelled with capital letters (O, A, E, B, C and sometimes R for the bedrock beneath), and each horizon corresponds to a distinct combination of pedogenic processes (organic accumulation at the surface, leaching in the middle, illuvial accumulation deeper down).

Figure 2.2 · Idealized soil profile and horizon nomenclature. The depth of each horizon and the contrast between them depend on climate, parent material and the amount of time that has elapsed since the surface stabilized. In dry climates, soils may be only weakly differentiated; in humid temperate climates, the contrasts can be very strong.

For the geo-archaeologist, soils matter for several interlocking reasons. First, soils develop on stable surfaces. The presence of a well-developed soil somewhere in a stratigraphic sequence — a so-called palaeosol — is therefore evidence that, at the time of that soil's formation, the surface was stable for long enough to allow horizons to develop. Palaeosols thus mark periods of geomorphic stability, which often correspond to periods of intense human occupation. Second, soils are reactive media: they record the chemical and biological signature of whatever has taken place on them. A soil enriched in phosphate is likely to record the presence of a midden, a stable or a cemetery; a soil enriched in lead is likely to record metal-working. Third, soils are the matrix within which most archaeological artefacts are preserved, and their characteristics determine what survives and what does not.

Table 2.2 — Master soil horizons and their typical features

Horizon	Position	Typical features	Archaeological significance
O	Surface	Organic litter; partially decayed plant material	Indicates vegetated, stable surface; pollen and macro-botanical preservation
A	Topsoil	Mineral soil mixed with humus; dark colored	Often the active surface; bioturbation; artefact lag
E	Below A	Eluvial horizon; light-colored, leached	Indicates leaching; common under temperate forests
B	Subsoil	Illuvial accumulation of clay, iron, organics	Cumulic B horizons can bury archaeological surfaces
C	Deepest	Weathered parent material, little pedogenesis	Provides depositional context for the soil above
R	Substrate	Consolidated bedrock	Stops vertical movement of artefacts and water

Table 2.2 — Master horizons of the standard soil-profile nomenclature, with notes on their archaeological significance.

A particularly informative class of soils for the geo-archaeologist is the anthrosol — a soil whose properties have been significantly altered by sustained human activity. Garden soils of Amazonia, the so-called terra preta, are the textbook example: dark-colored soils enriched in charcoal, phosphate and bone fragments, with a fertility far greater than that of surrounding tropical soils. Anthrosols are also widespread in long-occupied parts of the Old World, including the dark earths of north-western European towns and the orchard soils of Mediterranean garden hinterlands.

2.3 Paleoenvironmental reconstruction

Reconstructing past environments is one of the central goals of geo-archaeology. The reasoning is straightforward: a society's choices of settlement location, subsistence strategy and material culture were shaped by the environment in which it operated, and any attempt to understand those choices must therefore begin by reconstructing that environment. The technical challenge is harder. Past environments are no longer directly observable; they must be inferred from proxies — biological, chemical, physical or geomorphic markers preserved in the sedimentary record that respond systematically to particular environmental parameters.

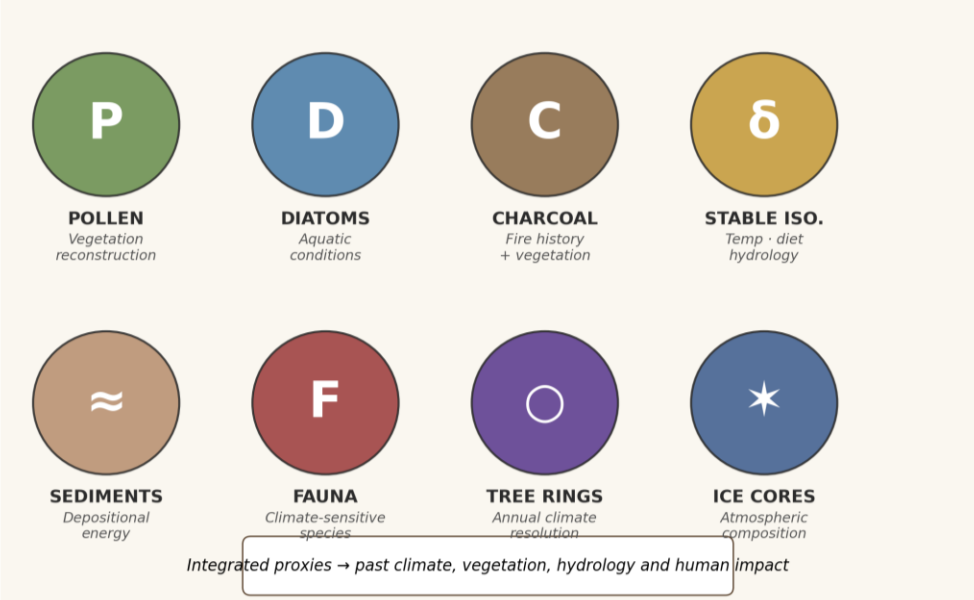

Figure 2.3 · Principal proxies used in paleoenvironmental reconstruction. Each proxy is sensitive to a different aspect of the past environment; integrating multiple proxies provides the most robust reconstructions.

Pollen analysis (palynology) is the classical paleoenvironmental proxy and remains one of the most powerful. Pollen grains are produced in enormous quantities by wind-pollinated plants, are distinguishable to genus or even species level under the microscope, and are remarkably resistant to decay in anoxic sediments. A pollen diagram from a peat bog, a lake core or an off-site sedimentary trap can document the changing composition of the regional vegetation over millennia. In archaeological contexts, palynology has been used to track Mesolithic Forest clearance, Neolithic cereal cultivation, the spread of olive in the Mediterranean, and the abandonment of agricultural land in periods of crisis.

Stable isotopes provide an entirely complementary class of proxies. The oxygen isotope composition of carbonate fossils, ice cores or speleothems is sensitive to temperature and to the

global ice-volume of the planet; the δ18O record of marine sediment cores is the principal basis for the global chronology of Pleistocene glaciations. The carbon isotope composition of plant remains is sensitive to the photosynthetic pathway used (C3 versus C4), to atmospheric CO2 and, indirectly, to humidity. The nitrogen isotope composition of bone collagen reflects the trophic level of the diet. These isotopic proxies are discussed in greater detail in Chapter 5.

Sediment cores themselves are paleoenvironmental archives. The grain-size and mineralogy of a lake-bottom core reflect the rate of erosion in the catchment and therefore, indirectly, the climate and vegetation. The presence or absence of varves — annually laminated couplets of light and dark sediment — provides a year-by-year chronology. Diatom assemblages preserved in lake sediments record changes in water chemistry. Charcoal particles record fire history, which in turn records both climate (lightning fires) and human activity (anthropogenic burning). Most of the great climate reconstructions of the last fifty years have been built on the multi-proxy analysis of long sediment cores from lakes, ocean basins and ice sheets.

2.4 Stratigraphy and site context

All of the principles introduced above converge in the practice of stratigraphic analysis at archaeological sites. The standard product of such analysis is a section drawing — a scaled vertical representation of the deposits exposed in an excavation cut, with each lithological unit identified, described and assigned a unit code. The geo-archaeologist's role in producing this drawing is partly methodological (ensuring that the descriptions follow a consistent vocabulary) and partly interpretive (proposing a sequence of depositional events that explains the observed succession).

Sites located in stable upland positions tend to have thin, slowly accumulating stratigraphies in which the human occupation horizons are sharply visible against the surrounding pedogenic background. Sites located in valley bottoms or on coastal plains tend to have thick, rapidly accumulating stratigraphies in which human occupation horizons are interbedded with alluvial, colluvial or aeolian deposits. Coastal sites add the additional complication of sea-level change: a shoreline occupied at a moment of relatively low sea-level may today be drowned, while a shoreline occupied at a moment of relatively high sea-level may be stranded several kilometers inland. The reconstruction of past shorelines is an active area of modern geo-archaeology, particularly in the Mediterranean and along the Gulf coast of the Middle East.

A general lesson can be drawn from all of this: there is no such thing as an isolated archaeological site. Every site sits within a sedimentary system that controls how it was deposited, how it has

been preserved, and how it can be approached today. Reading that sedimentary system is the central business of the geo-archaeologist.

Chapter 3 — Field and Laboratory Techniques

The methods discussed in this chapter are the operational core of geo-archaeology. They allow the principles introduced in Chapter 2 — superposition, sedimentation, pedogenesis and palaeoenvironmental change — to be brought to bear on a specific site or region. The chapter is organized in four parts: first the survey and mapping work that precedes any intrusive intervention; second the strategies by which samples are selected and collected; third the analyses performed on those samples in the laboratory; and finally, the specialized technique of soil micromorphology, which has emerged in recent decades as one of the most powerful tools for the in-situ interpretation of archaeological deposits.

3.1 Site survey and mapping

Survey and mapping are the preliminary phases of any geo-archaeological project. Their purpose is to characterize the spatial setting of the site or region before any sampling or excavation is undertaken, so that subsequent work can be properly contextualized. In practice, survey involves a combination of cartographic, geomorphological and archaeological observation.

Topographic mapping defines the physical setting. Until the 1990s, topographic maps for archaeological projects were drawn by hand using total stations and theodolites; today, the digital elevation model (DEM) — derived from photogrammetry, GNSS surveys, airborne LiDAR or open satellite-derived products such as SRTM and Copernicus DEM — is the standard product. A DEM at a horizontal resolution of one meter or better is sufficient to detect most archaeological micro-topography in open landscapes. Where vegetation cover is dense, only LiDAR-derived terrain models are likely to be useful, as discussed in detail in Chapter 7.

Geomorphological mapping superimposes process information on the topography. It identifies the active landforms (alluvial fans, terraces, dunes, slope deposits and so on), classifies the deposits associated with each, and proposes a relative chronology among them. The product is a geomorphological map at the same scale as the topographic base. Such a map is invaluable for predicting where archaeological sites are likely to be preserved and where they are likely to have been destroyed by erosion or buried by sedimentation. A site that has clearly been buried under five metres of late Holocene alluvium, for example, cannot be discovered by surface survey.

Pedestrian survey: In parallel with cartographic work, archaeological pedestrian survey records the actual distribution of surface artefacts. Survey teams walk transects across the landscape, recording artefact densities in pre-defined collection units. The results are typically expressed as density maps, with hot-spots interpreted as potential sites or activity areas. The reliability of pedestrian survey depends critically on visibility: a recently ploughed field with low vegetation cover provides excellent visibility, while a pasture or a forest may conceal sites entirely. This is one of the reasons why remote-sensing techniques discussed in later chapters have become so important.

The integration of these various data layers is now routinely undertaken within a geographic information system. GIS allows topography, geomorphology, surface artefact densities, satellite imagery and any number of other layers to be combined into a single analytical environment. Distance, slope, aspect, viewshed and visibility analyses can be performed quickly and at any scale. The use of GIS in geo-archaeology is so pervasive that the technology will be treated as a recurring presence in the rest of this report rather than as a separate topic.

3.2 Sampling strategies

Once a site or region has been characterized, the next operational step is sampling. A sampling strategy is the rule by which samples are selected from the universe of possible samples; the strategy chosen has profound consequences for the kinds of inferences that can subsequently be drawn from the data. Three sampling strategies are routinely used in geo-archaeology: random, systematic and stratified or targeted.

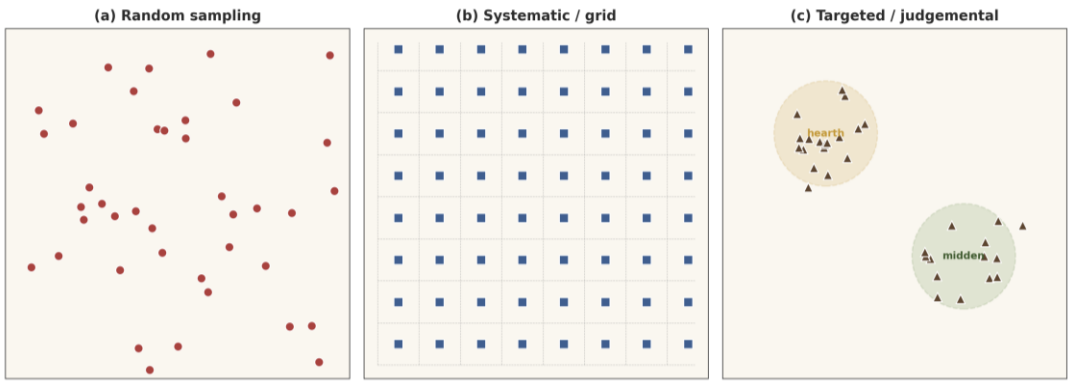

Figure 3.1 · Three common field-sampling strategies. (a) Random sampling — points are chosen at random within the area; (b) systematic sampling — points are placed on a regular grid; (c) targeted or transect sampling — points are clustered along a feature or transect of interest. Each strategy has different statistical properties.

Simple random sampling has the desirable statistical property that it produces an unbiased sample of the population. It is rarely used on its own in geo-archaeology, however, because it tends to leave large gaps in some parts of the area and clusters in others. Systematic sampling, in which sample points are placed on a regular grid, is more common because it ensures complete spatial coverage and makes mapping straightforward. The disadvantage of systematic sampling is that it can interact with periodic structures in the landscape — if the spacing of the grid happens to match the spacing of, say, archaeological field boundaries, the survey may either over- or under-represent the boundaries depending on phase.

Stratified or targeted sampling is the most flexible and the most commonly adopted strategy. The landscape or site is first divided into strata defined by some independent variable (geomorphological unit, soil type, distance from a known site), and then sampled separately within each stratum. This guarantees representation of all defined strata and allows the sampling effort to be concentrated where it is most likely to yield information. Targeted transects across known or suspected features serve a similar purpose.

Table 3.1 — Comparison of sampling strategies in geo-archaeology

Strategy	Strengths	Weaknesses	Best used when…
Random	Statistically unbiased	Gaps and clusters; inefficient	Sampling small areas with no a priori knowledge
Systematic	Complete coverage; easy to map	Can alias periodic features	Mapping unknown terrain; first-pass surveys
Stratified	Represents all defined strata	Requires prior stratification	Most regional geo-archaeological surveys
Targeted	Maximum information per sample	Biased; cannot estimate density	Following up known anomalies; section sampling

Table 3.1 — Comparison of sampling strategies, their relative strengths and weaknesses, and the situations in which each is most appropriate.

Within a single excavation section, a different kind of sampling decision is required: which layers to sample, and how. The standard practice is to collect column samples — continuous vertical sequences of small bulk samples from each lithological unit — together with spot samples from features of particular interest, such as hearths, floors or storage pits. Bulk samples are usually intended for grain-size analysis, chemistry and palaeoenvironmental work; oriented block samples are required for micromorphology; charcoal samples for radiocarbon dating; and sediment from light-tight sub-cores for OSL.

3.3 Sediment and soil analysis

Laboratory analysis of sediment and soil samples is one of the most labour-intensive components of any geo-archaeological project. The standard suite of analyses includes grain-size determination, the measurement of organic and carbonate content, soil chemistry (pH, electrical conductivity, exchangeable bases) and, increasingly, geochemistry by XRF or ICP-MS. Each of these analyses generates quantitative data that can be plotted as a depth profile and interpreted in the light of the stratigraphic context.

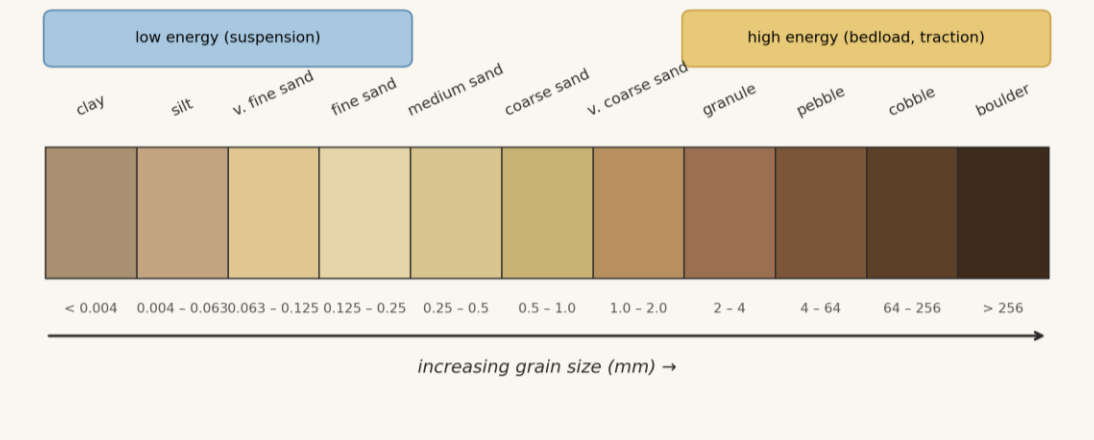

Figure 3.2 · The Wentworth grain-size scale used in routine sedimentological logging. The scale is logarithmic, with each class roughly twice the size of the next; the diameters are quoted in millimeters.

Grain-size analysis is performed either by traditional sieving (for sediments coarser than about 63 micrometers) or by laser diffraction (for finer sediments). The result is a distribution curve from which descriptive statistics — median, mean, sorting, skewness, kurtosis — can be extracted. These statistics are then interpreted in terms of depositional environment, using the diagnostic schemes summarized in Chapter 2. Two complementary representations are routinely used: the cumulative grain-size curve, which displays the percentage of the sample finer than each size class, and the frequency curve, which displays the percentage of the sample within each size class.

Organic-matter content is determined by loss on ignition. A weighed sample is dried, then heated to about 550 °C for several hours; the weight loss represents the organic fraction. A second heating step at about 950 °C drives off carbonate as CO2, allowing the carbonate fraction to be calculated. The resulting depth profiles of organic content and carbonate are diagnostic of pedogenic and depositional processes: a buried palaeosol, for instance, will appear as a peak in organic content; a calcic horizon will appear as a peak in carbonate.

Soil chemistry — pH, electrical conductivity, exchangeable bases — is determined by standard extraction protocols. These properties are sensitive to the climatic regime, to leaching, and to anthropogenic inputs. Elevated phosphate values are particularly diagnostic of past human activity, and many geo-archaeological surveys include simple P-spot tests as a rapid means of identifying buried occupation deposits in the field.

3.4 Micromorphology

Soil micromorphology is the microscopic study of undisturbed sediment and soil. The technique is conceptually simple: an oriented block of sediment is impregnated with resin, sliced into a thin section about 30 micrometers thick, and examined under a polarizing microscope. What this allows is the direct observation of structural features that are too small or too subtle to be detected in the field but that record critical information about depositional and post-depositional processes.

A trained micromorphologist can identify in thin section the difference between a primary occupation surface and one that has been trampled, the difference between an in-situ ash deposit and a redeposited one, the imprint of bioturbation by earthworms or termites, the chemical alterations associated with burning, and the residue of organic matter that has long since decomposed. The technique is particularly valuable at complex multi-period sites such as long-occupied tells, caves and rock shelters, where field interpretation alone is often inadequate to disentangle the sequence of events.

Limits of the method. Micromorphology is labour-intensive and requires specialized training. Preparing a single thin section can take several weeks, and the interpretation of the resulting images is a craft that develops only with extensive experience. For this reason, micromorphology is rarely used as a screening tool; it is applied selectively, to particularly informative or particularly problematic contexts. Even so, no other technique provides comparable information about the formation of an archaeological deposit.

The integration of micromorphological observation with geochemical and isotopic data — to which we turn in Chapter 5 — represents one of the most powerful combinations available to the modern geo-archaeologist. Detailed micromorphological logs from a single profile, augmented by XRF and stable-isotope data from the same samples, can produce a reconstruction of site formation processes that approaches the resolution of an annual record.

Chapter 4 — Dating Techniques

Dating is the chronometric backbone of archaeology. Without secure dates, stratigraphic sequences cannot be correlated between sites, the duration of cultural phases cannot be estimated, and the tempo of past human activity cannot be reconstructed. Dating methods can be classified along several dimensions: by the physical principle on which they rely (radiometric, luminescence, electron spin resonance, palaeomagnetic), by the kind of material they require (organic, mineral, ceramic), and by the time range over which they are applicable. The present chapter introduces the main families of dating techniques used in geo-archaeology, with particular attention to radiocarbon dating, dendrochronology and optically stimulated luminescence.

4.1 Radiometric methods

Radiometric dating exploits the fact that radioactive isotopes decay at a known and constant rate. If the initial amount of the parent isotope can be reasonably estimated and the present amount can be measured, the time elapsed since the system became closed can be calculated. The single most important radiometric method in geo-archaeology is radiocarbon dating, introduced by Willard Libby in 1949.

Radiocarbon dating exploits the fact that the carbon-14 isotope is continuously produced in the upper atmosphere by the interaction of cosmic-ray neutrons with nitrogen-14. Once it is produced, 14C mixes rapidly with the atmospheric carbon reservoir, is incorporated into living organisms by photosynthesis (and from there into the rest of the food chain), and is in approximate isotopic equilibrium with the atmosphere as long as the organism is alive. When the organism dies, no further 14C is incorporated, and the 14C already in the tissues begins to decay back to 14N with a half-life of 5,730 years. Measuring the ratio of 14C to stable 12C in a sample therefore gives an estimate of the time elapsed since the organism died.

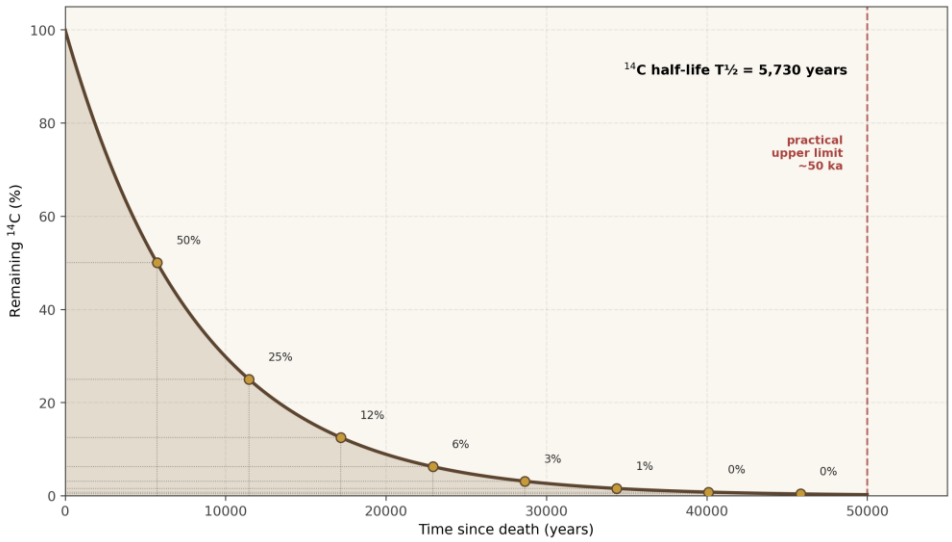

Figure 4.1 · Radioactive decay of carbon-14. After each half-life of 5,730 years, the amount of 14C remaining in a closed system is halved. In practice, radiocarbon dating becomes increasingly imprecise beyond about 50,000 years, when the residual 14C signal approaches the detection limit of modern accelerator mass spectrometers.

Several technical issues complicate radiocarbon dating in practice. The atmospheric 14C concentration has not been constant: it has fluctuated with solar activity, geomagnetic field strength and changes in the carbon cycle. Calibration curves — derived from independently dated material such as tree-ring sequences and U/Th-dated speleothems — are therefore required to convert raw radiocarbon ages into calendar ages. The current internationally accepted curve, IntCal20, allows calibration with appreciable precision back to 55,000 years before present. A second issue is contamination: even minute amounts of younger or older carbon can significantly distort the result, particularly for samples close to the limit of the method. A third issue is the reservoir effect: carbon in some environments (marine, freshwater carbonate-rich) is not in isotopic equilibrium with the atmosphere, so dates on samples from these environments require an additional reservoir correction.

Beyond radiocarbon, several other radiometric techniques are used in specific contexts. Uranium-series dating, based on the decay of various uranium isotopes through their daughter products, is applied to carbonate materials such as speleothems, corals and travertines, and reaches back to about 500,000 years. Potassium–argon dating and its successor argon–argon dating is applied to volcanic minerals and have been crucial for dating the early African Pleistocene hominin record. Cosmogenic nuclide dating, based on the in-situ production of isotopes such as 10Be and 26Al by cosmic-ray bombardment of exposed surfaces, allows the dating of surface exposure ages and is increasingly used in geomorphological geo-archaeology.

4.2 Dendrochronology

Dendrochronology — the science of dating events by means of tree rings — has the unique virtue of producing absolute dates with annual precision. The method depends on the fact that trees in temperate climates produce a distinct growth ring each year, and that the width and structure of that ring respond to the climatic conditions of the growing season. The ring-width sequence of a single tree therefore constitutes a climatic chronicle, dated absolutely if the date of cutting or growth-cessation is known.

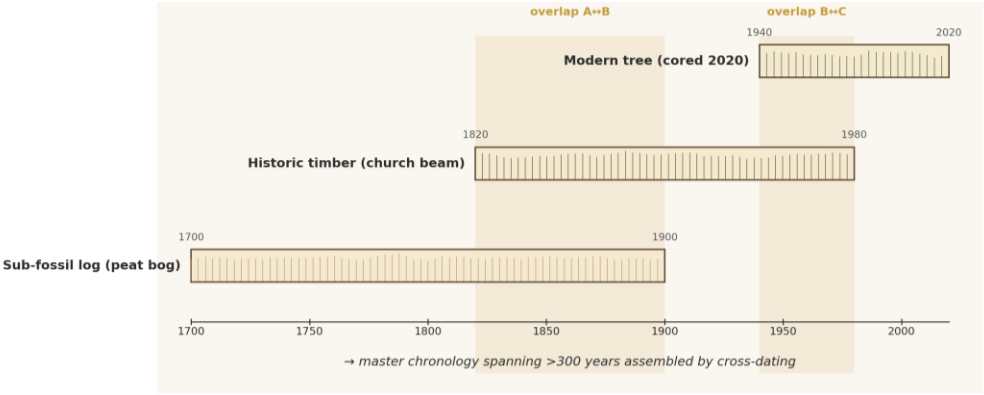

Figure 4.2 · The cross-dating principle. The ring-width sequence of a living tree can be matched to that of progressively older historical and archaeological timbers, extending the absolute chronology centuries or millennia into the past.

By cross-matching ring-width sequences from many trees of overlapping age, master chronologies have been constructed that extend back many millennia in some regions. The Hohenheim oak and pine chronologies of central Europe, for example, now reach back more than 12,000 years; the bristlecone-pine chronology of California reaches back nearly 9,000 years. These chronologies allow individual wooden artefacts — beams from medieval cathedrals, timbers from Bronze Age Lake dwellings, wooden coffins from prehistoric burials — to be dated to the calendar year of the tree's death.

Dendrochronology has two principal limitations. First, it requires preserved wood: the method is most useful in waterlogged sites, in dry rock shelters, and in built structures where timber has survived. Second, it requires the construction of a master chronology for the species and region in question. In areas where no master chronology yet exists, dendrochronology cannot be used. Recent efforts to extend dendrochronology to subtropical and tropical species are partially overcoming the second limitation, though the climatic signal in tropical tree rings is typically weaker than in temperate ones.

4.3 Optically Stimulated Luminescence (OSL)

Optically Stimulated Luminescence (OSL) dating measures the time elapsed since a mineral grain was last exposed to sunlight. The technique exploits the fact that natural radiation in the surrounding sediment continuously produces electron–hole pairs in the crystal lattice of common minerals such as quartz and feldspar, some of which become trapped at defect sites. When the grain is exposed to light, the trapped electrons are released and recombine, emitting a faint luminescence in the process and resetting the system. In the dark, the population of trapped electrons grows again. By measuring the accumulated luminescence (which scales with the burial dose) and the dose rate of the surrounding sediment, the burial age of the grain can be calculated.

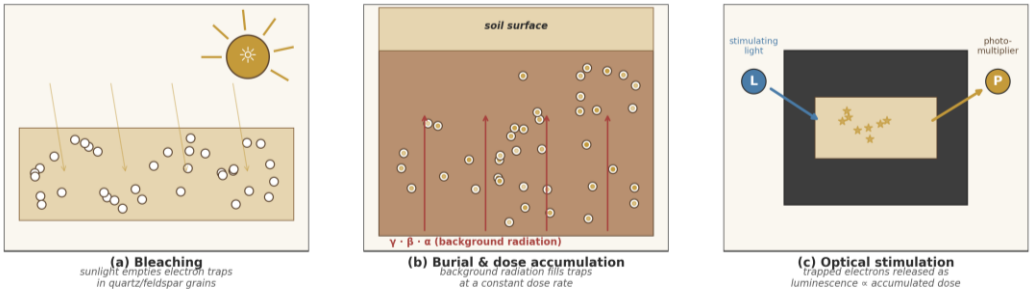

Figure 4.3 · Principle of Optically Stimulated Luminescence (OSL) dating. (1) Exposure to sunlight bleaches the grain, resetting the clock; (2) once buried, the grain accumulates trapped electrons at a rate determined by the surrounding radiation; (3) in the laboratory, optical stimulation releases the electrons and the emitted luminescence is measured.

The strength of OSL is that it dates the sediment itself rather than any organic inclusion. This makes it ideal for sites and contexts where no datable organic material is preserved — sand dunes, loess plateaus, aeolian-influenced cave deposits and many open-air Palaeolithic sites in arid regions. The effective range of OSL is approximately 100 years to 100,000 years for quartz, and somewhat longer for some feldspar protocols. Within that range, typical precision is around 5–10 per cent of the age.

Sampling for OSL requires special care. The sample must not be exposed to light during collection; this is normally achieved by hammering an opaque steel tube into the section and capping it before extraction. Laboratory preparation is performed under low-intensity red or sodium light. Modern single-aliquot regenerative-dose (SAR) protocols allow age determinations on individual

grains or small aliquots, which is particularly valuable for sediments with mixed populations of grains of different burial histories.

4.4 Relative dating and chronostratigraphy

Alongside the absolute techniques described above, geo-archaeology continues to make use of relative dating methods that establish only the order of events, not their date in calendar years. The most fundamental of these is straightforward stratigraphic ordering by the principle of superposition. Cross-cutting relationships among features — a pit dug through a floor, a wall built across an earlier road — provide additional relative-age constraints. Typological analysis of finds (ceramics, lithics, coins, metal objects) provides a culturally based relative chronology that can often be tied to the absolute chronology through a few well-dated reference points.

Chronostratigraphy, finally, is the formal process of correlating local stratigraphic sequences with the global stratigraphic record. This is most important for Pleistocene archaeology, where local sequences are correlated with the Marine Isotope Stage (MIS) record, the speleothem-based monsoon record from East Asian caves, and the polar ice-core records. The result is a global framework into which any archaeological sequence can be situated, at least at the resolution allowed by the available correlations.

Table 4.1 — Comparison of principal dating methods used in geo-archaeology

Method	Materials	Effective range	Typical precision
Radiocarbon (14C)	Organic carbon (charcoal, bone, plant remains)	0 – 55,000 yr BP	±20 – 200 yr
Dendrochronology	Wood with preserved rings	0 – 12,000 yr BP	annual
OSL (quartz / feldspar)	Sediment grains	100 – 500,000 yr	±5 – 10 %
U-series (U/Th, U/Pb)	Carbonates (speleothems, corals, travertine)	100 – 500,000 yr (U/Th)	±1 – 5 %
K–Ar / 40Ar/39Ar	Volcanic minerals	10 ka – billions yr	±0.5 – 2 %
Cosmogenic nuclides	Exposed rock surfaces	100 – 5,000,000 yr	±5 – 20 %
Palaeomagnetism	Sediments with magnetic minerals	millions yr	qualitative / chronostrat.

Table 4.1 — Comparison of principal dating methods. Effective range and typical precision vary with sample type and preservation; the values given are indicative.

Chapter 5 — Geochemical Analysis

Geochemistry, in the geo-archaeological context, is the study of the chemical composition of archaeological materials and their host sediments. The aim is twofold: to use chemical composition as a fingerprint that connects artefacts to their geological sources, and to use chemical variation through space and time as a record of past human activity. The chapter introduces three families of techniques in particular: X-ray fluorescence, stable-isotope analysis, and the recovery of ancient DNA from sediments.

5.1 X-ray fluorescence (XRF)

X-ray fluorescence (XRF) is now the workhorse of archaeological elemental analysis. The technique exploits a fundamental principle of atomic physics: when an atom is bombarded with high-energy X-rays, electrons may be ejected from inner shells. The resulting vacancy is filled by an electron falling from a higher shell, and a secondary X-ray is emitted whose energy corresponds exactly to the energy difference between the two shells. Since this energy difference is specific to each element, the spectrum of secondary X-rays provides a direct fingerprint of the elemental composition of the sample.

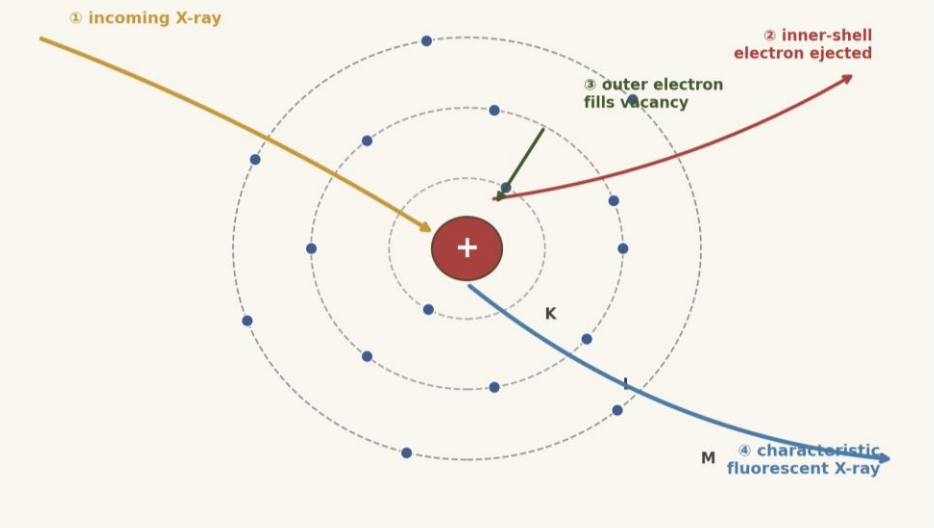

Figure 5.1 · Principle of X-ray fluorescence. A primary X-ray (red) ejects an inner-shell electron; an outer-shell electron drops to fill the vacancy and a secondary X-ray (yellow) is emitted with an energy that is characteristic of the element. The resulting spectrum is essentially a list of elements present in the sample.

Two implementations are widely used. Wavelength-dispersive XRF (WD-XRF) uses a crystal spectrometer to disperse the secondary X-rays and offers very high precision; it is the standard method for laboratory-based elemental analysis of geological materials. Energy-dispersive XRF

(ED-XRF) uses a solid-state detector to discriminate the X-ray energies directly, is somewhat less precise but considerably more flexible, and is the basis of the now-ubiquitous portable XRF (pXRF) field instruments. A modern pXRF analyzer is little larger than a handheld drill and can produce a multi-element analysis of a sediment, soil or artefact in a few minutes.

In archaeological applications, XRF is used routinely for two purposes. First, it allows the chemical sourcing of raw materials: obsidian, for example, has element ratios that vary characteristically among different volcanic sources, and obsidian artefacts from a single site can frequently be assigned to specific sources hundreds or thousands of kilometers away. Similar work has been done on ceramics, metals, ochres and many other materials. Second, XRF mapping of the chemistry of an archaeological deposit can reveal hidden patterns: elevated phosphorus in former animal pens, elevated heavy metals in metal-working areas, elevated calcium in burnt-bone concentrations. The portable XRF in particular has revolutionized this kind of in-situ chemical mapping.

5.2 Stable-isotope analysis

Stable-isotope analysis exploits subtle differences in the abundance of the stable isotopes of an element to track natural and anthropogenic processes. The most commonly measured isotope systems in archaeology are those of carbon (13C / 12C), nitrogen (15N / 14N), oxygen (18O / 16O), strontium (87Sr / 86Sr) and, more recently, sulphur (34S / 32S) and lead (208Pb / 207Pb / 206Pb).

Carbon and nitrogen isotopes in human and faunal bone collagen are the standard tools for dietary reconstruction. Plants are divided into two photosynthetic categories — C3 plants (most temperate cereals, fruits and vegetables) and C4 plants (millet, maize, sorghum and many tropical grasses) — with characteristically different δ13C values. Marine plants have still different δ13C values. The δ13C of the bone collagen of a consumer therefore reflects the dominant plant base of its diet, integrated over the lifetime of the individual. Nitrogen isotopes, meanwhile, become enriched in 15N by approximately 3–4 ‰ at each step up the food chain, so δ15N reflects the trophic level of the diet.

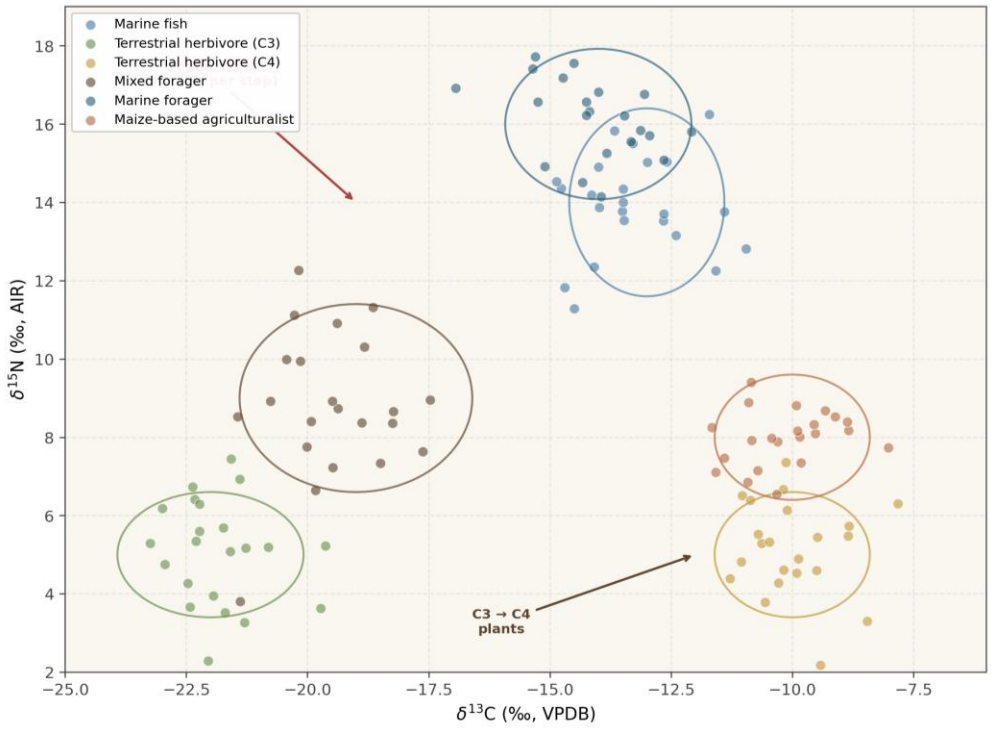

Figure 5.2 · Bivariate plot of δ13C and δ15N values in bone collagen. Different dietary categories — terrestrial herbivores eating C3 plants, C4-plant consumers, marine fish and mammals, and mixed human diets — plot in distinct regions of the diagram. The diagram is the workhorse of palaeodietary reconstruction.

Oxygen and strontium isotopes are used principally for the reconstruction of mobility. Oxygen isotope ratios in drinking water vary systematically with climate, altitude and distance from the coast; the δ18O of skeletal tissue reflects the water consumed during the formation of that tissue. Strontium isotope ratios, similarly, vary with the underlying geology; the 87Sr/86Sr ratio of dental enamel reflects the geological provenance of the food and water consumed during tooth formation in childhood. By comparing dental enamel with bone, archaeologists can identify individuals who grew up in one isotopic region and died in another — that is, individuals who were demonstrably mobile within their own lifetimes.

Table 5.1 — Common applications of stable isotopes in geo-archaeology

System	Material	Primary information	Key archaeological questions
δ13C / δ15N	Bone collagen	Dietary composition	C3 vs C4; marine input; trophic level
δ18O	Tooth enamel; carbonate; speleothem	Drinking-water; climate	Mobility; palaeoclimate; weaning
87Sr / 86Sr	Tooth enamel; bone	Geological background	Mobility; provenance of food / animals
δ34S	Bone collagen	Aquatic vs terrestrial	Marine input; freshwater input
208Pb / 207Pb / 206Pb	Metals; ceramics	Geological source of lead	Provenance of metal artefacts

Table 5.1 — Commonly used stable-isotope systems in geo-archaeology, the materials measured and the questions they help to address.

5.3 Ancient DNA from sediments

The recovery of ancient DNA (aDNA) from skeletal remains has transformed Pleistocene and Holocene archaeology over the last two decades. More recently, the same molecular methods have been applied directly to sediments — so-called sedaDNA. The principle is that DNA from organisms that lived, died or otherwise contributed material to a deposit can persist in the sediment matrix for tens of thousands of years, particularly in cold, dry or anoxic conditions. Targeted extraction and high-throughput sequencing can recover this DNA and identify the organisms that contributed it.

In geo-archaeological terms, sedaDNA opens two new windows. The first is the identification of hominin presence at sites where no skeletal remains have been preserved. Neanderthal and Denisovan DNA, for example, has now been recovered from cave sediments at sites where no fossil bones of these hominins are known. The second window is palaeoecological: the species composition of past faunas and floras can be reconstructed in remarkable detail from sedaDNA, complementing or replacing the more traditional macro-fossil and microfossil records.

As with all new techniques, sedaDNA must be interpreted carefully. Modern contamination is a constant risk; deeper layers can be contaminated by DNA percolating from above; and the relationship between DNA preservation and depositional environment is still being characterized.

Nevertheless, the technique is rapidly becoming a standard part of the geo-archaeologist's toolkit, particularly at deeply stratified Palaeolithic sites where every additional source of information is precious.

Chapter 6 — Visual Concepts I: Remote Sensing and Satellite Imagery

The remainder of this volume is concerned with what may be called the visual concepts of contemporary geo-archaeology — the imaging technologies, processing pipelines and analytical frameworks that have transformed the discipline over the last quarter of a century. The present chapter introduces the broad family of remote-sensing techniques based on satellite and aerial imagery; Chapter 7 will treat airborne LiDAR; and the second volume will continue with UAV photogrammetry, GIS and AI-assisted detection.

6.1 Principles of remote sensing

Remote sensing is the science of acquiring information about an object or area without making physical contact with it. In practice the term refers to the use of imaging sensors mounted on aircraft, satellites or other airborne platforms to record the electromagnetic radiation reflected or emitted by the Earth's surface. Each sensor is sensitive to a particular range of wavelengths within the electromagnetic spectrum, and each surface material — soil, vegetation, water, rock, built structure — has its own characteristic spectral signature determined by its chemical composition, structure and moisture state. By measuring the radiation reaching the sensor in several wavelength bands and combining these measurements, the analyst can identify and map surface materials over very large areas.

Figure 6.1 · The electromagnetic spectrum and the ranges sampled by common Earth-observation sensors. Optical sensors (Landsat, Sentinel-2) operate in the visible, near-infrared (NIR) and shortwave-infrared (SWIR); thermal sensors operate in the mid- and long-wave infrared; LiDAR uses a narrow band in the NIR; synthetic-aperture radar (SAR) such as Sentinel-1 operates at microwave wavelengths.

Three properties distinguish remote-sensing platforms from one another. Spatial resolution is the smallest object that can be resolved on the ground; it varies from kilometers for some meteorological sensors, through tens of meters for Landsat, ten meters for Sentinel-2, down to better than 0.5 meters for the latest commercial high-resolution platforms. Spectral resolution is the number and width of the bands in which the sensor measures radiation; multispectral sensors record a handful of broad bands, while hyperspectral sensors record hundreds of narrow bands. Temporal resolution is the frequency with which the same point on the ground is revisited; this varies from weeks (Landsat) down to days (Sentinel-2 in combination, or commercial constellations) or even multiple times per day for some new constellations.

Active versus passive sensing: A passive sensor records radiation produced elsewhere — most commonly sunlight reflected by the Earth's surface, or thermal radiation emitted by it. An active sensor produces its own radiation and records the return signal. LiDAR and SAR are the principal active systems used in archaeology. Active systems have several advantages: they work at night (LiDAR, SAR) and in any weather (SAR), and they can deliver direct three-dimensional information.

6.2 Landsat, Sentinel-2 and other platforms

The Landsat programme is the longest continuous record of the Earth's surface from space. Operated by NASA and the US Geological Survey, the programme began in 1972 with the launch of Landsat 1 and has now produced more than five decades of data. The current operational satellites are Landsat 8 (launched 2013) and Landsat 9 (launched 2021), both carrying the Operational Land Imager (OLI) and Thermal Infrared Sensor (TIRS). Landsat data are freely available worldwide and are particularly valuable for studies of long-term landscape change.

The European Sentinel-2 mission, operated by the European Space Agency as part of the Copernicus programme, has provided a complementary data stream since 2015. Sentinel-2 consists of two satellites (Sentinel-2A and -2B) in a phased orbit that provides a global revisit of five days. The Multispectral Instrument (MSI) on board records thirteen bands at spatial resolutions of 10 m (four visible/NIR bands), 20 m (six red-edge and SWIR bands) and 60 m (three atmospheric bands). Sentinel-2 data, like Landsat, are openly available.

A growing range of commercial high-resolution platforms now complements the freely available data. WorldView, GeoEye, Pléiades and others deliver imagery at sub-meter resolution; the more recent constellations of SkySat, Planet, and BlackSky deliver near-daily revisit at sub-3-metre

resolution. These commercial data are expensive but indispensable for detailed mapping of small sites and features. A separate category is the airborne hyperspectral sensor (such as AVIRIS or HyMap), which records hundreds of contiguous narrow bands and allows much finer spectral discrimination than is possible with multispectral satellites.

Table 6.1 — Specifications of common satellite platforms used in geo-archaeology

Platform	Operator	Spatial resolution	Revisit / availability
Landsat 8/9	NASA / USGS	30 m (15 m pan)	16 d each (~8 d combined); free
Sentinel-2A/2B	ESA Copernicus	10 / 20 / 60 m	5 d (combined); free
Sentinel-1A/1B (SAR)	ESA Copernicus	5 × 20 m	6 d (combined); free
WorldView-3	Maxar	0.31 m (pan) / 1.24 m (MS)	1–3 d; commercial
Pléiades Neo	Airbus	0.30 m (pan)	daily; commercial
Planet SkySat	Planet Labs	0.5 m	sub-daily; commercial
Planet Dove	Planet Labs	3 m	daily; commercial

Table 6.1 — Indicative specifications of commonly used satellite platforms. The market evolves rapidly; specifications should always be checked against current documentation.

6.3 Spectral indices for archaeology

A spectral index is a simple arithmetic combination of two or more spectral bands designed to highlight a particular surface property. Indices are routinely calculated as the first step in any archaeological analysis of multispectral imagery, because they reduce the high-dimensional spectral data to a small number of physically meaningful layers that are easier to interpret visually and computationally.

The most widely used index in any environmental application of remote sensing is the Normalized Difference Vegetation Index, or NDVI. NDVI is calculated as (NIR − RED) divided by (NIR + RED), where NIR is the reflectance in the near-infrared band and RED is the reflectance in the red band. Healthy vegetation strongly absorbs red light (used in photosynthesis) and strongly reflects near-infrared light (which would otherwise overheat the plant), so vegetation pixels have high NDVI values; bare soil and water have low values. NDVI is sensitive to differences in plant vigour, and these differences in turn can reveal buried archaeological features.

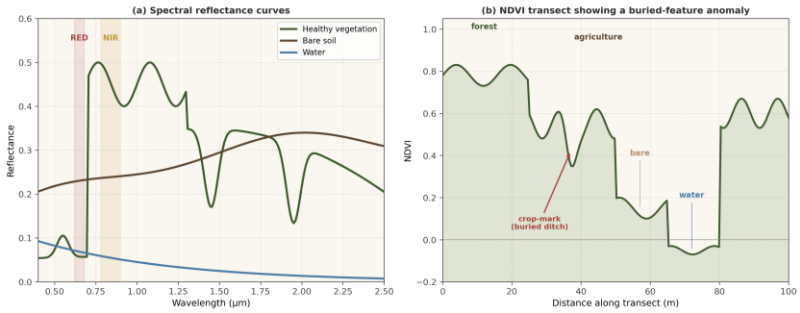

Figure 6.2 · The NDVI principle for detecting buried archaeological features. (a) Healthy vegetation has high NIR reflectance and low red reflectance, producing high NDVI values; bare soil and stressed vegetation have lower NDVI. (b) Across a transect, a buried wall produces lower NDVI because plants growing above it have less soil moisture and root depth.

The reason that NDVI reveals buried features is straightforward. A buried wall or pavement reduces the depth of soil available to plant roots, restricts moisture retention, and modifies surface drainage. Plants growing over the wall are therefore drought-stressed compared to those in adjacent areas; their NDVI is lower; and the plan of the wall appears in the NDVI image as a linear or rectilinear anomaly. Conversely, plants growing over a buried ditch — where soil is deeper and moisture greater — appear more vigorous; their NDVI is higher; and the ditch appears as a positive anomaly. These crop-marks have been known to aerial archaeologists since the 1920s, but the satellite era has made it possible to look for them systematically over entire regions.

Table 6.2 — Spectral indices commonly used in archaeological remote sensing

Index	Formula	Detects	Typical use
NDVI	(NIR − RED) / (NIR + RED)	Plant vigour	Crop-marks; buried features
EVI	Enhanced vegetation index	Plant vigour (corrected)	As NDVI, in high-biomass areas
NDWI	(GREEN − NIR) / (GREEN + NIR)	Surface water	Wetlands; palaeochannels
NDMI	(NIR − SWIR1) / (NIR + SWIR1)	Vegetation water content	Soil-moisture anomalies
BSI	Bare-soil index	Bare soil exposure	Erosion; ploughed sites
NBR	(NIR − SWIR2) / (NIR + SWIR2)	Burnt area	Fire history; site destruction

Table 6.2 — Standard spectral indices and their typical application in archaeological prospection. NIR = near-infrared; SWIR = shortwave infrared; GREEN, RED = corresponding visible bands.

Two related indices deserve specific mention. The Normalized Difference Water Index (NDWI) replaces the red band of NDVI with the green band; it is sensitive to liquid water at the surface and is useful for mapping palaeochannels, wetlands and other water-related archaeological features. The Bare Soil Index (BSI) combines visible and SWIR bands to highlight bare soil; it is useful for picking out sites where ploughing has brought sub-surface anthropic deposits to the surface.

More sophisticated processing techniques — principal-components analysis, spectral mixture analysis, tasseled-cap transformation, and unsupervised classification — extend the range of features that can be detected from multispectral imagery. These methods become particularly powerful when combined with the machine-learning pipelines discussed in the next volume.

6.4 Synthetic Aperture Radar

The optical remote-sensing systems discussed in Sections 6.1 through 6.3 are passive: they record the solar radiation reflected from the Earth's surface and are therefore dependent on daylight and on clear-sky conditions. A complementary class of active remote-sensing systems addresses these limitations by transmitting their own radiation and recording the portion that is reflected back. The most important active system for archaeological purposes is synthetic aperture radar (SAR), which operates in the microwave region of the spectrum and is therefore unaffected by cloud cover, by atmospheric water vapour, or by the diurnal cycle. The principal SAR missions used in current archaeological practice are the European Sentinel-1 constellation, which operates in the C-band, and the older RADARSAT and ALOS missions, which operate in C-band and L-band respectively.

The physics of radar backscatter differs fundamentally from that of optical reflectance. The intensity of the backscattered signal depends on the surface roughness at the scale of the radar wavelength (a few centimeters for C-band), on the dielectric properties of the surface materials (particularly their water content), and on the geometric orientation of the surface relative to the radar antenna. Smooth surfaces such as paved roads, calm water and dry bare soils produce specular reflection away from the radar and return very weak signals. Rough surfaces such as cultivated fields, dense vegetation and disturbed ground produce strong diffuse backscatter. The dielectric contrast between dry and wet soils is particularly large, with the result that recently irrigated or rain-soaked fields appear significantly brighter than dry fields in C-band imagery.

The archaeological applications of SAR fall into three broad categories. The first is the detection of sub-surface features that produce subtle topographic or moisture anomalies invisible to the optical eye. Particularly in arid environments, SAR has been used to detect buried palaeo-channels, infilled archaeological features, and walls that have been completely levelled at the surface. The second is the monitoring of vulnerable archaeological landscapes through interferometric techniques (InSAR), which use the phase information of two successive SAR acquisitions to detect ground displacement at the millimetric scale. InSAR has been used to monitor the subsidence of dewatered wetland archaeological sites, the slow movement of historic structures, and the gradual deformation of tells under modern agriculture. The third is the integration of SAR observations with optical and elevation data into multi-modal classification pipelines that exploit the complementary information content of each sensor.

6.5 Hyperspectral imaging

A further extension of optical remote sensing replaces the small number of broad spectral bands of conventional multi-spectral sensors with the hundreds of narrow contiguous bands of hyperspectral sensors. The principal civilian hyperspectral missions used in archaeological work include the EnMAP mission of the German Aerospace Center, the PRISMA mission of the Italian Space Agency, and the now-retired Hyperion sensor aboard EO-1. Hyperspectral sensors deployed aboard manned aircraft and increasingly aboard UAVs provide an even finer spectral resolution at the cost of substantially higher operational complexity.

The principal archaeological advantage of hyperspectral imaging is the ability to identify surface materials by their full spectral signature rather than by a small number of band ratios. Specific minerals, vegetation stress conditions, soil organic matter content, and even some classes of archaeological residue have characteristic spectral features (narrow absorption bands at particular wavelengths) that can be detected in hyperspectral data but not in conventional multi-spectral data. The principal disadvantages are the operational complexity of hyperspectral acquisition, the much larger data volumes that result, and the substantially greater processing burden of the resulting datacubes. The published archaeological literature on hyperspectral imaging is small but is expanding rapidly as commercial UAV-mounted hyperspectral systems become available.

6.6 — Cloud computing platforms for remote sensing

A development of the past decade that has reshaped the practice of archaeological remote sensing is the emergence of cloud-based platforms that provide pre-processed satellite imagery together with analytical infrastructure in a single integrated environment. The principal platforms in current use are Google Earth Engine, the Copernicus Data and Information Access Services, and Microsoft's Planetary Computer. Each platform hosts a curated archive of multi-decadal satellite imagery from the principal civilian missions, together with derived products (cloud masks, vegetation indices, land-cover classifications), and provides programmatic access through scripting interfaces that allow large-area analyses to be conducted in a few minutes rather than the days or weeks that would have been required with downloaded imagery.

The implications for archaeology have been substantial. Analyses that previously required either a dedicated computing infrastructure or a major institutional investment can now be conducted by an individual researcher with a laptop and a web browser. Multi-temporal analyses spanning the full Landsat archive (1972 to the present) are particularly well-suited to the cloud-platform model, as are large-area comparative analyses across multiple regions. The principal methodological caveats are the dependence on the curated archives provided by the platforms (which are not always identical to the official mission archives) and the dependence on the continued operation of the platforms themselves, which are commercial or quasi-commercial services subject to change. The published best practice is to document the platform version and the imagery snapshot used in any published analysis with the same care as one would document any other data source.

Chapter 7 — Visual Concepts II: LiDAR and Topographic Imaging

If satellite remote sensing has expanded the spatial scale of archaeological prospection, airborne Light Detection and Ranging (LiDAR) has revolutionized its precision. LiDAR is the single most important imaging technology to have entered the geo-archaeological toolkit in the past twenty years. Its ability to penetrate vegetation cover and reveal the underlying ground surface has uncovered entire archaeological landscapes that had eluded conventional survey, most spectacularly in the forested lowlands of Central America, Cambodia and the eastern United States.

7.1 Principles of LiDAR

LiDAR is an active remote-sensing system. The sensor — typically mounted on a fixed-wing aircraft, a helicopter or a UAV — emits a rapid sequence of laser pulses, usually at a near-infrared wavelength around 1,064 nanometers. Each pulse travels to the ground, is reflected back, and is detected by the sensor. The time-of-flight between emission and detection, together with the precise position and orientation of the sensor (determined by GNSS and an inertial measurement unit), allows the three-dimensional position of the reflecting surface to be calculated with centimetric precision.

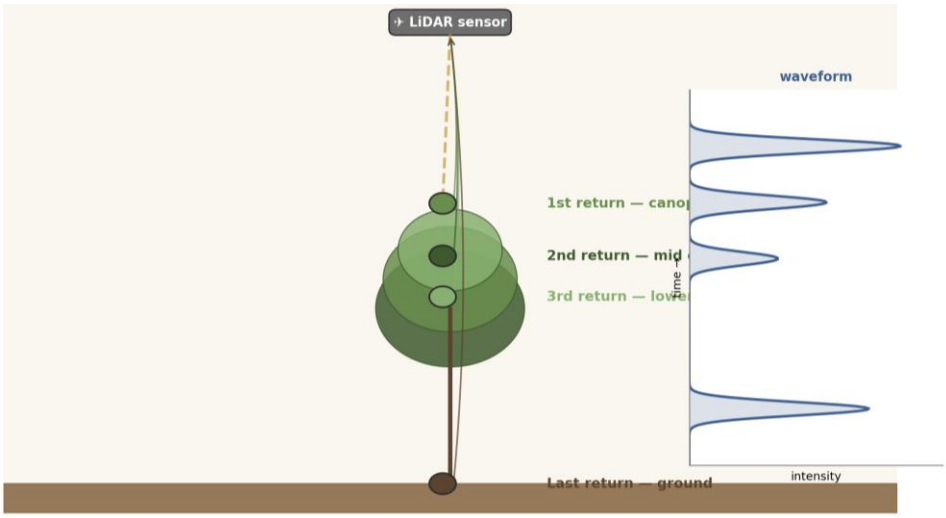

Figure 7.1 · Multiple-return LiDAR. A single laser pulse may be partly reflected by the upper canopy and partly transmitted through; further partial reflections occur at intermediate vegetation layers, and the final return comes from the ground. The full waveform of returns is recorded and used to reconstruct the vertical structure of the canopy and the bare-earth surface beneath it.

The transformative property of LiDAR is its capacity to record several returns from a single pulse. A pulse fired into a forest canopy is partly reflected by the upper leaves, partly transmitted through the gaps, partly reflected by mid-canopy branches, and partly transmitted further to be reflected by lower vegetation and finally by the ground. Modern systems record up to five or more discrete returns per pulse, or the full waveform of the return signal. By processing this multi-return information, the analyst can separate canopy returns from ground returns and reconstruct the bare-earth surface beneath even dense vegetation.

7.2 Vegetation penetration and bare-earth modelling

The end products of LiDAR processing are two digital models. The Digital Surface Model (DSM) records the elevation of the highest reflecting surface at each location — generally the top of the

canopy, or the roof of a building. The Digital Terrain Model (DTM) records the bare-earth elevation, derived by filtering out the canopy and other above-ground returns. For archaeological purposes, the DTM is the model of interest, because it reveals the micro-topography of the ground surface.

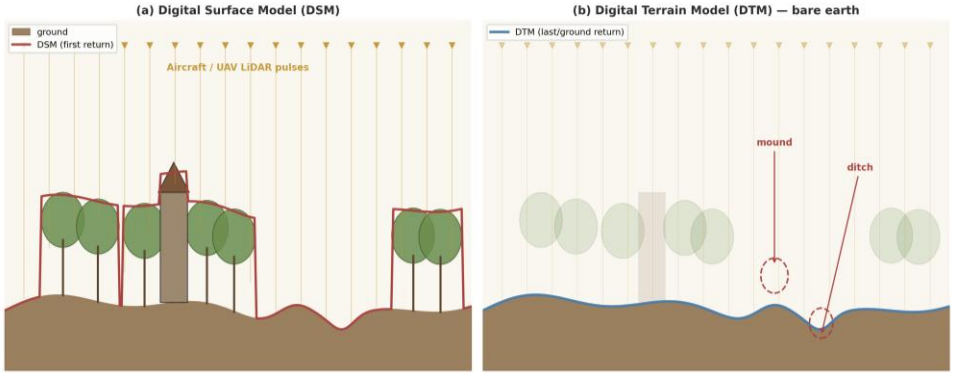

Figure 7.2 · The contrast between a Digital Surface Model (top) and a Digital Terrain Model (bottom) for the same patch of vegetated landscape. Removing the canopy reveals a low earthwork — possibly a former enclosure bank — that is completely invisible in standard imagery.

The success of vegetation removal depends on the density of the canopy, the density of the LiDAR returns and the sophistication of the filtering algorithms. In open woodland, a return density of even a few points per square meter is sufficient to produce a high-quality DTM. In closed tropical rainforest, return densities of 15 to 25 points per square meter are typically required, and a small but significant proportion of the ground may remain unsampled. Even so, the resulting DTMs reveal archaeological features that no other technique could have detected. The discovery of extensive Maya urban networks in the Guatemalan Petén — pyramids, causeways, agricultural terraces — beneath what had been described as virgin rainforest is the most celebrated example.

7.3 Applications in geo-archaeology

Beyond the dramatic discovery cases, LiDAR has found steady application in three more routine areas of geo-archaeological research. The first is the systematic mapping of earthwork landscapes — Iron Age enclosures, Roman field systems, medieval ridge-and-furrow — in regions where modern land use makes ground-level survey impractical. LiDAR-based mapping in the United Kingdom, Germany, the Netherlands and Belgium have produced inventories of such features at a scale unimaginable a generation ago.

The second application is geomorphological. High-resolution DTMs allow the precise mapping of fluvial terraces, palaeochannels, landslide complexes, coastal palaeo-shorelines and other

landforms that constitute the physical setting of archaeological sites. A LiDAR-derived geomorphological map at 50-centimetre resolution offers far more information than any traditional cartographic product and feeds directly into questions of site location, taphonomy and preservation.

The third application is the analysis of standing remains. Terrestrial LiDAR (or close-range LiDAR mounted on a tripod or on a UAV) can record the three-dimensional geometry of standing walls, rock-cut features, cave passages and other heritage structures with millimetric precision. This is increasingly the standard for monument recording and for monitoring the long-term preservation of vulnerable sites.

Looking ahead: This concludes Volume I of the report. Volume II will take up the visual-concepts thread with UAV photogrammetry and integrated GIS analysis (Chapter 8), the contribution of machine learning and deep learning to all of the techniques discussed so far (Chapter 9), an extended treatment of site-formation processes and a series of case studies that illustrate how the methods are deployed in practice (Chapters 10 and 11), and a final chapter on the ethical and heritage-management dimensions of the discipline (Chapter 12). A consolidated bibliography and a visual atlas will close the report.

7.4 Visualization techniques for LiDAR-derived models

A bare-earth digital elevation model derived from LiDAR is, in itself, a relatively uninformative raster of elevation values. The features of archaeological interest — earthworks, terraces, hollow ways, defensive ditches and structural footings — are detected only when the elevation model is rendered through one of several specialized visualization techniques. Each technique emphasises different aspects of the topography and is suited to different feature classes; the published best practice in archaeological LiDAR analysis is to apply several techniques in parallel and to inspect the resulting visualizations side-by-side.

The most familiar visualization is the hillshade, in which a single light source illuminates the elevation model from a specified azimuth and inclination, and the resulting brightness of each pixel is determined by the angle between the local surface normal and the light direction. The hillshade is intuitive and visually compelling, but it has the well-known limitation that linear features oriented parallel to the light direction are invisible. The standard response is to compute hillshades from several azimuths and to combine them into a multi-directional hillshade, but more principled alternatives have been developed over the past two decades.

The sky-view factor is a visualization that computes, for each pixel, the proportion of the upper hemisphere that is visible from that pixel (taking the surrounding topography into account. Concave features such as ditches, hollow ways and quarries appear dark because much of the sky is occluded by the surrounding higher ground; convex features such as banks, mounds and tells appear bright because their summits have an unobstructed view of the sky. The sky-view factor is direction-independent and is therefore an excellent companion to the multi-directional hillshade. The local relief model subtracts a smoothed version of the elevation model from the original, with the result that gentle regional slopes are removed and only the small-scale topographic variation remains; the resulting visualization is particularly effective for archaeological features superimposed on substantial regional relief.

Beyond these three principal techniques, a variety of more specialized visualizations exist: the openness positive and negative (related to the sky-view factor but using a different angular integration), the simple local relief model, the slope shade, and various hybrid visualizations that combine information from several sources. The Relief Visualization Toolbox developed by the Slovenian research group at the Institute of Anthropological and Spatial Studies has become the de facto standard implementation of these techniques and is freely available.

7.5 Drone-borne and bathymetric LiDAR

The discussion in earlier sections has focused on the airborne LiDAR systems mounted on manned aircraft, which have been the workhorses of large-scale archaeological LiDAR for the past two decades. Two recent developments are extending the range of LiDAR-based methods. The first is the emergence of small LiDAR sensors mountable on consumer-grade UAVs. These drone-borne systems are typically less accurate and have shorter range than their airborne counterparts, but they can be deployed for individual sites and small landscapes at a fraction of the cost of a manned-aircraft survey. The published applications include the documentation of vegetated archaeological monuments that are not readily mappable by photogrammetric techniques, the rapid response to threatened sites where a manned-aircraft survey could not be organized quickly, and the routine site-scale monitoring that supports cultural-heritage management.

The second development is bathymetric LiDAR, which uses green-wavelength lasers capable of penetrating shallow water. Bathymetric LiDAR has been used to map the submerged components of coastal archaeological landscapes, including ancient harbours, fish traps, and offshore extensions of terrestrial sites. The technique is limited to water depths of less than approximately

fifty meters in clear water and considerably less in turbid water, which excludes many submerged archaeological landscapes, but for the shallower coastal contexts to which it applies the resulting bathymetric models are of unprecedented resolution and accuracy.

Chapter 8 - Visual Concepts III: UAV Photogrammetry and GIS

The introduction of small unmanned aerial vehicles (UAVs) to civilian use during the early 2010s changed the operational scale at which geo-archaeologists could acquire high-resolution three-dimensional data. Where airborne LiDAR (Chapter 7) provides regional-scale topographic models acquired from manned aircraft, UAV photogrammetry provides site-scale and excavation-scale data acquired by an individual researcher in a single day of fieldwork. The technical foundation of UAV photogrammetry is the algorithmic framework known as Structure-from-Motion (SfM), which reconstructs three-dimensional geometry from overlapping two-dimensional photographs without the need for survey-grade stereo cameras or pre-calibrated rigs. SfM has effectively democratized three-dimensional documentation in archaeology, and it now constitutes the standard method for recording excavated surfaces, individual artefacts, standing monuments and entire landscapes.

This chapter describes the workflow by which UAV photogrammetry products are generated, the principal sources of error and uncertainty in those products, and the role of Geographic Information Systems (GIS) in integrating photogrammetric outputs with other spatial data. Particular attention is given to the choices that the geo-archaeologist must make at each stage of the workflow, because those choices determine the resolution and the absolute accuracy of the resulting model, and therefore the questions to which it can ultimately be applied.

8.1 The photogrammetric workflow

The complete workflow from UAV acquisition to a usable orthomosaic or digital elevation model passes through five well-defined stages. Each stage has its own technical literature and its own internal trade-offs; the following description summarizes the principal considerations at each stage and identifies the key decisions left to the researcher.

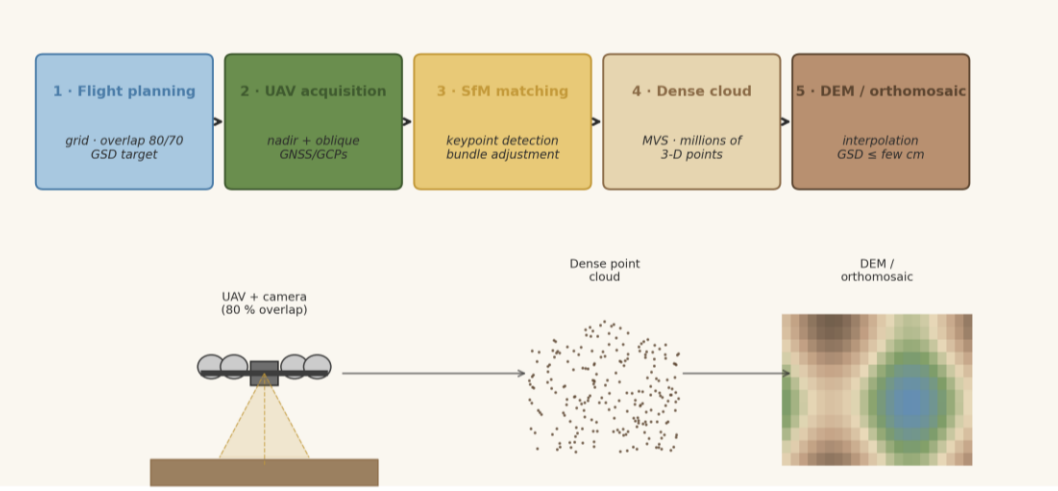

Figure 8.1 · The five-stage Structure-from-Motion (SfM) workflow, from flight planning through orthomosaic generation. Each stage propagates errors to the next, so the final accuracy is bounded by the weakest link.

The first stage is flight planning. The UAV must fly a pre-defined trajectory such that every point on the ground appears in a minimum of three overlapping photographs taken from different viewpoints. The standard industry recommendation is 80 % forward overlap and 70 % side overlap, although larger overlaps are advisable for sites with low texture (sandy surfaces, modern fields) or steep relief. The ground sample distance (GSD) — the linear ground dimension of one pixel — is determined by the focal length of the camera, the size of its sensor, and the flying altitude. A typical small UAV carrying a 20-megapixel camera flying at 60 m altitude will produce imagery with a GSD of approximately 1.5 cm, which is adequate for the documentation of all but the smallest archaeological features.

The second stage is image acquisition. The UAV flies the planned trajectory, recording GNSS coordinates and orientation for each photograph. For archaeological work that requires absolute (geo-referenced) accuracy at the centimeter level, a network of ground control points (GCPs) must be installed across the site before flight and surveyed with a differential GNSS receiver or a total station. The GCPs serve as anchor points during the bundle adjustment of the next stage, and their distribution across the site determines the homogeneity of the final positional accuracy. A common rule of thumb is one GCP for every five photographs, distributed both horizontally and, where relief permits, vertically.

The third stage is image alignment, in which the SfM algorithm identifies distinctive key points (corners, blobs, intensity gradients) in every photograph and matches them across the overlap regions. From the geometry of these matched points, the algorithm jointly estimates the position and orientation of every camera at the moment of capture, along with the three-dimensional

coordinates of the matched key points themselves. This joint estimation is the bundle adjustment, and it is the mathematical core of SfM. The output of the alignment stage is a sparse point cloud of typically a few hundred thousand points, together with refined exterior orientation parameters for every photograph.

The fourth stage is dense reconstruction. With camera parameters now known, the algorithm proceeds to a multi-view stereo (MVS) computation that estimates a depth for every pixel of every input photograph. The result is a dense point cloud containing tens of millions of points for a typical site-scale survey. This stage is computationally the most expensive in the workflow — a dense reconstruction from one thousand 24-megapixel photographs may take several hours on a workstation equipped with a high-end GPU.

The fifth and final stage converts the dense point cloud into the products that are normally consumed by archaeologists: a digital elevation model (DEM, normally a regular raster grid of elevations), an orthomosaic (a single seamless image of the site projected onto the DEM and corrected for parallax), and a textured three-dimensional mesh suitable for visualization or three-dimensional printing. Each of these products inherits the positional and elevational accuracy of the underlying dense cloud, which in turn inherits the accuracy of the camera-position estimates and the GCP survey.

8.2 Sources of error and good practice

Several systematic and stochastic errors affect SfM outputs in archaeological contexts, and a competent geo-archaeologist needs to anticipate them. The most pervasive systematic error is the so-called bowl effect, a slight curvature of the reconstructed surface arising from the joint estimation of camera focal length during bundle adjustment. The effect is minimized by including oblique photographs in the survey (not only nadir views) and by distributing GCPs across the full extent of the surveyed area, including at its margins. A second common error is loss of texture, which prevents the SfM algorithm from finding matching key points; the most frequent culprits in archaeological work are uniform sandy surfaces, freshly excavated clays, and the polished stones of paved spaces. Texture loss is treated by introducing artificial fiducial markers or by acquiring photographs at lower altitude where individual grains become resolvable.

A third class of error originates in the GNSS positioning of the UAV itself. Most consumer UAVs use single-frequency GNSS receivers that achieve positional accuracies of two to five metres in absolute terms, even though their relative accuracy between consecutive photographs is much

higher. For archaeological work that requires sub-centimeter absolute accuracy, the only reliable solution is to use real-time-kinematic (RTK) GNSS UAVs in combination with surveyed GCPs, or to fly a conventional UAV and rely entirely on GCPs for absolute georeferencing. The recent generation of RTK UAVs has reduced the need for dense GCP networks but has not eliminated it: a quality survey still requires at least four well-distributed GCPs to detect and correct for any residual systematic distortion.

Table 8.1 · Common UAV platform classes used in geo-archaeology

Platform class	Typical payload	Endurance	Typical GSD	Best use in geo-archaeology
Consumer multirotor	20 MP camera	20–30 min	1–3 cm	Single excavation surfaces, small monuments
Prosumer multirotor	42 MP camera, RTK	30–45 min	0.5–1.5 cm	Site-scale survey, accurate DEMs
Fixed-wing UAV	24 MP camera	60–90 min	3–10 cm	Landscape-scale survey, regional mapping
Hybrid VTOL	Multispectral, LiDAR	60–120 min	2–8 cm + LiDAR	Multi-sensor surveys, vegetated terrain

Table 8.1 · Common UAV platform classes used in geo-archaeology, with their typical performance characteristics.

The choice of platform follows the requirements of the survey. For single excavation surfaces, a consumer multirotor is adequate and inexpensive; for site-scale survey requiring sub-centimeter absolute accuracy, a prosumer RTK multirotor is the current standard; for landscape-scale work covering many square kilometers, fixed-wing platforms are more efficient because of their longer endurance. The increasing availability of small LiDAR sensors mountable on UAVs is gradually blurring the boundary between photogrammetric and LiDAR-based surveys, particularly for sites with significant vegetation cover.

8.3 Geographic Information Systems

A Geographic Information System (GIS) is software for storing, manipulating and analysing data that have an explicit spatial reference. In a typical geo-archaeological GIS, the photogrammetric and LiDAR products described above are integrated with archaeological survey data, with documentary sources (historical maps, gazetteers), and with environmental layers (geology, soils, hydrology) into a single analytical environment. The result is more than a digital map: it is a research instrument that allows the geo-archaeologist to interrogate the relationships between

sites and landscapes, to model the visibility of monuments, to predict the location of undiscovered sites, and to manage cultural heritage at scales beyond the individual site.

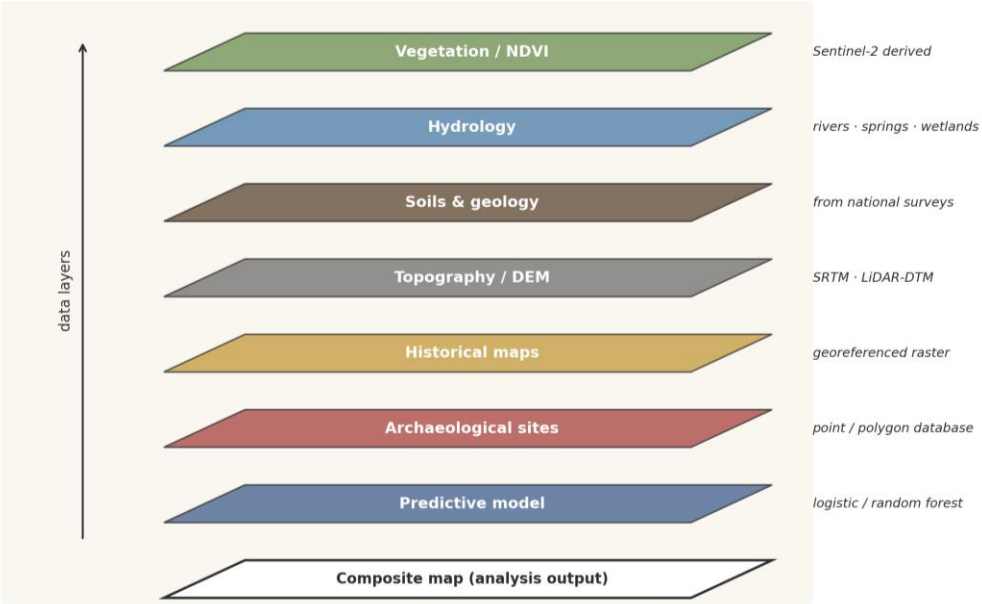

Figure 8.2 · The conceptual model of a GIS as a stack of co-registered spatial layers. Each layer represents one phenomenon; analytical operations combine layers to produce derived products such as predictive maps.

The conceptual model of a GIS is built around layers. Each layer represents one phenomenon (vegetation, hydrology, soils, archaeological sites) and is stored either as a raster (a regular grid of pixel values) or as a vector (a set of points, lines or polygons with attached attributes). Layers are co-registered to a common spatial reference frame, which means that they can be combined, overlaid and compared in any meaningful way. The principal operations performed on layers fall into a small number of well-defined categories, summarized in Table 8.2 below.

Table 8.2 · Principal spatial operations in archaeological GIS

Operation class	Typical input	Typical output	Geo-archaeological use
Buffer	Vector layer	Polygon at fixed distance	Catchment of springs, defensible perimeters
Overlay (intersect)	Two vector layers	Spatial intersection	Sites on particular soil types
Raster algebra	Multiple rasters	New raster from formula	NDVI, slope-weighted erosion potential
Viewshed	DEM + observer point	Visible / invisible mask	Visibility of monuments from each other
Least-cost path	DEM + friction surface	Optimal route between points	Reconstructed ancient roads
Density estimation	Point layer	Continuous surface of density	Site distribution patterns
Predictive modelling	Sites + environmental	Probability surface	Likelihood of undiscovered sites

Table 8.2 · Principal spatial operations in archaeological GIS, with examples of how each is used in geo-archaeology.

Each of these operations corresponds to a substantive archaeological question. The buffer operation answers the question 'how far is each site from the nearest water source?' The overlay operation answers on which soil type is each site located?' Viewshed analysis answers 'from which points in the landscape is this monument visible?' Least-cost-path analysis estimates the most efficient travel route between two locations given the topography and other costs, and is widely used to model ancient roads, transhumance routes and trade networks. Density estimation produces continuous surfaces of site density that can be related to environmental variables. And predictive modelling combines all of the above to identify zones of high probability of finding undiscovered sites — a procedure of considerable practical importance for cultural-heritage management in advance of infrastructure projects.

8.4 Integration: the digital geo-archaeological landscape

The genuine power of UAV photogrammetry and GIS lies not in either technique used in isolation but in their integration with the techniques surveyed in earlier chapters. A typical modern workflow at a Bronze Age tell, for example, might begin with a regional UAV survey that produces a sub-decimeter DEM of the entire archaeological landscape. The DEM is then loaded into a GIS, where it is overlaid with geological maps, soil maps, hydrological data, and the locations of all known sites in the region. A least-cost-path analysis identifies probable routes between the principal sites, and a viewshed analysis identifies the locations from which the tell would have been visible. Targeted survey, guided by the resulting maps, may then identify previously unknown sites or features that allow the analyst to test specific hypotheses about settlement choice, defensibility, or visibility politics.

At the site scale, the same workflow produces a centimeter-resolution DEM of the standing remains, an orthomosaic for the production of plans, and a textured three-dimensional model of the site as a whole. These products are then integrated with sub-surface geophysics, with the stratigraphic record from excavation, with the dating sequence (Chapter 4) and with the chemical record from soil and sediment samples (Chapter 5). The result is a multi-dimensional digital representation of the site — a representation in which spatial, temporal and compositional information are all accessible from a single environment, and in which any further question can be answered by an additional query rather than a fresh field campaign.

Two cautionary remarks are in order. The first concerns the seductive precision of digital products. A DEM with a 2 cm GSD looks more authoritative than a hand-drawn site plan, but its appearance of precision can mask substantial errors in absolute georeferencing, in the interpolation of bare-earth surfaces from incomplete dense clouds, or in the underlying photographic acquisition. A well-trained geo-archaeologist learns to treat digital products with the same scepticism applied to any other piece of evidence and to estimate their error budgets explicitly. The second concerns the long-term curation of digital data. Photogrammetric models, GIS projects and large rasters are at risk of being unreadable within a decade because of format obsolescence and the rapid evolution of software. Sustained curatorial effort — in the form of open data formats, persistent identifiers, and properly staffed digital repositories — is a non-trivial component of any digitally based research programme.

8.5 Worked example: error budget for a tell-scale photogrammetric survey

To make the discussion of errors and accuracy concrete, the present section walks through a realistic error budget for a representative tell-scale photogrammetric survey. The scenario is a 200-metre by 250-metre Bronze Age tell, surveyed with a prosumer-grade RTK multirotor UAV carrying a 42-megapixel camera, flown in a double-grid pattern at 50 meters above ground level with 80 % forward overlap and 70 % side overlap. Twelve ground control points are surveyed across the site using a differential GNSS receiver with a horizontal accuracy of two centimeters and a vertical accuracy of three centimeters.

The first error contribution is the intrinsic accuracy of the imagery. At the chosen flight altitude and camera configuration, the ground sample distance is approximately 0.7 cm per pixel. Sub-pixel key point matching achieves a horizontal accuracy of approximately one-quarter of a pixel under good conditions, giving a horizontal error of approximately 0.2 cm at the center of each photograph. Toward the photograph edges, the error rises to approximately 0.5 cm because of lens distortion and projective foreshortening. The second contribution is the camera-position uncertainty propagated through the bundle adjustment. With twelve well-distributed GCPs of two-centimeter horizontal accuracy, the residual GCP error contributes approximately 0.8 cm horizontal and 1.2 cm vertical to the final model. The third contribution is the GCP survey itself, with the two and three centimeter horizontal and vertical accuracies cited above.

Combining these contributions in quadrature gives a total expected horizontal accuracy of approximately 2.2 cm and a vertical accuracy of approximately 3.4 cm at the center of the surveyed area, rising to approximately 3.5 cm horizontally and 4.5 cm vertically toward the margins. These figures are well within the requirements for the documentation of standing architecture, the production of accurate excavation plans, and the comparison of repeated surveys over multiple seasons. They are not adequate, however, for the documentation of individual artefacts at sub-millimeter resolution, which requires the dedicated close-range photogrammetric techniques discussed in the next section.

8.6 Close-range and micro-photogrammetry

Photogrammetry can be deployed at scales much smaller than those of the typical UAV survey. Close-range photogrammetry, in which a handheld camera is moved around a target object at distances of one to two meters, has become a standard technique for the documentation of individual artefacts, of small excavation features such as hearths or burials, and of architectural details on standing monuments. The mathematical foundation is identical to that of UAV

photogrammetry, but the practical workflow differs in several respects. The camera is moved manually rather than autonomously; lighting must be controlled to avoid specular reflections and harsh shadows; and the absolute scale is established not by GNSS coordinates but by a calibrated reference object included in the field of view.

Micro-photogrammetry extends the same technique to the scale of microscopic features. With macro lenses and dedicated close-up rigs, individual lithic edges, ceramic surface treatments, and micro-stratigraphic details visible only under magnification can be recorded as three-dimensional models with sub-micron resolution. The principal application is the documentation of use-wear and manufacturing traces on stone tools, for which the resulting models can be analyzed quantitatively to distinguish different working motions, different worked materials, and different stages of the operational sequence. The published literature on micro-photogrammetric use-wear analysis is small but growing rapidly, and the technique is poised to replace the qualitative microscopic analyses that have dominated lithic studies for the past five decades.

8.7 Four-dimensional archaeology

A natural extension of three-dimensional photogrammetric documentation is the addition of time as a fourth dimension. By acquiring photogrammetric surveys of an excavation at the end of each working day, or after each major stratigraphic transition, the excavator produces a time-indexed sequence of three-dimensional models that documents the progressive removal of deposits. The four-dimensional dataset can be replayed in software to reconstruct the state of the excavation at any past moment, to visualize the geometry of deposits that have since been removed, and to verify the consistency of the stratigraphic interpretation against the actual depositional sequence.

The methodological implications of four-dimensional documentation are still being worked out in the published literature. On the positive side, the technique provides a level of post-excavation accountability that has not previously been available; on the negative side, it adds substantial overhead to the daily routine of fieldwork and produces datasets whose long-term storage and curation are themselves a significant challenge. The largest published four-dimensional archaeological dataset, from the Çatalhöyük excavations in central Anatolia, exceeds one terabyte of registered point-cloud data and is being curated through a dedicated long-term archive. As storage costs continue to fall and as photogrammetric processing software continues to mature, four-dimensional documentation is likely to become standard practice within the next decade.

8.8 Predictive modelling in GIS

Predictive modelling — the estimation of the probability that a given location contains an undiscovered archaeological site — is one of the principal applications of GIS in contemporary geo-archaeology. The methodological foundation is straightforward. A training dataset is assembled consisting of the locations of known sites and an equal or larger number of locations known not to contain sites. For each location, a vector of environmental covariates is extracted from the GIS: elevation, slope, aspect, distance to permanent water, soil type, geological substrate, and any other variables thought to influence settlement choice. A statistical or machine-learning model is fitted to this training set such that, given a covariate vector, it predicts the probability of site presence. The fitted model is then applied to every location in the study area to produce a continuous probability surface.

The choice of statistical model for predictive archaeology has evolved substantially over the past three decades. The earliest published models, dating from the 1980s, used simple weighting schemes in which each covariate was assigned a weight by expert judgement and the location score was the weighted sum. The 1990s saw the introduction of logistic regression, which estimated the weights statistically from the training data and produced calibrated probability estimates. The 2000s saw the introduction of generalized additive models and decision trees, which allowed non-linear and interactive effects of the covariates. The 2010s saw the introduction of random forests and gradient-boosted trees, which routinely outperformed the earlier models on benchmark datasets. The 2020s have seen the introduction of deep-learning models that take raw remote-sensing imagery as input rather than pre-computed covariates.

Each generation of models has come with its own methodological caveats. The principal recurring concern is the difficulty of constructing a representative negative-example set, since locations 'known not to contain sites' are in fact only known not to contain sites that have been found. Without explicit attention to this difficulty, the resulting probability surfaces are likely to reflect the spatial pattern of past archaeological survey rather than the spatial pattern of past human settlement. A secondary concern is the temporal heterogeneity of the training data: a single composite training set may contain sites of widely different ages whose locational preferences are not the same, and the resulting model may be a poor predictor for any single period. Recent best practice addresses these concerns through period-specific models, through careful documentation of survey intensity in the negative-example set, and through explicit estimation of the spatial autocorrelation of the residuals.

Chapter 9 - Artificial Intelligence and Machine Learning in Geo-archaeology

The fifth and most recent generation of geo-archaeological methods is rooted in artificial intelligence, and specifically in the family of techniques known as machine learning. Where earlier generations of the discipline depended on manual interpretation of stratigraphic sections, photographs and maps, the most recent generation increasingly depends on algorithms that learn to make those interpretations from labelled examples. The applications fall into three principal categories. First, machine-learning models are used as detectors: given a satellite image, a LiDAR-derived elevation model, or an aerial photograph, they identify the location of probable archaeological features such as burial mounds, ditches, structures, or linear earthworks. Second, machine-learning models are used as classifiers: given a recovered artefact, a sherd, or a sediment sample, they assign it to a typological or compositional class. Third, machine-learning models are used as predictors: given a regional environmental dataset and the known location of archaeological sites, they predict the probability of undiscovered sites at every point in the landscape.

This chapter introduces the technical foundations of these applications, the principal model families currently in use, the practical workflows that have emerged in the literature, and the methodological and ethical concerns that the use of these methods raises. It assumes familiarity with the remote-sensing and GIS techniques discussed in Chapters 6, 7 and 8, but does not assume any background in computer science.

9.1 The principle of supervised learning

The dominant paradigm in archaeological machine learning is supervised learning. The analyst assembles a training dataset consisting of input examples (image patches, sediment spectra, artefact photographs) paired with output labels (presence or absence of a site, ceramic type, raw-material class). A model — a parametric mathematical function — is then fitted to the training data such that, given an input, it produces an output that matches the label as closely as possible. Once trained, the model is applied to new, unlabeled inputs to produce predictions. The quality of those predictions depends in the first instance on the quality and the representativeness of the training data, and only secondarily on the architecture of the model itself.

Several model families have proved useful in geo-archaeological practice. Logistic regression and decision trees are appropriate for tabular data with a moderate number of well-defined input

variables (for example, predicting site presence from environmental covariates such as elevation, slope, soil type and distance to water). Random forests and gradient-boosted trees are more powerful generalizations that work well on the same kind of tabular data and are often the default choice in geo-archaeological predictive modelling. Support vector machines have been used successfully for the classification of hyperspectral data. For image data, however, the dominant family for the past decade has been the convolutional neural network, which is introduced in the next section.

9.2 Convolutional neural networks

Convolutional neural networks (CNNs) are a class of deep neural networks specifically designed for the processing of grid-structured data such as images. The fundamental insight underlying their architecture is that the features relevant to image classification are local (an edge, a texture, a small structural element) and that the same feature can occur anywhere in the image. CNNs exploit this insight by replacing the fully connected matrix multiplications of ordinary neural networks with convolutions — small, sliding filters that are applied identically to every region of the input. The result is a network that is both far smaller and far better suited to spatial data than a general-purpose neural network of comparable performance.

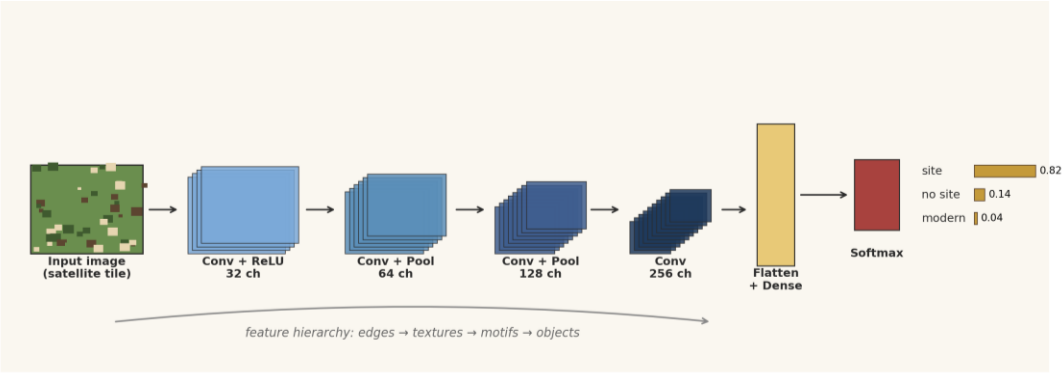

Figure 9.1 · Schematic of a convolutional neural network classifier. The input image passes through several convolutional layers that extract a hierarchy of features, before a flattening and a dense layer produce per-class score. The example illustrates a three-class problem distinguishing archaeological sites from natural landscapes and modern disturbance.

A typical CNN for archaeological feature detection consists of a sequence of convolutional layers, each of which extracts features at a progressively coarser spatial scale. The earliest layers learn to detect simple primitives such as edges, oriented gradients and small blobs. The intermediate layers combine these primitives into more complex motifs — for example, the geometry of a circular ditch, the silhouette of a rectangular foundation, or the brightness pattern of a crop-

mark. The deepest layers integrate these motifs into representations that are diagnostic of the target object class. After the convolutional stack, a flatten operation reshapes the spatial feature map into a vector, which is fed into a small number of fully connected layers and ultimately into a SoftMax output layer that produces a probability score for each class.

Training a CNN consists of finding values for its millions of parameters that minimize the discrepancy between its predictions on the training data and the corresponding labels. The standard algorithm is stochastic gradient descent, in which the network parameters are repeatedly adjusted in the direction that most rapidly reduces a chosen loss function (typically the cross-entropy between predicted and true labels). The training proceeds in epochs, each of which passes the entire training set through the network once. Convergence is monitored on a held-out validation set that does not participate in the parameter updates; training is terminated when the validation loss stops decreasing, even if the training loss is still falling, in order to avoid the well-known pathology of overfitting.

9.3 Object detection: YOLO and related models

Image classification — assigning a single class label to an entire image — is only one of the tasks of interest to the geo-archaeologist. More frequently, the task is object detection: given an aerial photograph or a LiDAR-derived hillshade of a landscape, locate every archaeological feature in the scene and assign each a class label and a bounding box. Object detection is conceptually harder than classification because the number of objects in the input is unknown in advance and because the objects may occur at very different spatial scales.

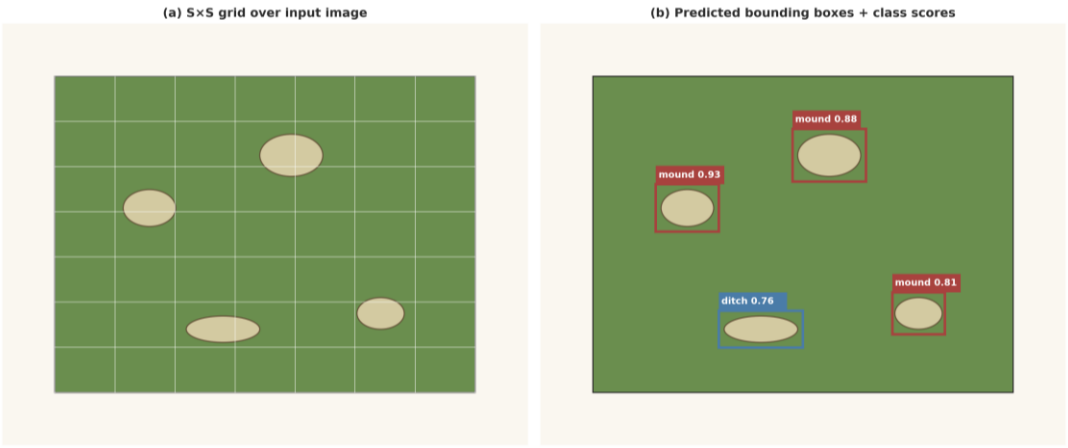

Figure 9.2 · YOLO-style single-pass object detection. Panel (a) shows the input image with an S×S grid overlay; the network simultaneously predicts for each grid cell the bounding box, class label and confidence score of any contained object. Panel (b) shows the resulting bounding boxes after non-maximum suppression and a confidence threshold.

Two main approaches to object detection have come to dominate the literature. The first family, exemplified by the R-CNN series of networks (Region-based CNN, Fast R-CNN, Faster R-CNN), separates the problem into two stages. A first stage proposes candidate regions in the image that might contain an object; a second stage classifies the contents of each candidate region and refines its bounding box. The second family, exemplified by the YOLO series (You Only Look Once) and by the SSD (Single Shot Detector) family, treats object detection as a single regression problem. The image is divided into a grid of cells, and the network predicts, for every cell, the bounding box parameters and class scores of any object whose center falls within that cell. After post-processing to remove redundant detections, the result is the list of detected objects together with their bounding boxes and class scores.

In archaeological applications, the choice of detector is governed less by raw accuracy than by the geometry of the targets and by the available training data. For dispersed, well-separated objects such as burial mounds in a forest steppe, YOLO-style detectors are normally adequate and computationally efficient. For dense, overlapping targets such as terrace systems on steep mountain slopes, the two-stage R-CNN family typically performs better at the cost of greater training and inference time. The published archaeological literature has used both families with reported precision and recall in the range of 0.7 to 0.95, depending on the homogeneity of the dataset, the size of the training set, and the difficulty of the target class.

9.4 Evaluation and overfitting

The evaluation of machine-learning models in geo-archaeology is more subtle than the evaluation of classical statistical models, and a careful treatment of evaluation is one of the principal methodological responsibilities of the modern practitioner. The fundamental rule is that a model's performance must be evaluated on data that the model has never seen during training. Performance on the training set itself is uninformative, because the model can in principle memorize the training examples and produce excellent results on them while producing arbitrary results on new data — the phenomenon of overfitting.

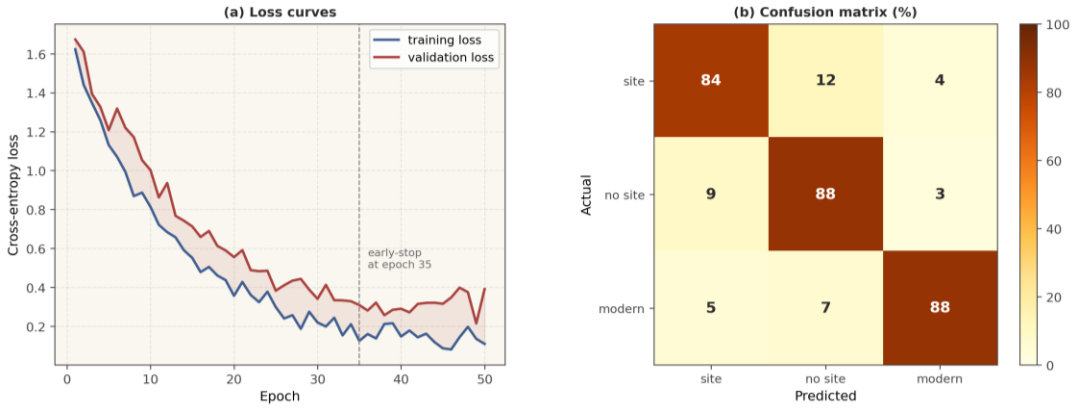

Figure 9.3 · Diagnostic plots from training a CNN classifier. Panel (a) shows the evolution of training and validation loss over epochs; the divergence after epoch ~35 is the signature of incipient overfitting and indicates the appropriate early-stopping point. Panel (b) shows the resulting confusion matrix on the held-out test set.

The diagnostic plot of training and validation loss over training epochs is the principal tool for detecting overfitting. In a well-behaved training run, both losses decrease together as the network learns features that generalize. At some point, the training loss continues to decrease while the validation loss flattens out and eventually rises; this divergence indicates that the network is beginning to memorize idiosyncrasies of the training set that do not generalize to new data. The standard mitigations are early stopping (terminating training at the point of minimum validation loss), data augmentation (artificially increasing the size and variability of the training set by applying random transformations to the input), and regularization (penalizing large network weights in the loss function).

Beyond the loss curves, a battery of summary metrics is reported for any deployed model. For classification problems, the principal metrics are accuracy (the fraction of examples correctly classified), precision (the fraction of positive predictions that are correct), recall (the fraction of true positives that are predicted as positive), and the F1 score (their harmonic mean). The

confusion matrix shown in Figure 9.3(b) decomposes these metrics per class. For object-detection problems, the standard metric is mean average precision (mAP), which combines precision and recall across a range of intersection-over-union thresholds. Reporting all of these metrics, rather than only accuracy, is essential because most archaeological datasets are heavily imbalanced — sites are rare compared to no-sites — and an apparently high accuracy can mask catastrophic failures on the minority class.

Table 9.1 · Standard evaluation metrics for machine-learning models

Metric	Definition	Why it matters in archaeology
Accuracy	Correct predictions ÷ total predictions	Misleading with imbalanced classes (sites are rare)
Precision	True positives ÷ (true positives + false positives)	Rate of false alarms among predicted sites
Recall	True positives ÷ (true positives + false negatives)	Rate of missed sites among real sites
F1 score	Harmonic mean of precision and recall	Single summary balancing the two
mAP	Mean average precision across IoU thresholds	Standard for object detection
κ (Cohen's kappa)	Agreement above chance	Useful when classes are imbalanced

Table 9.1 · Standard evaluation metrics for machine-learning models in geo-archaeology.

9.5 Methodological and ethical concerns

The deployment of machine learning in geo-archaeology raises a number of concerns that are not always given the attention they deserve in the published literature. The first concerns the geographical and cultural bias of training data. Most published CNN models for archaeological detection have been trained on data from western Europe, North America, or a small number of well-studied regions of the Maya lowlands. Their applicability to landscapes and material cultures outside these regions is unclear, and the uncritical transfer of trained models from one cultural region to another can introduce systematic biases into the resulting archaeological maps. The geo-archaeological community has only recently begun to address this problem through the assembly of geographically diverse benchmark datasets.

The second concern is the question of explainability. CNNs and related models are widely regarded as black boxes whose internal decision processes are not directly interpretable. Recent work in explainable AI has produced techniques such as saliency maps, class activation maps, and feature attribution that can highlight the regions of an input image that most strongly influenced a prediction, but the interpretive value of these techniques in archaeological contexts is still being explored. Where models are used to support consequential decisions — for example, the allocation of cultural-heritage protection to particular landscapes — the inability to explain the model's reasoning is a serious limitation that must be acknowledged explicitly.

The third concern is the disclosure of site locations. A successful detector applied to a satellite image of an unprotected landscape can produce a precise inventory of previously unknown sites within a few hours of inference time. Publication of such an inventory in the form of an open dataset creates a significant risk of looting. The same is true of large training datasets that include the locations of vulnerable sites. The current best practice is to redact precise coordinates from published outputs, to register detection results with appropriate cultural-heritage authorities before any public release, and to consider the differential vulnerability of sites in regions with limited enforcement capacity. These are not abstract concerns: documented cases of looting following the publication of remote-sensing site inventories now exist in the literature, and the geo-archaeological community has a continuing responsibility to address them.

None of these concerns argues against the use of machine learning in geo-archaeology. They argue, instead, for the development of an explicitly methodological subfield within geo-archaeology dedicated to the appropriate, transparent and ethically responsible use of these techniques. The body of work surveyed in the present chapter is the foundation of that subfield, and the case studies presented in Chapter 11 illustrate both its successes and its limitations.

9.6 Semantic segmentation and the U-Net family

The CNN architectures discussed in Section 9.2 produce single-class labels for whole input images. A more demanding task in geo-archaeological applications is semantic segmentation, in which the network must produce a class label for every pixel of the input, so that the spatial extent of each detected feature is delineated rather than merely localised. Semantic segmentation networks have a fundamentally different architecture: instead of progressively down sampling the input to a small classification head, they pair the down sampling path with an up sampling path that progressively restores the spatial resolution to that of the original input.

The result is a network that takes an image of size H × W as input and produces a pixel-wise classification of the same size as output.

The most widely used segmentation architecture in archaeological practice is the U-Net, introduced by Ronneberger and colleagues in 2015 for biomedical image segmentation and rapidly adapted to remote-sensing tasks. The U-Net combines the down sampling and up sampling paths with skip connections that pass high-resolution feature maps directly from the down sampling path to the corresponding up sampling layer. The result is a network that can produce sharp segmentation boundaries without losing the global context provided by the deepest layers. Variants such as the U-Net++ and the Attention U-Net have improved on the original architecture by adding additional skip connections and attention mechanisms; the best-performing variants on archaeological remote-sensing tasks routinely achieve intersection-over-union scores above 0.8 on validation tiles.

The practical workflow for archaeological semantic segmentation closely parallels the classification workflow but differs in one important respect: the training annotations must consist of pixel-wise masks rather than image-level labels. The production of these masks is laborious and is normally the principal practical bottleneck in the deployment of a segmentation pipeline. Various strategies are used to reduce the annotation burden, including the use of weakly supervised approaches that learn from image-level labels alone, the use of semi-supervised approaches that propagate sparse annotations to nearby pixels, and the use of synthetic training data generated procedurally. None of these strategies eliminates the need for high-quality annotated data, but they reduce the volume of manual annotation required to bring a model to operational performance.

9.7 Transfer learning and pre-trained models

The training of a CNN from random initial weights requires a training dataset of several thousand examples per class and several hours to several days of GPU computation. For most archaeological applications, the available training data are far smaller than this — typically a few hundred examples per class in the best-documented studies. Transfer learning addresses this constraint by starting from a network that has already been trained on a large generic dataset (typically ImageNet, with its more than a million natural images across 1,000 classes) and adapting it to the archaeological task by retraining only the final layers or the entire network at a low learning rate.

The empirical performance of transfer learning in archaeological applications has been remarkably consistent. Across a range of detection and classification tasks, the use of an ImageNet-pre-trained network as the starting point routinely yields validation accuracies five to fifteen percentage points higher than the same network trained from random weights on the same archaeological data. The principal exception is when the input modality differs substantially from the pre-training modality — for example, when single-channel LiDAR-derived hillshades are used as input and the pre-trained network expects three-channel RGB. In these cases, the pre-trained weights of the first convolutional layer must be adapted or replaced, and the benefit of transfer learning is correspondingly reduced. Recent work has produced large pre-trained models specifically for remote-sensing modalities, partially addressing this limitation.

9.8 Vision transformers

The CNN architecture, which has dominated computer vision since the publication of AlexNet in 2012, has begun to be displaced by an alternative architecture known as the vision transformer. Vision transformers, introduced by Dosovitskiy and colleagues in 2020, divide the input image into a sequence of small patches, encode each patch as a vector, and apply the self-attention mechanism of the transformer family of language models to those vectors. The principal advantage of the resulting architecture is that any patch can attend to any other patch directly, without the locality bias imposed by the sliding convolutional filters of a CNN; the principal disadvantage is that the self-attention mechanism scales quadratically with the number of patches, making vision transformers more computationally demanding than CNNs of comparable performance for high-resolution inputs.

The application of vision transformers to archaeological remote-sensing tasks is still in its infancy. The few published studies report performance comparable to that of well-tuned CNNs, with no clear winner across the surveyed tasks. The principal advantage of vision transformers in the archaeological context appears to be their ability to integrate information across large spatial extents, which is particularly useful for the detection of linear features such as ancient roads, paleochannels, and field systems that may extend for kilometres across the input image. The principal disadvantage is the comparatively large training data requirement of vision transformers, which has so far limited their use to the best-documented archaeological remote-sensing datasets.

Chapter 10 - Site Formation Processes

The archaeological record that confronts the excavator is never a direct snapshot of past human behavior. It is the residue of that behavior after a long sequence of cultural and natural transformations, each of which has selectively preserved, destroyed, moved, or altered the material remains. The systematic study of these transformations is the subject of site formation theory, the most influential statement of which remains the work of Michael Schiffer in the 1970s and 1980s. Schiffer drew the now-canonical distinction between cultural formation processes — the deliberate or incidental actions of human beings that produce the archaeological record — and natural formation processes — the geological, biological and chemical processes that subsequently modify it. The intellectual project of geo-archaeology can in many respects be reduced to the systematic investigation of the second of these two classes of processes.

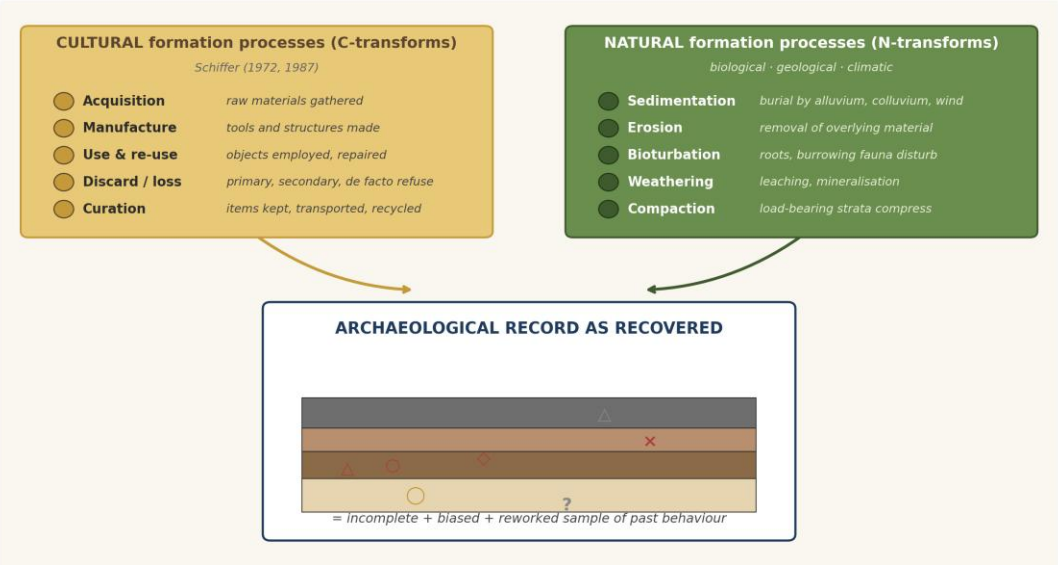

Figure 10.1 · Schiffer's distinction between cultural (C-transforms) and natural (N-transforms) formation processes. The two classes operate in sequence and in parallel to produce the archaeological record as ultimately recovered.

10.1 Cultural formation processes

Cultural formation processes are the totality of past human behaviours that contribute material residues to the archaeological record. Schiffer identified five principal phases: acquisition (the procurement of raw materials), manufacture (the transformation of raw materials into finished tools, ornaments and structures), use and reuse (the deployment of those finished items in routine activities), discard or loss (the deposition of material into the archaeological context), and curation (the deliberate retention or transport of items beyond their initial context). Each of these phases leaves a characteristic residue. Manufacturing debris is concentrated near

workshops; primary refuse is found at the locus of use; secondary refuse is concentrated in middens; de facto refuse — items abandoned in place when a site is suddenly vacated — preserves spatial associations that the other classes of residue lose.

The interpretation of cultural formation processes requires attention to scale. At the scale of a single hearth, the question is whether the surrounding artefact scatter reflects primary refuse from the use of the hearth or secondary refuse swept toward it during cleaning. At the scale of a single structure, the question is whether the contents of the floor reflect normal habitation or a violent abandonment event. At the scale of a settlement, the question is the relationship between the residential and the disposal zones, and whether the gradient between them reflects systematic urban management or accidental accumulation. At each scale, the practical task of the excavator is to read the spatial distribution of materials as evidence for the behavioral processes that produced it.

10.2 Natural formation processes

Natural formation processes act on the archaeological residue from the moment it is deposited. The principal classes of process are sedimentation, erosion, bioturbation, chemical weathering, and mechanical disturbance. Sedimentation — the accumulation of material on top of the archaeological deposit by alluvial, colluvial, aeolian or pedogenic processes — is generally favorable to preservation, since it buries and protects the deposit. Erosion is the inverse and is generally unfavorable: it may remove the overlying sediments and expose the deposit to weathering and looting, or it may rework the deposit itself, redistribute artefacts down-slope and destroy spatial associations. Bioturbation — the mixing of sediments by the activities of plants and animals — is pervasive in temperate soils and is one of the principal causes of the apparent stratigraphic disturbance that excavators commonly encounter. Chemical weathering — the leaching, dissolution and precipitation of minerals in the soil solution — selectively destroys some classes of material (bones in acidic soils, metals in waterlogged conditions) while preserving others.

A particularly important class of natural processes is taphonomy, the systematic study of what happens to organic remains after death. The term was originally coined for the study of palaeontological assemblages, but its application to archaeology has proved extraordinarily fruitful. The taphonomic sequence proceeds through five stages: the living assemblage of organisms in the past landscape, the death assemblage immediately following mortality, the buried assemblage that becomes part of the sedimentary record, the fossil assemblage that

survives the subsequent diagenetic alteration, and the recovered assemblage that is ultimately collected by the excavator. At each transition, certain individuals or certain elements are systematically removed; the recovered assemblage is therefore a heavily biased sample of the original living assemblage, and any reconstruction of past faunal communities, palaeodemographic patterns or palaeodietary regimes must explicitly correct for these biases.

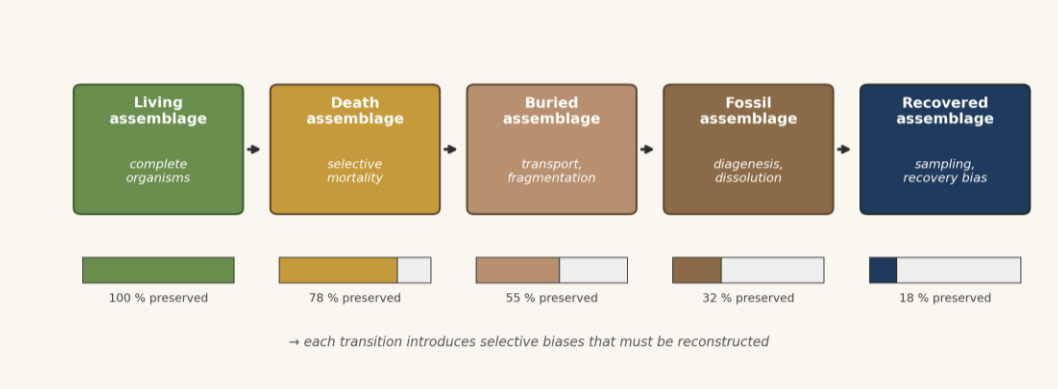

Figure 10.2 · The taphonomic sequence from living to recovered assemblage. Each transition removes a fraction of the original material, so the recovered assemblage represents only a small and selectively biased sample of the original community.

Taphonomic indicators are the principal evidence by which the excavator reconstructs the histories of individual specimens. Weathering stages on bone surfaces record exposure to subaerial conditions before burial. Carnivore tooth-marks record post-mortem scavenging. Cut-marks record human butchery. Trampling abrasion records the passage of feet over surfaces. Burning records exposure to fire, whether deliberate (cooking) or incidental (post-depositional). Patterns of long-bone breakage record the difference between fresh-bone breakage during marrow extraction and dry-bone breakage by trampling or post-depositional processes. The careful inventory of these indicators on individual specimens is laborious but is the only direct route to inferring the cultural and natural processes that produced the assemblage.

10.3 Disturbance and integrity

The combined effect of cultural reworking, natural disturbance, and biased recovery produces archaeological assemblages whose integrity — the degree to which the spatial and temporal associations of the original deposit have been preserved — is variable. The assessment of integrity is one of the central interpretive tasks of geo-archaeology and is typically carried out through a combination of stratigraphic, sedimentological, and statistical procedures. Stratigraphic analysis (Chapter 2) identifies the principal depositional units and the surfaces that

separate them. Sedimentological analysis characterizes the depositional energy and the post-depositional processes (bioturbation, pedogenesis, illuviation) that have modified each unit. Statistical analysis of the artefact assemblage looks for indicators of disturbance — refittable elements separated by tens of centimeters, vertical distributions inconsistent with primary deposition, anomalous spatial clustering of differentially weathered specimens.

The recognition that no archaeological assemblage is perfectly preserved should not be read as a counsel of despair. It is, on the contrary, a precondition for productive interpretation. An archaeology that ignores the formation history of its evidence will mistake taphonomic patterns for behavioural ones; an archaeology that engages with the formation history will systematically distinguish what the past did from what subsequent processes have done to it. The mature geo-archaeology of the early twenty-first century is committed precisely to that systematic distinction.

10.4 Practical implications for excavation

The theoretical framework summarized in this chapter has direct practical implications for the way excavations are conducted. The first is that excavation is itself a destructive process, and therefore that the documentation of context must be exhaustive and irreversible. A modern excavation produces, alongside the recovered artefacts and ecofacts, a complete archive of section drawings, plans, photographs, three-dimensional point clouds, stratigraphic descriptions, sediment samples and dating samples. The geo-archaeologist's principal contribution to this archive is the sedimentological and pedological description of each context, the systematic collection of samples for laboratory analysis, and the integration of all of this into a coherent depositional history of the site.

The second practical implication is that single-context recording — the procedure of treating every distinguishable depositional unit as a separate entity, with its own number, its own description, and its own list of contained finds — is not a matter of administrative convenience but a methodological necessity. Each context corresponds, in principle, to a single depositional event whose history must be reconstructed individually. The Harris matrix, introduced in the 1970s, is the standard graphical representation of the resulting stratigraphic sequence and is the foundation on which all subsequent chronological and behavioural interpretation rests.

The third practical implication is that any chronological model derived from an archaeological site is only as good as the formation-history model on which it rests. A radiocarbon date on

charcoal from a buried surface dates that charcoal, not necessarily the activity associated with the surface; if the charcoal was reworked from an older context, the date may be older than the use of the surface by an unknown margin. The systematic identification of such taphonomic complications, and the corresponding adjustment of chronological interpretations, is one of the principal contributions that geo-archaeology makes to the modern excavation programme.

10.5 Anthropogenic soils and dark earths

A specific class of formation processes that deserves separate treatment is the formation of anthropogenic soils — soils whose properties have been substantially altered by sustained human activity over decades or centuries of occupation. The most thoroughly studied class of anthropogenic soils is the Amazonian terra preta, a dark, fertile soil that occurs in discontinuous patches across the Amazon basin in association with pre-Columbian habitation sites. Terra preta soils are characterized by elevated concentrations of organic carbon (typically two to three times the background level), elevated phosphorus and calcium, abundant ceramic fragments and charcoal particles, and a pH closer to neutral than the surrounding acidic forest soils. The fertility of terra preta is several times that of surrounding soils and persists for centuries after the original occupation, raising both scientific questions about its mode of formation and practical questions about its potential for sustainable tropical agriculture.

The published understanding of terra preta has converged on a multi-pathway model of formation. The dark color derives largely from biochar — charcoal produced at low temperatures and incorporated into the soil through the disposal of cooking residues and the maintenance of household fires. The phosphorus and calcium are derived from animal bones, fish remains and ash. The ceramic fragments are the residue of broken cooking and storage vessels. The microbial community of the resulting soil is distinct from that of surrounding soils and contributes to the unusual stability of the carbon stocks. The combination of these inputs over decades or centuries produces a soil that bears the chemical signature of the occupation and that, once formed, is remarkably stable in tropical conditions.

Comparable anthropogenic soils have been documented in several other parts of the world. The dark earths of north-western European medieval towns, the orchard and garden soils of Mediterranean and Near Eastern long-occupied landscapes, and the agricultural terraces of the Andean highlands are all examples of soils whose properties have been transformed by sustained human activity. In each case, the geo-archaeological challenge is to identify the diagnostic signature of the anthropogenic component against the background of natural pedogenesis, and

to use that signature to reconstruct the history and intensity of past occupation. The combination of micromorphological observation, chemical analysis, isotopic measurement and dating allows this reconstruction to be carried out with increasing precision.

10.6 Preservation of organic materials

The preservation of organic materials in archaeological contexts is governed by a small number of well-understood environmental parameters: oxygen availability, moisture, temperature, pH, and the presence of microbial communities capable of metabolising the material in question. The general rule is that organic materials are preserved in conditions that exclude one or more of the requirements of the principal decomposition pathways. Anaerobic conditions exclude the aerobic bacteria and fungi that are responsible for most decomposition in surface soils. Continuously waterlogged conditions exclude oxygen and limit microbial activity. Continuously frozen conditions exclude microbial activity entirely. Continuously desiccated conditions exclude the water required for microbial metabolism. Highly acidic or highly alkaline conditions exclude many microbial taxa and slow the decomposition of resistant organic materials such as keratin, lignin, and chitin.

The distinct preservation environments of the archaeological record correspond directly to these mechanisms. Waterlogged wetland sites preserve wooden structures, leather, plant remains and human bodies through anaerobic conditions. The intertidal and subtidal portions of submerged coastal sites preserve organic materials through a combination of waterlogging and burial. Permafrost preserves organic materials through continuous freezing, and the recent retreat of cold-climate permafrost has exposed substantial new archaeological assemblages that are now at risk of rapid decomposition. Hot, dry desert sites preserve organic materials through desiccation; the well-known textiles of Egyptian tombs and the preserved bodies of the Tarim Basin are examples. Acid bog environments preserve bodies through a combination of anaerobic conditions and the tannic-acid suppression of microbial activity; the well-known bog bodies of north-western Europe are the canonical examples.

Each preservation environment is fragile in distinctive ways. Waterlogged sites are at acute risk from drainage of the surrounding water table, whether through anthropogenic drainage works or through climate-driven water-table decline. Permafrost sites are at acute risk from rising temperatures, which have already exposed and damaged numerous archaeological deposits across the circumpolar Arctic over the past two decades. Desert sites are at risk from changing precipitation patterns and from human use, particularly tourism. Bog sites are at risk from peat

extraction and from agricultural conversion. The combination of climate change, infrastructure development, and resource extraction is placing unprecedented pressure on these specialised preservation environments, and the geo-archaeological monitoring of vulnerable sites is now an urgent practical priority in many parts of the world.

10.7 Bioturbation in detail

Bioturbation — the mixing of sedimentary deposits by the activities of living organisms — is the most pervasive natural formation process at temperate-zone archaeological sites and deserves a more detailed treatment than the brief mention in Section 10.2. The principal bioturbating organisms are earthworms, ants and termites, burrowing mammals (moles, voles, rabbits), and the root systems of trees and shrubs. The intensity and depth of bioturbation depend on the soil type, the climate, the vegetation cover, and the time elapsed since the deposition of the deposit in question. Under typical temperate forest conditions, the upper 30 to 50 cm of the soil profile is intensively bioturbated and is essentially structureless from a stratigraphic point of view; the deeper horizons are progressively less affected but are rarely entirely undisturbed.

The archaeological consequences of bioturbation are several. Vertical displacement of artefacts is the most direct: small artefacts can be transported upward by the casting activity of earthworms or downward by the entry of artefacts into root and animal burrows. The result is a vertical distribution of artefacts that does not directly reflect the stratigraphy of the original deposit and that must be interpreted with explicit attention to the bioturbation history. Horizontal displacement is generally smaller in magnitude but can be significant for very small artefacts in actively bioturbated layers. Spatial reorganization can erase the primary distribution of artefacts around features such as hearths or workshops, leaving a residual distribution that reflects subsequent natural processes rather than past behaviour. The detection of these effects in the field is one of the principal practical responsibilities of the modern excavator, and the appropriate response is normally a combination of refined recording (in which spatial coordinates are recorded for every find rather than only for the largest), explicit modelling of the bioturbation depth, and statistical analysis of the resulting distributions.

Chapter 11- Case Studies

The methods surveyed in the preceding chapters acquire their practical meaning only when applied to specific archaeological problems. The present chapter selects two recent case studies that have transformed the way geo-archaeology is practiced in the early twenty-first century. The

first is the application of airborne LiDAR to the Maya lowlands, an undertaking that began with a small-scale survey at Caracol in 2009 and that has since expanded into the largest single archaeological remote-sensing programme ever conducted. The second is the application of convolutional neural networks to the automatic detection of Roman roads in the Mediterranean and northern European landscapes, an undertaking that illustrates the integration of remote sensing, machine learning, GIS and field verification into a single coherent workflow.

11.1 Airborne LiDAR in the Maya lowlands

The Maya lowlands of southern Mexico, Guatemala, Belize and Honduras pose a distinctive challenge to archaeological survey. The landscape is densely forested, and the canopy cover prevents the use of conventional aerial photography for the detection of buried features. For most of the twentieth century, the mapping of Maya sites depended on ground survey by archaeologists who walked transects through the jungle and recorded the visible mounds, plazas and causeways that they encountered. The procedure was extraordinarily labour-intensive: a single site such as Caracol, in western Belize, required several decades of ground survey to be partially mapped. The resulting site maps, however valuable, were known to be incomplete in unknown but probably substantial proportions.

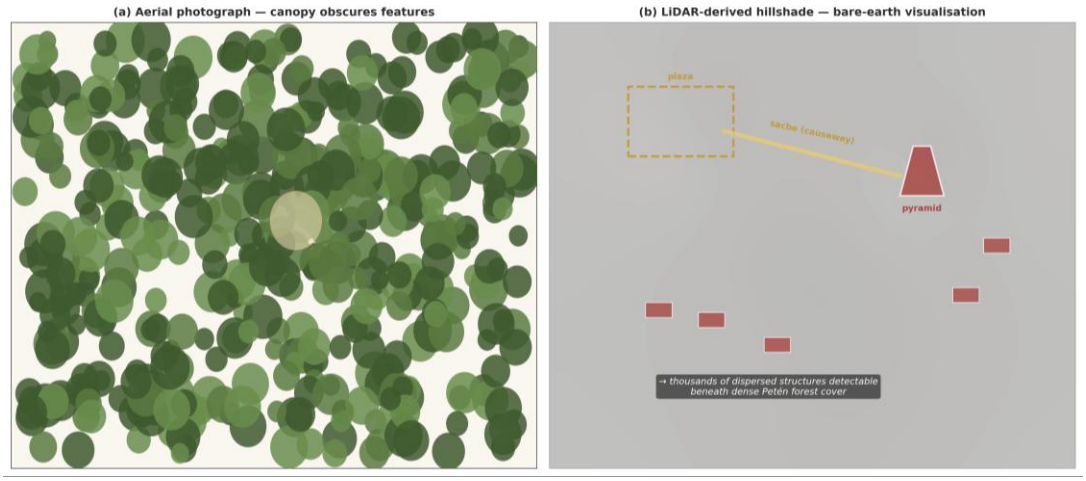

Figure 11.1 · The contrast between conventional aerial imagery and airborne-LiDAR bare-earth visualizations over the Maya lowlands. Panel (a): under closed canopy, structures are not detectable from above. Panel (b): the LiDAR-derived hillshade reveals plazas, pyramids and the sacbe causeway network in a single visualization.

The first systematic application of airborne LiDAR to the Maya problem was conducted at Caracol by Arlen and Diane Chase in 2009, in collaboration with the National Center for Airborne Laser Mapping at the University of Houston. The 2009 survey covered approximately 200 km² of the

Caracol periphery and identified thousands of previously unknown structures, terraces and roads in a single week of acquisition followed by several months of processing. The published results, which appeared in 2011 and 2014, demonstrated unambiguously that the visible-from-the-ground portion of the Caracol landscape represented only a small fraction of the actual archaeological record. The published density of structures was several times higher than the previous ground-survey estimate, and the spatial pattern of those structures revealed an organization of agricultural terraces, residential platforms and inter-site causeways that had not been suspected from the earlier work.

The success of the Caracol survey prompted a much larger programme, the Pacunam LiDAR Initiative, which acquired more than 2,000 km² of LiDAR data across the central Maya lowlands of Guatemala between 2016 and 2018. The published synthesis of that programme, by Marcello Canuto and colleagues in Science in 2018, reported the detection of more than 60,000 previously unknown structures, including residential platforms, defensive fortifications, agricultural fields and a substantial inter-site road network. The implication for Maya demography was substantial: previous estimates of the regional population had been based on the visible sites, and the much larger number of detected structures suggested a population two to three times the previously accepted estimate, occupying a much more intensively managed agricultural landscape than had been envisaged.

The Maya LiDAR programme illustrates the principal strengths and limitations of the technique. On the strengths side, LiDAR penetrates the canopy and produces bare-earth elevation models with sub-decimeter vertical accuracy over hundreds of square kilometers, transforming the spatial scale at which regional archaeology can be conducted. It is non-invasive, leaves no physical trace on the landscape, and produces a digital archive that is reusable for indefinite future analysis. On the limitations side, LiDAR detects only those features that have surface topographic expression: structures completely levelled by erosion, agricultural reworking or modern construction are invisible. Field verification of detected features remains essential, and the published Pacunam programme has been accompanied by an extensive ground-truth campaign that systematically samples the LiDAR-detected structures to confirm their archaeological character and to establish their chronology.

11.2 Machine-learning detection of Roman roads

The Roman road network is one of the most thoroughly documented infrastructure systems of the ancient world. Major roads are listed in the third-century Itinerarium Antonini and depicted

on the medieval copy of the imperial road map known as the Peutinger Table. Minor roads are partially recorded in regional inscriptions and itineraries, but the great majority of the network has not been mapped from documentary sources. Over the past two centuries, archaeologists and ancient historians have devoted enormous effort to mapping the surviving traces of Roman roads through field walking, the inspection of historical cadastral records, and the analysis of aerial photographs. The cumulative result is a set of regional maps of variable completeness, with substantial gaps in remote, vegetated or modernized landscapes.

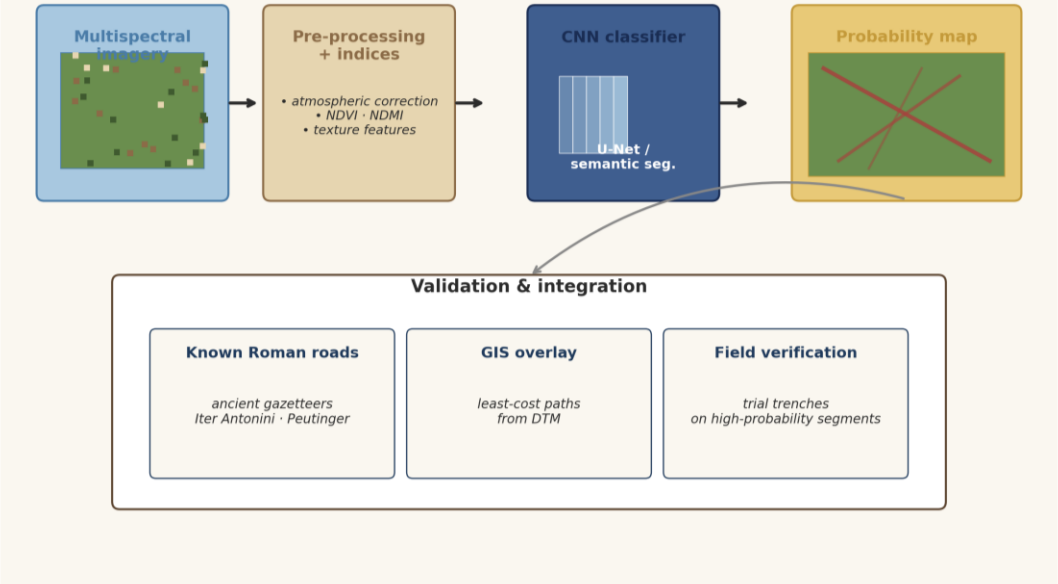

Figure 11.2 · A representative end-to-end workflow for the AI-assisted detection of Roman roads. Multispectral imagery is pre-processed into vegetation and texture indices, a convolutional neural network is trained on known road segments to produce a probability map, and the result is integrated with GIS modelling and field verification.

The use of convolutional neural networks for the automatic detection of road traces in remote-sensing data has matured rapidly during the past decade. The general workflow, illustrated in Figure 11.2, begins with the acquisition of multispectral satellite imagery (typically Sentinel-2 or commercial high-resolution imagery) and the calculation of a battery of derived indices: NDVI for vegetation vigour, NDMI for moisture, texture features capturing the smoothness of the surface, and panchromatic-band derivatives for fine spatial detail. A semantic-segmentation CNN — typically a U-Net or one of its variants — is then trained on tiles of imagery in which the location of known road segments has been annotated. The trained network is applied to a much larger area to produce a probability map of road presence, which is then thresholder, vectorized, and integrated with a least-cost-path model derived from a digital elevation model. The output of the

integrated workflow is a set of candidate road segments ranked by detection probability and by consistency with the expected route geometry.

The published applications of this workflow have been concentrated in two regions: the western Iberian Peninsula, where work by Hèctor Garcia-Molsosa and colleagues has demonstrated the successful detection of previously unmapped segments of the network linking Augusta Emerita to the Atlantic coast; and the Roman provinces of Britain, where the comparable network of Roman roads is partially preserved in modern field boundaries and partially obliterated by post-medieval agriculture. In both cases, the published results report precision in the range of 0.75 to 0.85 on validation tiles, with the principal source of false detections being natural linear features (rivers, geological lineaments, modern field boundaries) that mimic the spectral and textural signature of Roman roads. Field verification of high-probability detections has, in several cases, confirmed previously undocumented segments of the network and has led to revisions of the published regional maps.

11.3 Lessons from the case studies

The two case studies share a number of methodological lessons that have broader implications for the practice of geo-archaeology in the digital era. The first lesson is that the integration of multiple data sources is more powerful than any single source in isolation. The Maya LiDAR programme is most effectively deployed in conjunction with ground survey, historical maps and palaeoclimatic data; the Roman roads workflow is most effectively deployed in conjunction with GIS-based least-cost-path modelling and documentary evidence. In both cases, the published results that have most influenced the broader discipline are those that have explicitly integrated multiple lines of evidence rather than relying on a single technical innovation.

The second lesson is that the role of the human expert remains essential. Neither LiDAR nor CNN detection produces interpreted archaeological maps directly; both produce digital products that must be inspected, evaluated, edited and verified by trained archaeologists familiar with the regional context. The most successful published programmes have been those that have invested heavily in the human-expert side of the workflow rather than treating the technical side as autonomous. This is a methodological observation, not a sentimental one: the comparative experiments published in the literature have repeatedly shown that the precision and recall of fully automated workflows are several percentage points below those of human-supervised workflows.

The third lesson is the importance of open data. Both the Maya LiDAR programme and the published Roman roads workflows have benefited substantially from the willingness of their authors to release training data, trained models, and intermediate processing products to the wider community. The cumulative result has been a rapid acceleration in methodological development, as the techniques first demonstrated for one region or one feature class have been adapted by other groups to other regions and other classes. The continued maintenance of open data and open software repositories is one of the principal infrastructural responsibilities of the geo-archaeological community in the years ahead.

11.4 Palaeo-shorelines and ancient ports of the Mediterranean

A third case study illustrates the application of geo-archaeological methods to coastal landscapes whose configuration has changed substantially since antiquity. The Mediterranean coast has experienced both eustatic sea-level changes (driven by the global volume of ice) and local tectonic and isostatic movements (driven by regional crustal processes) over the past several thousand years, with the result that many ancient harbours, beaches, and coastal settlements are no longer in the positions they occupied when they were in use. Some are now submerged; others are stranded several kilometers inland; in both cases their reconstruction requires the integration of geo-archaeological evidence with palaeo-environmental modelling and historical documentation.

The well-documented case of the Hellenistic and Roman port of Ephesus, on the Aegean coast of modern Türkiye, illustrates the principal methodological challenges. The ancient harbour, which was the second-largest port of the eastern Mediterranean during the Roman imperial period, is now stranded approximately eight kilometers inland behind a thick alluvial plain built up by the Cayster river. Geo-archaeological coring of the alluvial plain has reconstructed the progressive infilling of the ancient harbour through five distinct sedimentary phases over the past two millennia. The first phase preserves the marine sediments of the open harbour; the second records the progressive accumulation of estuarine deposits as the river delta advanced; the third records the deliberate dredging that the city authorities undertook to maintain the harbour; the fourth records the eventual abandonment of the harbour as dredging became uneconomic; and the fifth records the alluvial fan deposits that buried the ancient shoreline. The integration of these sedimentary records with the historical record of port maintenance documented in inscriptions and chronicles produces a remarkably detailed picture of the interaction between human and natural processes over two millennia.

Comparable studies have been published for the ancient ports of Marseille, Naples, Alexandria, Tyre, and several smaller harbours of the Black Sea. In each case, the methodological core is the same: deep sedimentary cores extracted from the modern coastal plain, integrated with archaeological observations of the present configuration of the harbour and with documentary evidence of its ancient configuration. The resulting reconstructions feed directly into broader discussions of the connectivity of the ancient Mediterranean, the resilience of its maritime infrastructure, and the differential vulnerability of coastal settlements to environmental change — discussions whose relevance to the present is, of course, increasingly acute.

The same approach is now being deployed along the coasts of the Persian Gulf and the southern Caspian, where the combined effects of late-Quaternary sea-level change, active tectonics and human modification of the shoreline make the reconstruction of palaeo-shorelines particularly demanding. The U-series and ESR dating of raised coral-reef terraces on Kish and Qeshm Islands (Preusser et al., 2003; Pirazzoli et al., 2004) has constrained the Holocene-to-late-Pleistocene uplift history of the inner Persian Gulf and is now being integrated with the active-tectonic record of the Zagros deformation front (Fathian et al., 2022, 2026). Along the south-eastern Caspian, the multi-decadal synthesis of Lahijani et al. (2026) documents the cyclical formation and desiccation of coastal lagoons over historical and instrumental time scales, providing a directly comparable Iranian counterpart to the Mediterranean studies summarised above. The integration of these coastal records with the geo-archaeological record of the adjacent inland sites — the Gohar Tappeh proto-historic site on the south-eastern Caspian plain (Bakhtiarizadeh et al., 2018; Nazari et al., 2021) is a particularly clear example — is one of the priorities of the UNESCO Chair on Coastal Geo-Hazard Analysis programme.

11.5 Iranian Bronze Age tells

A fourth case study, particularly relevant to the institutional context of the present report, concerns the geo-archaeology of Bronze Age tells in the Iranian Plateau. Tells — artificial mounds formed by the accumulated debris of successive occupation phases — are the characteristic settlement form of the agricultural societies of the Near East from the Neolithic onward. They preserve in stratified form the entire history of a single locality, and they are therefore of exceptional value for the reconstruction of long-term cultural and environmental change. The Iranian Plateau contains many hundreds of substantial tells, of which only a small fraction has been investigated systematically. The well-known sites of Tepe Sialk, Tepe Hissar, Tepe Yahya, Shahr-e Sukhteh, and Konar Sandal are representative.

The geo-archaeological investigation of an Iranian tell typically combines several of the methods discussed in earlier chapters. A regional remote-sensing survey using CORONA satellite imagery from the 1960s — before the recent expansion of irrigated agriculture obscured many archaeological landscapes — provides the baseline map of the tell and its hinterland. Targeted geophysical survey using gradiometry and electrical resistivity identifies the layout of the buried architecture within the tell. Sedimentological and geochemical analysis of borehole cores reconstructs the depositional sequence of the tell and identifies discrete occupation phases. Pollen and phytolith analysis of selected horizons reconstructs the vegetation of the immediate hinterland during each phase. Dating of charcoal and bone samples produces an absolute chronology of the occupation sequence. The synthesis of these datasets supports a reconstruction of the long-term trajectory of the settlement and of its interaction with the surrounding environment.

The principal published example of this integrated approach is the synthesis of the Tepe Sialk excavations, which combines decades of stratigraphic work with new sedimentological, palynological, and radiocarbon evidence to reconstruct the occupation of the site from the early Neolithic through the late Iron Age. The resulting reconstruction documents repeated cycles of expansion and contraction, the progressive aridification of the surrounding plain, and the eventual abandonment of the site in the late first millennium BCE. Comparable but less complete reconstructions have been published for several of the other major Iranian tells, and the geo-archaeology of the Iranian Plateau remains an active and underexploited area of research.

Two more recent contributions further illustrate the integrated approach. The OSL dating programme on the south ziggurat at Tepe Sialk (Fazeli Nashli et al., 2023) produced refined chronological constraints on the construction and use phases of one of the largest pre-Achaemenid monumental structures of the central Iranian Plateau, and demonstrated that optically stimulated luminescence dating, when carefully applied to mud-brick and adobe contexts, can provide age control where charcoal is unavailable or contaminated. In a different but complementary register, the archaeoseismological investigation of the Gohar Tappeh proto-historic site on the south-eastern Caspian plain (Bakhtiarizadeh et al., 2018; Nazari et al., 2021) used the stratigraphy and damage record of a long-occupied tell as the primary archive for surface-rupture history along the active Khazar Fault. The combined treatment of a tell as both an archaeological and a paleoseismic archive — with the destruction layers, repair-and-rebuild sequences, and offset architectural features read in tandem with the active-fault geology — is

one of the methodologically distinctive contributions of the recent Iranian geo-archaeology to the international literature.

11.6 Synthetic remarks

The case studies presented in Sections 11.1 through 11.5 illustrate the application of geo-archaeological methods at scales ranging from individual sites to entire regions and at chronological depths ranging from the present back to the Pleistocene. They share several common features. First, in each case the productive insight has come from the integration of multiple independent lines of evidence rather than from any single technical innovation. Second, in each case the published results have built incrementally on earlier work by other researchers, with new techniques producing refinements of older interpretations rather than wholesale replacements. Third, in each case the methodological agenda for the next decade is reasonably clear, and the principal obstacles to further progress are the practical ones of funding, infrastructure, and long-term curatorial commitment.

Chapter 12 - Ethics, Heritage and Future Directions

The preceding eleven chapters have surveyed the principal methods of contemporary geo-archaeology and have illustrated their application through selected case studies. The present chapter steps back from the technical content to consider the ethical, professional and disciplinary frameworks within which those methods are deployed, and to project where the discipline is most likely to move during the next decade. Geo-archaeology, like every other archaeological subfield, operates within a complex web of obligations — to the material record itself, to the communities whose past is being investigated, to the public that supports the research financially, and to the future researchers who will inherit the datasets currently being produced. A technically competent practice that ignored these obligations would not, in the modern sense of the term, be a responsible practice.

Figure 12.1 · Six principles framing ethical practice in contemporary geo-archaeology, organised around the central commitment to the long-term stewardship of the material and digital archaeological record.

12.1 Stewardship of the material record

The first ethical commitment of any archaeological practice is the stewardship of the material record itself. Archaeological sites and the deposits they contain are finite, non-renewable resources: once excavated, they cannot be excavated again, and the act of excavation is irreversibly destructive. The geo-archaeologist therefore bears a particular responsibility for the documentation of contexts that are about to be destroyed, for the curation of the samples and records that result from that documentation, and for the long-term accessibility of those samples and records to future researchers.

In practical terms, stewardship requires the maintenance of physical archives (sediment samples, dating samples, artefacts and ecofacts) in conditions that preserve them indefinitely, and the maintenance of digital archives (photographs, plans, point clouds, GIS projects, laboratory results) in formats and on infrastructures that remain readable as software evolves. Both requirements are easier to state than to implement. The infrastructure of physical archives in most countries is under chronic financial pressure, and the rapid evolution of digital formats places digital archives at continuous risk of obsolescence. The recent emergence of FAIR data principles — findable, accessible, interoperable, reusable — provides a useful framework for

digital curation, but its successful implementation requires sustained institutional commitment and, in most cases, dedicated funding lines that do not yet exist in the typical archaeological project budget.

12.2 Community engagement and descendant rights

The second ethical commitment is engagement with the communities whose past is being investigated. The relationship between archaeologists and descendant communities has evolved substantially over the past several decades. The earlier model of archaeology as an extractive enterprise — in which trained outsiders conducted excavations, removed materials to distant institutions, and published interpretations in academic journals that the source communities never read — has been replaced, at least in principle, by a model of collaborative engagement in which descendant communities participate in the design, conduct and publication of archaeological research.

Geo-archaeology poses some distinctive challenges to this collaborative model because of the technical specialization of its methods. A community member may have an immediate intuition for the meaning of a recovered artefact but is unlikely to have an immediate intuition for the significance of an XRF spectrum or a CNN probability map. The responsibility of the geo-archaeologist is therefore not only to invite engagement but to engage in the patient and often time-consuming work of communicating technical results in terms that are accessible to non-specialists. The published literature contains several models of successful long-term engagement of this kind, particularly in indigenous contexts in the Americas, Australia, and the Arctic, and these models repay careful study by practitioners working in any culturally sensitive landscape.

A particular set of obligations attaches to the treatment of human remains. The geo-archaeologist may be involved in the dating of skeletal material (Chapter 4), in the isotopic analysis of bone for palaeodietary or palaeomobility reconstruction (Chapter 5), or in the sedimentological analysis of mortuary contexts (Chapter 2). In all of these cases, the obligations to the descendant communities of the individuals being studied take precedence over the strictly methodological considerations. The principle of free, prior and informed consent, formalized in several international instruments and adopted by most national professional societies, is the practical anchor for these obligations. Where descendant communities have expressed objections to particular analytical procedures, those objections are not negotiable on technical grounds.

12.3 Site protection and the disclosure of locations

The third ethical commitment is the protection of sites from harm caused by their disclosure. Archaeological sites are vulnerable to looting, to opportunistic damage by infrastructure projects, and to incidental damage by tourism. The publication of precise location data, particularly for sites of high commercial value (gold-bearing burials, intact ceramics, well-preserved stelae) can directly increase the risk of looting. This is not a theoretical concern: documented cases now exist in which the publication of survey reports has been followed by waves of organised looting in the surveyed area, with measurable losses to the material record.

The remote-sensing and machine-learning methods discussed in Chapters 6, 7 and 9 amplify this concern because they make it possible to produce large inventories of previously unknown sites in a short time. An unsupervised release of such an inventory in an open data format would constitute a direct contribution to the looting risk. The community has gradually adopted a set of protective practices: precise coordinates are redacted from published outputs; detection results are registered with the appropriate cultural-heritage authorities before any release; differential vulnerability of sites in regions with limited enforcement capacity is taken into account in publication decisions; and access to high-resolution training data is restricted to vetted research collaborations. These practices add overhead to the publication process but are now generally accepted as the minimum standard of responsible practice.

12.4 Open science and responsible AI

The fourth ethical commitment is to the transparency and reproducibility of the research process. The methods surveyed in this report depend in many cases on substantial software infrastructure and on training datasets whose composition affects the conclusions. The reproducibility of the results, by colleagues or by the original authors at a later date, requires the publication not only of the conclusions but of the data, the code, and the parameters that produced them. The general framework of open science addresses this requirement at the level of the publication record; the specific issues raised by machine-learning models — the curation of training data, the documentation of model architectures, the release of trained model weights, the disclosure of computational provenance — are still under active discussion in the broader scientific community and require ongoing attention in geo-archaeological practice.

The methodological concerns surveyed in Section 9.5 — geographical bias, model explainability, and the differential vulnerability of culturally sensitive landscapes — are inseparable from the broader ethical commitments outlined here. A responsible deployment of machine learning in

geo-archaeology must therefore include explicit attention to the composition and provenance of its training data, to the interpretability of its decisions, to the differential consequences of its predictions across different cultural and geographical contexts, and to the accountability structures that govern its use. These are not optional refinements: they are conditions on the legitimacy of the research itself, and the community has begun to address them through revised peer-review standards, registered-report formats for AI-driven studies, and the development of community-curated benchmark datasets that represent a wider geographical and cultural range than the early literature.

A second, related dimension of responsible AI concerns the disclosure of AI use in authored scholarly work. The same large-language-model and generative tools that are now being deployed for the analysis of imagery are also being used — routinely and on a substantial scale — in the drafting, structuring and editorial preparation of scientific manuscripts and monographs. The emerging norm, increasingly codified in publisher guidelines and in research-integrity policies, is that the use of artificial intelligence as a writing or editorial aid should be disclosed openly, that the scientific judgements and the responsibility for the content must remain with the human author, and that AI tools should not be listed as co-authors. The present book follows this norm: the methodology note in the Abstract and in Section 1.4 discloses the use of artificial intelligence as a drafting, structuring and editorial aid, while making explicit that all scientific judgements, the selection of case studies, the interpretation of the cited literature, and the final formulations of every section remain those of the author. This open declaration is itself an instance of the responsible-AI practice that this section advocates.

12.5 Future directions

A speculation about the future of a rapidly evolving discipline is necessarily provisional, but several trends are sufficiently well established to merit explicit mention. The first is the continued integration of multi-sensor remote sensing. The combination of LiDAR, hyperspectral imagery, synthetic-aperture radar, and UAV photogrammetry into a single fused dataset is already standard in the most advanced research programmes; the principal remaining challenge is the development of analytical workflows that exploit the full information content of these fused datasets rather than reducing them to their lowest common denominator. The next decade will likely see the emergence of multi-modal foundation models — large neural networks pre-trained on diverse sensor data and fine-tuned to specific archaeological tasks — that genuinely exploit this integrated information.

The second trend is the increased use of low-cost, autonomous sensor networks. The historical model of archaeological data collection — a single field season followed by a multi-year laboratory and publication cycle — is being supplemented by continuous monitoring programmes in which networks of inexpensive sensors record environmental conditions at archaeological sites over years or decades. The data streams from these networks are most directly useful for the management of vulnerable sites in changing climates, but they are also opening new analytical possibilities for the study of long-term human-environment interactions.

The third trend is the convergence of geo-archaeology with palaeogenomics and palaeoproteomics. The rapid expansion of ancient DNA and protein analysis over the past decade has produced reconstructions of past populations, diets, and pathogen exposures at a resolution that was not previously available. The integration of these biomolecular records with the geo-archaeological reconstruction of past environments and depositional contexts is one of the most productive interdisciplinary frontiers of the current decade and is likely to remain so.

The fourth trend is the increasing involvement of the public in geo-archaeological research. The community-science model that has proved successful in astronomy, ornithology, and other observational sciences is gradually being adapted to archaeology, with citizen volunteers contributing to the annotation of remote-sensing imagery, the monitoring of vulnerable sites, and the digitization of historical records. The technical infrastructure for community participation has matured rapidly, and the principal remaining challenges are the design of meaningful tasks and the maintenance of long-term volunteer engagement.

Taken together, these trends suggest a geo-archaeology that will be more integrative, more continuous, more biomolecular and more participatory than the discipline as it stands today. They do not suggest a geo-archaeology that will be more automated in any reductive sense: the role of the trained interpreter, of the contextually informed analyst, and of the locally engaged collaborator will remain central. The methods will change, sometimes rapidly; the methodological responsibilities will not.

12.6 Climate change and threatened sites

A specific application of the broader ethical commitments of the discipline concerns the response of geo-archaeology to climate change. The archaeological record is at risk from climate change in several distinct ways, and the methodological response of the discipline is still being worked out. The principal risks fall into four broad categories. Coastal sites are at risk from rising sea levels

and from increased storm activity, which are accelerating the erosion of vulnerable shorelines and submerging the archaeological deposits of many coastal regions. Arctic and high-altitude sites are at risk from permafrost thaw, which is exposing organic remains that have been protected by freezing for millennia and that decompose rapidly once exposed to oxic conditions. Arid-zone sites are at risk from changing precipitation patterns, which are altering the moisture regime of preserved organic materials and accelerating the decomposition of textiles, basketry, and other moisture-sensitive remains. Sites in regions of changing fire regime are at risk from wildfires whose frequency and intensity are increasing, with documented losses across western North America, southern Europe, and Australia over the past decade.

The methodological response to these threats has several components. The first is the systematic monitoring of vulnerable sites through repeated remote-sensing observation, integrated with on-the-ground documentation where resources permit. The second is the development of triage frameworks for the allocation of limited investigative and protective resources to the most vulnerable sites. The third is the rapid documentation, through the methods discussed in earlier chapters, of sites whose survival is judged to be unlikely. The fourth is the integration of climate-driven archaeological loss into the broader political case for emissions reduction, on the grounds that the irreversible destruction of cultural heritage is one of the most concrete manifestations of climate-change impact on human societies. None of these components is methodologically complete, and the geo-archaeological literature on climate-threatened sites has expanded substantially over the past five years as the underlying problem has become more acute.

12.7 Decolonization and the future of the discipline

A further dimension of contemporary geo-archaeological practice that deserves explicit mention is the broader project of decolonization of the archaeological disciplines. The historical roots of much modern archaeology in the colonial enterprises of the nineteenth and early twentieth centuries are well documented, and they have left enduring traces in the institutional structures, the publication conventions, and the conceptual vocabulary of the discipline. The decolonisation project, which has accelerated substantially over the past decade, seeks to identify these traces, to acknowledge their consequences, and to develop alternative practices that do not perpetuate the asymmetries of the colonial relationship.

The implications for geo-archaeology are several. The methodological agenda has historically been set by researchers based in the global North, with the result that the published literature is heavily biased toward the landscapes and material cultures of Europe and North America and

that the analytical infrastructure (radiocarbon laboratories, OSL laboratories, isotopic facilities) is heavily concentrated in those regions. The redistribution of analytical capacity to regions where the relevant material is located is a substantive priority for the next decade, and several international programmes are now actively supporting the development of regional laboratory networks in the Middle East, South America, Africa, and South-East Asia. The publication record itself is gradually shifting in the same direction, with regional journals and open-access platforms supporting researchers who have historically faced barriers to publication in the established international literature.

These developments are not, in any meaningful sense, departures from the technical content surveyed in earlier chapters of this report. They are, instead, the institutional and ethical conditions under which that technical content is most productively deployed. A discipline that takes both its technical methods and its institutional ethics seriously is in a stronger position to make sustained contributions to human knowledge than one that takes only one of them seriously. The next decade of geo-archaeology will, with any luck, be a period in which both have continued to develop in parallel.

Chapter 13 - Paleoseismology and Archaeoseismology

The Iranian Plateau is one of the most seismically active continental regions on Earth, lying within the broad zone of convergence between the Arabian and Eurasian plates that extends from the Caucasus through Anatolia, Iran and the Hindu Kush (Vernant et al., 2004; Allen et al., 2004). The accumulated record of historical earthquakes in this region, spanning approximately two and a half millennia and preserved partly in chronicles, partly in inscriptions and partly in the physical fabric of long-occupied cities, is among the longest and most detailed in the world (Ambraseys & Melville, 1982; Berberian, 2014). The investigation of that record through the combined methods of paleoseismology — the geological identification of pre-historical earthquakes — and archaeoseismology — the recognition of earthquake damage in archaeological deposits and standing monuments — has become one of the principal contributions of Iranian Earth science to the international literature of the discipline. A substantial part of the present synthesis draws on the integrated paleoseismic, morphotectonic and archaeoseismic programmes pursued over the past two decades along the major fault systems of the Alborz, the Zagros and the Iranian interior (Ritz et al., 2006, 2012; Nazari et al., 2009, 2010, 2014, 2021; Hollingsworth et al., 2010; Foroutan et al., 2012, 2014; Rizza et al., 2011, 2013; Faridi et al., 2017, 2019, 2023; Kamali et al., 2023; Fathian et al., 2021, 2026), and on the Persian translations of the standard methodological

references (Nazari, 2017; Nazari & Ghorashi, 2021) which have made the discipline accessible to a substantially wider Iranian readership. The present chapter introduces the methods of paleoseismology and archaeoseismology, surveys the principal active fault systems of the Iranian Plateau, and reviews the major regional case studies in which these methods have been deployed.

13.1 Definitions and methodological foundations

Paleoseismology is the branch of seismology that investigates earthquakes that occurred before the establishment of modern instrumental recording. Its central methodological insight, developed in the 1970s by researchers including Kerry Sieh on the San Andreas Fault in California, is that surface-rupturing earthquakes leave a distinctive stratigraphic signature in the Quaternary deposits that bury and overlie the rupturing fault plane. By excavating a trench across an active fault and reading the offsets, the colluvial wedges and the disrupted layers exposed in the trench walls, a competent investigator can identify the individual earthquakes that have ruptured the fault during the past several thousand years and, with appropriate dating, can place each event in absolute time. The resulting earthquake history is the foundation on which long-term seismic hazard assessments are built.

Archaeoseismology, by contrast, infers past earthquakes from their effects on the human-built environment. Standing walls, paved floors, vaulted ceilings, decorative columns, water-supply systems and burial monuments are all sensitive to seismic shaking and may preserve a record of past earthquakes that is independent of, and complementary to, the geological record from trenches. The interpretive challenges of archaeoseismology are substantial: damage caused by earthquakes must be distinguished from damage caused by warfare, by gradual structural decay, by deliberate demolition and by the routine pillaging of stone for re-use. The mature practice of archaeoseismology depends therefore on a careful catalogue of diagnostic indicators, on the joint interpretation of archaeological and geological evidence, and on cross-validation against any available historical documentation.

The integration of paleoseismology, archaeoseismology and historical seismology in a single research programme is a relatively recent development. The model proposed by Berberian for the Iranian Plateau, in which the historical earthquake catalogue is used to date individual ruptures identified in trenches and to constrain the seismogenic behaviour of named faults, has been particularly influential and is the methodological foundation on which much of the contemporary Iranian work in the field rests.

13.2 Trenching and the identification of paleoearthquakes

The principal field method of paleoseismology is the excavation of a trench across an active fault, oriented perpendicular to the surface trace and extending to a depth sufficient to expose the late Quaternary stratigraphy in both the hanging-wall and the footwall blocks. The trench walls are cleaned, photographed, and logged in detail at decimeter resolution; every distinguishable stratigraphic unit is assigned a number and described in terms of its sedimentology, its pedogenic features, its content of organic material suitable for dating, and its geometric relationships to the fault plane and to the neighbouring units. The resulting trench log is the primary document from which the earthquake history is reconstructed.

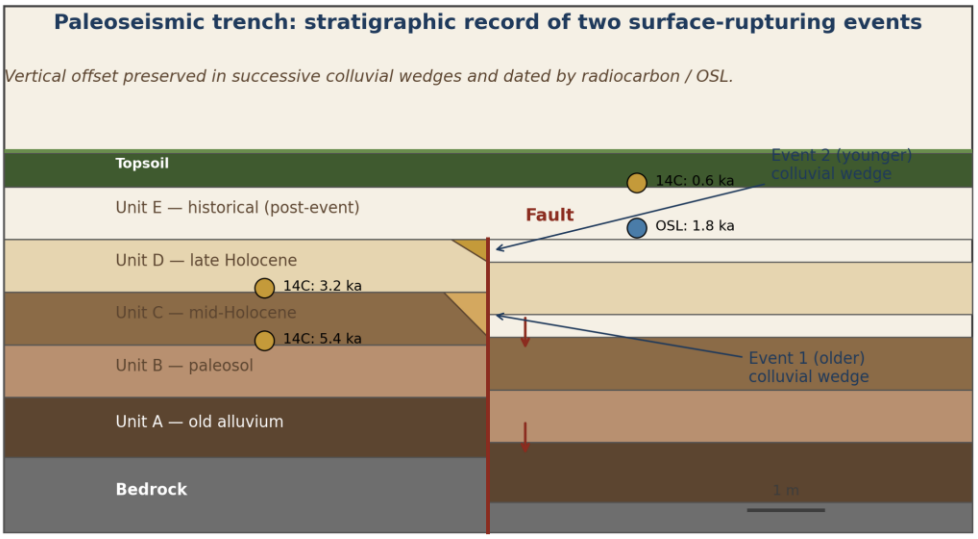

Figure 13.1 · Schematic cross-section of a paleoseismic trench. Successive stratigraphic units are offset by the fault to different degrees, indicating multiple rupturing events; the colluvial wedges at the base of the free face and the dating samples (^{14}C and OSL) together constrain the timing of each event.

Three principal lines of evidence support the identification of individual paleoearthquakes in a trench. The first is the differential offset of stratigraphic units: an older unit is offset by the cumulative slip of every earthquake that has occurred since its deposition, while a younger unit is offset only by the events that have occurred since the unit itself was laid down. The difference in offset between an older and a younger unit therefore records the slip of the events that occurred between them. The second line of evidence is the colluvial wedge: when a surface-rupturing earthquake produces a free face at the fault, the over-steepened slope above the rupture rapidly collapses, producing a wedge-shaped deposit of poorly sorted material against

the fault scarp. Successive colluvial wedges, stratigraphically distinguishable, record successive earthquakes. The third line of evidence is the upward termination of the fault plane against a buried surface, indicating that the fault did not rupture through the unit overlying that surface and therefore constraining the upper bound on the age of the most recent event.

The dating of paleoearthquakes proceeds through the methods discussed in Chapter 4. Charcoal samples within the offset stratigraphy are dated by radiocarbon and provide a chronological anchor for the units they belong to. Sand and silt units suitable for optically stimulated luminescence dating are sampled with light-tight tubes and yield depositional ages with characteristic uncertainties of approximately ten per cent. Tephra layers, where present, provide isochronous markers that can sometimes be correlated to known regional eruptions. The Bayesian framework of OxCal and similar software combines all of these constraints with the stratigraphic ordering imposed by the trench geometry to produce posterior distributions of the timing of each individual event.

13.3 Archaeological markers of past earthquakes

The archaeological record provides a distinctive and complementary set of indicators of past seismicity. The most direct of these are physical damage features in the standing fabric of historical monuments: the collapse of vaults and arches, the toppling of columns in a preferential direction, the rotation of capitals on their bases, the spalling of corner stones, the systematic cracking of walls along characteristic diagonal patterns, and the kinematic offset of paved surfaces. These features are routinely diagnostic when several of them occur together and when the spatial pattern of damage is consistent with the radiation pattern expected from a nearby earthquake source. Single features, in isolation, are often ambiguous and may equally be the product of structural decay, of warfare, or of subsequent reconstruction.

More indirect markers include the chronological discontinuities in the occupation sequence of long-occupied sites. The abandonment of urban quarters, the construction of major rebuilding episodes, the introduction of seismic-resistant architectural features, and the appearance of repair-and-recovery patterns in the stratigraphic record are all suggestive of a seismic crisis. None of these markers is uniquely diagnostic, and each requires careful evaluation against alternative causes. The integration of archaeoseismic indicators with the historical record of attested earthquakes is therefore essential. When the chronological and spatial pattern of archaeological damage matches an event documented in the historical sources, the joint identification is robust;

when no such documentary support exists, the archaeoseismic identification remains a working hypothesis.

Table 13.1 · Principal archaeological markers of past earthquakes and their diagnostic value

Indicator class	Typical observation	Diagnostic value
Preferential collapse	Columns toppled in a consistent direction	High when pattern is regional
Rotated masonry	Capitals or stones rotated on their seating	High
Diagonal wall cracks	Symmetric X-pattern in standing walls	Moderate to high
Offset paving	Step or shift across a previously continuous surface	High
Sealed collapse layer	Thick destruction stratum over occupation surface	Moderate
Sudden site abandonment	Sealed in-place artefact assemblage	Moderate; needs corroboration
Repair-and-rebuild seq.	Anomalous reconstruction phase	Moderate; needs corroboration
Seismic-resistant architecture	Wooden tie beams, base isolation	Indirect evidence of awareness

Table 13.1 · Principal archaeological markers of past earthquakes and their diagnostic value, summarizing the framework systematized by Stiros, Galadini, Sintubin and others.

13.4 The Iranian Plateau as a seismotectonic laboratory

The Iranian Plateau provides an unusually favourable setting for the integration of paleoseismic, archaeoseismic and historical methods. Three factors account for this. The first is the sustained tectonic activity of the region: the Arabia–Eurasia convergence rate of approximately 22 mm/yr at the Strait of Hormuz is absorbed by a network of active faults distributed across the Zagros, the Iranian interior and the Alborz, which produce a high rate of moderate and large earthquakes. The second is the antiquity of urban occupation: Iranian cities such as Tabriz, Rey (now part of Tehran), Esfahan, Shiraz and Mashhad have continuous occupation histories of one to two and a half millennia, during which any seismic crisis has left some trace in the documentary or archaeological record. The third is the existence of a substantial corpus of Persian and Arabic chronicles, geographical treatises, biographical dictionaries and administrative records that

document earthquakes from late antiquity onward, providing a chronological backbone unequalled in most of the seismically active world.

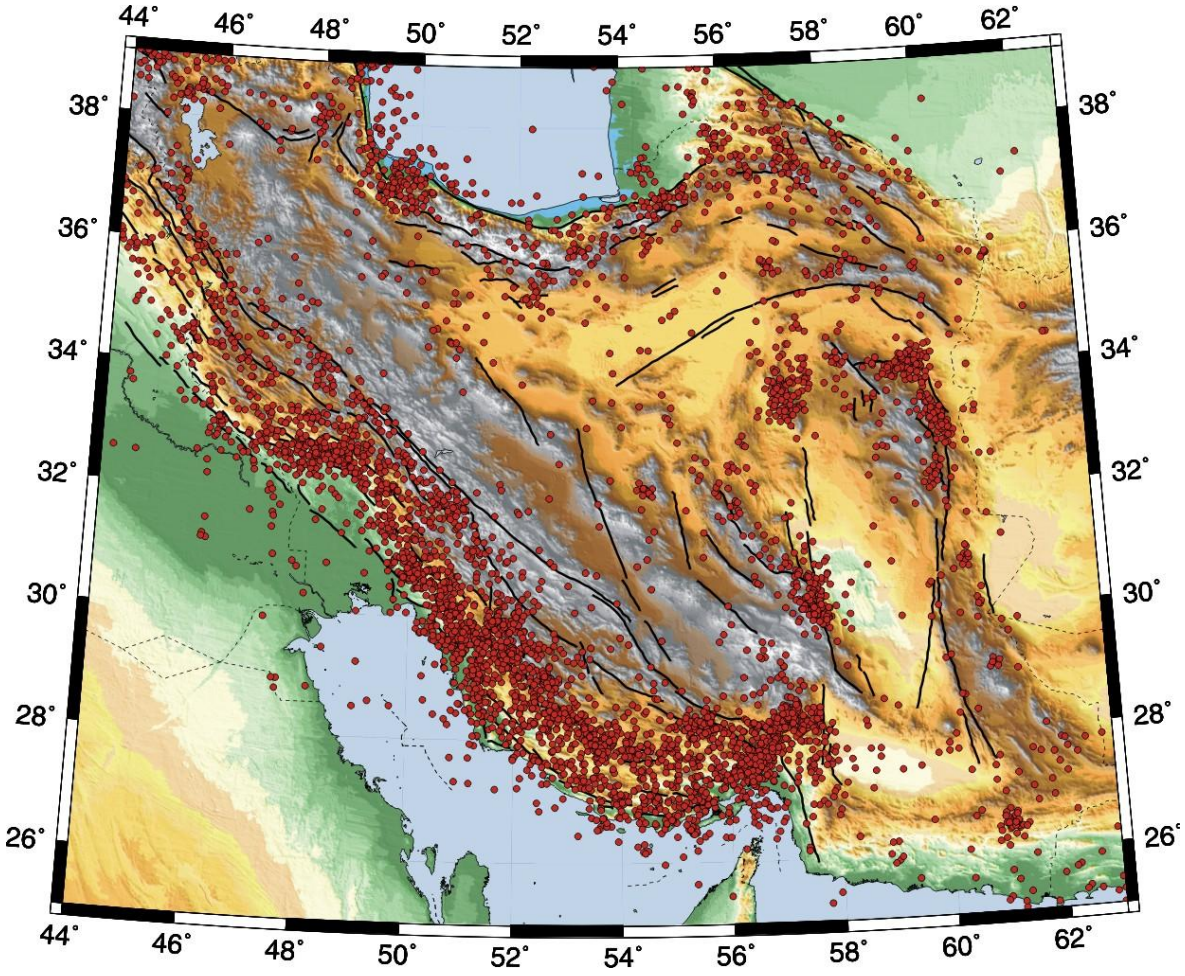

Figure 13.2 · A simplified map of the major active faults in Iran, overlaid on an SRTM DEM. Red circles represent instrumentally recorded earthquakes with a magnitude larger than 5.

The principal active fault systems of the Iranian Plateau fall into three broad groups. The Zagros fold-and-thrust belt, in the south-west, accommodates the bulk of the convergence between Arabia and central Iran through a system of blind thrust faults and large-scale folding (Berberian, 1995; Talebian & Jackson, 2004); major historical earthquakes here include the destructive events of Silakhor (1909), Firuzabad–Kojur and the Hamadan series, with the 2017 Sarpol-e Zahab event and the recent investigation of the south-western edge of the Fars Arc (Fathian et al., 2026) adding important new constraints on the kinematics of this segment. The Alborz mountain belt, north of Tehran, accommodates partitioned convergence and dextral strike-slip through a network of named faults including the North Tehran Fault (Ritz et al., 2012), the Mosha Fault (Ritz et al., 2006), the Khazar Fault (Nazari et al., 2021), the Taleghan Fault (Nazari et al., 2009), the

Firouzkuh Fault (Nazari et al., 2014) and the Astaneh Fault (Hollingsworth et al., 2010; Rizza et al., 2011); the Alborz has produced the catastrophic earthquakes of 856 CE (Qumis), 1177 (Rey), 1665 (Damghan), and the Rudbar–Manjil event of 1990. The interior of the Iranian Plateau, between the Zagros and the Alborz, is traversed by major strike-slip faults including the Doruneh Fault in the north-east (Solaymani Azad et al., 2015), the Main Recent Fault east of the Zagros, the Nayband and Anar faults in the central Plateau (Foroutan et al., 2012, 2014), and the Sabzevaran–Gowk–Nayband system in the south-east that ruptured during the Bam earthquake of 2003 (Talebian et al., 2004; Jackson et al., 2006).

13.5 Case studies: paleoseismology and archaeoseismology in Iran

13.5.1 The Mosha Fault and the seismic history of the Tehran region

The Mosha Fault, a 200-km-long oblique-slip structure that runs along the southern flank of the Central Alborz immediately north of Tehran, is one of the most thoroughly investigated faults in the Iranian seismotectonic literature. Its proximity to the modern capital — with a metropolitan population approaching ten million — makes the quantification of its seismogenic behaviour a matter of considerable practical importance. The combined paleoseismic and morphotectonic programme led by Ritz, Nazari and colleagues over the past two decades (Ritz et al., 2006; Ritz et al., 2012; Nazari et al., 2009; Nazari et al., 2010) has identified surface-rupturing earthquakes recorded along the Mosha, North Tehran, Taleghan and Astaneh faults during the past several millennia. The most recent ruptures of the North Tehran and Taleghan faults are constrained to the historical period and tentatively correlated with the destructive earthquakes documented in early Islamic chronicles, in particular the 958 CE Taleghan event and the 1177 CE Rey earthquake. The associated horizontal slip rates — on the order of two to three millimetres per year for the Mosha–North Tehran system and of approximately two millimetres per year for the Astaneh fault (Hollingsworth et al., 2010; Rizza et al., 2011) — place these faults among the most active structures of the Alborz and imply a substantial contribution to the seismic hazard of the Tehran region.

Complementary work on the Astaneh fault (Hollingsworth et al., 2010; Rizza et al., 2011) and on the Firouzkuh fault further east (Nazari et al., 2014) has produced a regional picture in which the eastern Alborz is segmented into several seismogenic units, each capable of producing $M \geq 7$ earthquakes at intervals of one to several thousand years. The Astaneh fault, in particular, is now understood to have ruptured during the great 856 CE Qumis earthquake, one of the most destructive events recorded in the Iranian historical catalogue (Hollingsworth et al., 2010). The

integration of this paleoseismic record with the historical earthquake catalogue of the Tehran region — which includes the destructive events of 958, 1177, 1665 and 1830, alongside many smaller events — has supported a substantial revision of the seismic-hazard maps used by Iranian building-code authorities (see also Nazari & Ghorashi, 2021, for the translated reference text on paleoseismic method).

13.5.2 The North Tabriz Fault and the recurrent destruction of Tabriz

The North Tabriz Fault is a 150-km-long dextral strike-slip structure that passes immediately north of the historic city of Tabriz in northwestern Iran. The city has been destroyed by major earthquakes on at least four occasions during the past millennium: 858, 1042, 1721 and 1780 CE. The historical record of these destructions, preserved in Persian and Arabic chronicles, is unusually detailed and includes descriptions of the patterns of damage, of casualty figures, and of the rebuilding efforts that followed. Paleoseismic trenching of the North Tabriz Fault by Hessami et al. (2003), the morphotectonic and geodetic work of Rizza et al. (2013), the regional fault-pattern analysis of Faridi et al. (2017, 2019) on the adjacent Qoshadagh structure, and the recent neotectonic synthesis of Faridi et al. (2023) has identified surface ruptures correlated with the events of 1042 and 1721, with characteristic single-event displacements of three to four metres consistent with the M ≈ 7.4 magnitudes inferred from the historical descriptions. The combined paleoseismic and historical record indicates a recurrence interval of approximately 250 to 400 years for major events on this fault, with the time elapsed since the most recent rupture (1780) approaching the lower bound of the expected interval.

13.5.3 The 2003 Bam earthquake and the citadel of Arg-e Bam

The Bam earthquake of 26 December 2003, a Mw 6.6 event on a previously unmapped strand of the Bam Fault in southeastern Iran, killed approximately 26,000 people and destroyed the substantial Sasanian-to-Islamic adobe citadel of Arg-e Bam, one of the largest mud-brick complexes in the world (Talebian et al., 2004; Jackson et al., 2006; Fielding et al., 2005). The earthquake provided an unusually well-documented instance of the rapid destruction of a major historical monument by a moderate-magnitude event, and the subsequent reconstruction of the citadel by the Iranian Cultural Heritage Organization has been accompanied by extensive archaeoseismic study of the collapse pattern. The combined InSAR, field-mapping and aftershock-relocation work (Talebian et al., 2004; Fielding et al., 2005; Jackson et al., 2006) has documented the systematic preferential collapse of the citadel walls in directions consistent with the inferred radiation pattern of the earthquake source, has identified evidence for earlier

seismic damage in the lower stratigraphic units of the citadel, and has informed the development of modern conservation practices for adobe heritage in seismically active regions.

13.5.4 Persepolis and Tepe Sialk: earthquakes in the deep history of Iran

The application of archaeoseismic methods to the principal Achaemenid monumental site of Persepolis, founded by Darius I at the end of the sixth century BCE, has produced suggestive but not yet conclusive evidence for at least one major seismic event during the long period between the abandonment of the site in late antiquity and its modern excavation. The preferential collapse of standing columns toward the southeast, the systematic toppling of capitals in a consistent direction, and the damage patterns in the surrounding palace complexes have been interpreted by Berberian and others as indicators of strong ground motion from a nearby source. The specific source is debated; the Kazerun Fault, the Main Recent Fault and several smaller structures of the central Zagros are all plausible candidates. The chronological constraint on the inferred event is poor and would benefit from further dating work on the destruction stratigraphy.

At Tepe Sialk, near Kashan in central Iran, the long Neolithic to Iron Age occupation sequence preserves several discontinuities in the form of thick destruction layers separating successive habitation phases. The interpretation of these layers as seismic in origin has been proposed by several authors on the basis of their thickness, their spatial extent across the site, and the pattern of repair-and-rebuild that follows them. As with Persepolis, the evidence is suggestive rather than conclusive, and the principal contribution of these case studies to date has been the identification of well-preserved sequences in which more focused future work may successfully resolve the seismic component of the depositional history.

13.6 Integration with the historical earthquake record

The Iranian historical earthquake catalogue, compiled and revised over several decades (Ambraseys & Melville, 1982; Berberian & Yeats, 1999, 2001; Berberian, 2014), contains approximately 1,500 events from the early historical period to the present, with reasonably reliable parametric data for events from the eighth century onward. The catalogue draws on a wide range of sources: Persian chronicles such as the Tarikh-e Tabari and the Tarikh-e Bayhaqi; Arabic geographical and historical works including those of al-Tabari, al-Mas’udi and al-Mustawfi; later European travelers' accounts; and the systematic seismological observations of the past century. The integration of this catalogue with the paleoseismic record (Hollingsworth et al., 2010

for the 856 CE Qumis event on the Astaneh fault; Ritz et al., 2012 for the North Tehran fault; Nazari et al., 2014 for the Firouzkuh fault; Foroutan et al., 2014 for the Nayband fault; Kamali et al., 2023 for the Doroud fault) has produced a multi-millennial earthquake history for the principal Iranian fault systems that is, in several respects, the most detailed available for any seismically active region of the world.

The contemporary research agenda in Iranian paleoseismology and archaeoseismology may be summarized under three broad headings. The first is the systematic trenching of the major faults of the Zagros, the central Iranian interior and the Alborz, with the aim of producing complete earthquake histories for each major segment back at least to the late Pleistocene. The second is the systematic archaeoseismic study of the principal historical cities of Iran — Tabriz, Tehran/Rey, Qazvin, Esfahan, Shiraz, Yazd, Kashan, Bam and others — using the standing fabric and the excavated stratigraphy as evidence for past events. The third is the integration of these field datasets with regional GPS observations, with InSAR-derived interseismic strain maps, and with modern instrumental seismicity to produce a coherent seismotectonic model of the Iranian Plateau as a whole. The model, when complete, will provide the scientific foundation for the seismic-hazard assessment that the Iranian population — concentrated in cities of high vulnerability located on or near major active faults — urgently requires.

13.7 GPS, InSAR and the modern instrumental record

The reconstruction of past earthquakes from geological and archaeological evidence is complemented, at the shortest time scales, by the direct instrumental observation of present-day crustal deformation. The Iranian Plateau has been the subject of a substantial GPS observation programme since the late 1990s, conducted jointly by Iranian institutions including the National Cartographic Centre, the International Institute of Earthquake Engineering and Seismology, the Geological Survey of Iran, and a number of European partners. The cumulative result, summarised by Vernant et al. (2004) and refined in numerous subsequent studies, is a velocity field for the Iranian Plateau that documents approximately 22 mm/yr of north–south Arabia–Eurasia convergence at the Strait of Hormuz, decreasing northward as it is absorbed by deformation along the Zagros, the central Iranian blocks, and the Alborz–Kopet Dagh.

The interferometric synthetic-aperture radar (InSAR) method, introduced to Iranian seismology in the early 2000s and now applied systematically to every $M \geq 5.5$ earthquake in the region, provides a second instrumental data stream. InSAR measures the line-of-sight displacement of the ground surface between two satellite acquisitions with millimetric precision, and the

resulting interferograms can be inverted to constrain the geometry and the slip distribution of the rupture that caused the displacement. The application of InSAR to recent Iranian earthquakes — the 2003 Bam event (Talebian et al., 2004; Fielding et al., 2005; Jackson et al., 2006), the 2010–2011 South Rigan (Baluchestan) sequence (Walker et al., 2013), the 2012 Ahar earthquakes (Copley et al., 2013), and the 2017–2018 Sarpol-e Zahab seismic sequence (Fathian et al., 2021) — has, in each case, identified the precise location of the rupturing fault, often a previously unmapped structure, and has constrained its kinematic behaviour with a resolution that ground-based surveys cannot match. The integration of GPS-derived strain accumulation, InSAR-constrained coseismic rupture, and paleoseismically dated rupture history provides the most complete picture of seismogenic behaviour that is currently available for any active fault.

13.8 The 1990 Rudbar–Manjil earthquake

The Rudbar-Manjil earthquake of 20 June 1990, a Mw 7.4 event in the western Alborz, killed approximately 40,000 people and is the most destructive Iranian earthquake of the twentieth century. The event ruptured a previously unmapped left-lateral strike-slip fault that has subsequently been named the Rudbar Fault, and produced a 60-kilometre surface rupture with maximum left-lateral displacements of approximately three metres. The geographical extent of damage was substantial: the towns of Rudbar, Manjil and Lushan were almost entirely destroyed, and damage extended to the cities of Rasht and Qazvin and to numerous villages of the surrounding mountains. The dam at Manjil, built across the Sefid Rud, was severely damaged but did not fail; its emergency response and subsequent reinforcement have become a textbook example of dam-engineering response to a near-source large earthquake.

The post-event field response to the Rudbar–Manjil earthquake produced one of the most thoroughly documented surface ruptures in the Iranian seismotectonic literature. The integrative synthesis of Berberian (2014), drawing on two decades of post-event fieldwork by Iranian and international teams, has reconstructed the rupture geometry, the slip distribution, the aftershock pattern, and the broader seismotectonic context of the event in unusual detail. The earthquake itself was preceded by a foreshock sequence that began approximately three weeks earlier and that was, in retrospect, recognizable as anomalous; the question of whether prospective recognition of foreshocks could be operationally useful for earthquake forecasting in the Iranian context remains a subject of active research.

Subsequent paleoseismic trenching of the Rudbar Fault has identified evidence for at least two earlier surface ruptures during the late Holocene, with characteristic recurrence intervals of one

to two thousand years. The implication that the 1990 event was the first major rupture of the Rudbar Fault for at least a millennium is consistent with the absence of any clear historical record of comparable destruction in this part of the Alborz, although the early historical record for this specific area is unusually sparse.

13.9 The 2017 Sarpol-e Zahab earthquake and the Zagros seismotectonic framework

The Sarpol-e Zahab earthquake of 12 November 2017, a Mw 7.3 event in the north-western Zagros, killed approximately 630 people and destroyed extensive sectors of the eponymous town as well as numerous nearby villages on both sides of the Iran–Iraq border. The earthquake ruptured a previously unmapped blind thrust fault associated with the active deformation of the High Zagros, and the subsequent InSAR and aftershock analyses — in particular the detailed treatment of the 2017–2018 seismic sequence by Fathian et al. (2021), which combined InSAR observations, aftershock relocation and seismic inversion — have substantially refined the seismotectonic model of this segment of the mountain belt. The kinematic behaviour of the rupture — an oblique thrust with a substantial right-lateral component — and the spatial offset between the surface trace of the previously mapped Mountain Front Fault and the actual rupture plane have important implications for the seismic hazard assessment of the Zagros foothills more broadly. The companion study of Fathian et al. (2026), which extends the active-tectonic record into the offshore Persian Gulf, demonstrates that the Zagros deformation front continues into the marine domain and that the seismotectonic framework of the south-western Iran–Iraq border region cannot be assessed in isolation from the broader onshore–offshore propagation of contraction within the Arabia–Eurasia collision system.

The post-event analysis of the Sarpol-e Zahab earthquake has illustrated a methodological pattern that recurs frequently in Iranian active tectonics: the actual rupture of a major earthquake is often produced by a previously unmapped fault that does not correspond exactly to the principal mapped structure of the region. The implications for paleoseismology are significant. The complete characterization of seismic hazard in a tectonically complex region cannot rely solely on the mapped principal structures; it must include systematic identification of the secondary blind structures that frequently produce moderate-to-large earthquakes. The integration of seismic-reflection imaging of the subsurface, of high-resolution topographic analysis (Chapter 7), of GPS-derived strain mapping, and of historical earthquake re-analysis is required to identify and characterize these structures before, rather than after, they rupture.

13.10 The Bam citadel revisited: archaeoseismic methodology

The detailed archaeoseismic study of the Arg-e Bam citadel, conducted in the years following the 2003 earthquake, provides one of the clearest illustrations of the integrated methodology now used in the discipline. The citadel, a vast adobe complex with a continuous occupation history from the Achaemenid period through the early twentieth century, contains stratified deposits whose total thickness exceeds twenty metres in the higher sectors. The interpretation of these deposits as a record of multiple seismic events in addition to the 2003 destruction has emerged from the systematic application of several lines of evidence.

The first line of evidence is the radial pattern of wall collapse documented in the 2003 destruction. The collapse direction at every recognizable section of standing wall was measured and tabulated during the months following the event by the multi-institution rapid-response team whose principal results are reported in Talebian et al. (2004), Fielding et al. (2005) and Jackson et al. (2006). The resulting rose diagram of collapse directions, when compared with the radiation pattern of the rupture as inferred from instrumental seismology and from the InSAR-derived slip distribution, was found to be statistically consistent — providing, in effect, a calibration of the relationship between strong ground motion and architectural collapse direction for this specific building tradition. The same methodology has subsequently been applied to the earlier collapse stratigraphies preserved within the citadel mound, with the result that at least two pre-2003 destruction layers can be identified with collapse-direction patterns suggestive of ground motion from sources at known azimuths to the citadel.

The second line of evidence is the chronology of these earlier destructions. The lowest of the two pre-modern destruction layers has been radiocarbon-dated to the late Sasanian period, broadly consistent with regional historical references to a major earthquake in the Kerman region during the late sixth or early seventh century CE. The upper destruction layer has been dated to the seventh or eighth century of the Islamic calendar, broadly consistent with a poorly documented but apparently substantial Kerman earthquake of approximately 1450 CE. The chronological consistency of the dated destruction stratigraphy with the independent historical record substantially strengthens the archaeoseismic interpretation.

The third line of evidence is the engineering response visible in the rebuilt fabric of the citadel. The post-Sasanian rebuilding, which is the most extensive single phase, introduced architectural features — wooden tie beams within the adobe walls, deeper foundations, and a generally lower wall-to-floor ratio — that are interpretable as deliberate seismic-resistance measures by the

rebuilders. The post-1450 rebuilding shows similar but less extensive engineering response, and the modern reconstruction now under way is using all of this historical evidence to inform the development of conservation practices that respect both the historical character of the citadel and the seismic environment in which it must continue to stand.

13.11 Historical earthquakes and the Persian chronicle tradition

The exceptional richness of the Iranian historical earthquake record derives partly from the seismic activity of the region and partly from a sustained tradition of historical writing in Persian and Arabic that extends from late antiquity to the present. The chronicles, geographical works, biographical dictionaries and administrative records of this tradition contain references to several hundred earthquakes that occurred before the establishment of instrumental recording, providing a chronological backbone for the seismicity of the past two millennia that few other regions of the world can match.

The reconstruction of historical earthquakes from textual sources is a specialized philological enterprise that requires its own methodology. The principal sources for Iranian historical earthquakes include the early Islamic chronicles such as the Tarikh-e Tabari (composed around 910 CE), the Tarikh-e Bayhaqi (eleventh century), the Mojmal al-Tawarikh (twelfth century), and the geographical works of al-Mas'udi, al-Istakhri and al-Mustawfi. From the Mongol period onward, the principal sources expand to include the Jami' al-Tawarikh of Rashid al-Din (early fourteenth century) and a substantial body of regional histories of individual cities and provinces. From the Safavid period onward (sixteenth century onward), the documentary record is enriched by European travelers' accounts, by Safavid and Qajar administrative records, and eventually by the early seismological observations of the late nineteenth and early twentieth centuries.

The integration of these textual sources with the geological and archaeological records is a labour-intensive task that has been undertaken systematically by Nicholas Ambraseys and Charles Melville, whose 'A History of Persian Earthquakes' (1982) remains the standard reference work, and by Manuel Berberian, whose more recent monograph 'Earthquakes and Coseismic Surface Faulting on the Iranian Plateau' (2014) provides a comprehensive update incorporating four further decades of work. The combined catalogue contains approximately 1,500 events, of which several hundred have sufficiently well-constrained location and magnitude to be useful for hazard analysis. The catalogue is open to ongoing refinement: every new philological discovery, every new paleoseismic trench, and every new archaeoseismic study contributes to the gradual improvement of the picture.

13.12 Implications for seismic-hazard assessment in Iran

The practical objective of paleoseismic and archaeoseismic research is to support the seismic-hazard assessment that informs building codes, urban planning, and emergency-response preparation. The Iranian seismic-hazard map produced by the Building and Housing Research Centre, originally published in 1999 and revised on several subsequent occasions, is the principal authoritative document in this domain. The map identifies four zones of relative hazard across the country and specifies the corresponding design ground accelerations to be used in structural engineering. The accuracy of the map depends in the first instance on the underlying earthquake catalogue and on the seismotectonic models used to extrapolate from the catalogue to the prediction of future ground motion.

The contribution of paleoseismology and archaeoseismology to this hazard-assessment effort is substantial. Paleoseismic data extend the earthquake catalogue back several millennia beyond the limits of the historical record, identifying low-frequency events whose recurrence is too long to be captured in the historical period. Archaeoseismic data complement the paleoseismic record in regions where geological exposure is poor but where long-occupied historical sites preserve evidence of past earthquakes in their built fabric. The integration of paleoseismic, archaeoseismic, historical, and instrumental data produces the magnitude-frequency relationships and the source-zone models that are required for probabilistic seismic-hazard analysis.

Several specific gaps in the current Iranian hazard model have been identified by the integrated paleoseismic and archaeoseismic work of the past two decades. The first is the underestimation of the maximum magnitude on several of the major faults of the Alborz and the Central Iranian interior, whose paleoseismically demonstrated rupture lengths and slip-per-event are consistent with magnitudes one half to one full unit larger than the historical maxima. The second is the under recognition of blind thrust faults beneath some of the major Iranian cities themselves — the discovery of the active Pardisan thrust beneath central Tehran (Talebian et al., 2016) is a particularly clear example — and in the Zagros foothills, where the Sarpol-e Zahab earthquake (Fathian et al., 2021) and several other recent events have demonstrated such structures to be capable of damaging earthquakes despite the absence of a clearly defined surface trace. The third is the temporal clustering of major events on the principal Iranian faults, with the implication that periods of elevated seismic activity may follow long quiescences. A fourth and broader gap, recently highlighted by the onshore–offshore analysis of the Fars Arc of the south-eastern Zagros

(Fathian et al., 2026), is the propagation of active deformation into the marine domain of the Persian Gulf, which lies outside the conventional scope of the onshore hazard models but is directly relevant to the seismic safety of the coastal infrastructure and the offshore hydrocarbon installations of southern Iran. Each of these gaps motivates an active research programme whose continuing output will progressively refine the hazard model on which the safety of the Iranian population ultimately depends.

Chapter 14 - Paleoclimatology and the Archaeological Past

The climate of the present is one moment in a continuum of climatic states that has varied substantially over the time scales relevant to archaeology. The Holocene — the interglacial period that began approximately 11,700 years ago and within which the entire span of agriculture, urbanization, state formation and recorded history has unfolded — was once thought to have been climatically quiescent compared with the dramatic excursions of the preceding glacial cycle. The work of the past three decades has substantially modified that view (Mayewski et al., 2004; Wanner et al., 2008, 2011). The Holocene has now been shown to contain repeated climatic events at scales from the global to the regional, including several abrupt shifts of sufficient amplitude to have affected agricultural productivity, water availability, and the viability of settlement in particular regions. The systematic reconstruction of this Holocene climate variability, and the investigation of its consequences for past human societies, defines the discipline of paleoclimatology in its archaeological application. For the Iranian Plateau and the wider south-west Asian region, the empirical basis for this work now rests on an expanding network of well-dated lake-sediment, peat-bog and speleothem archives, with the most recent contributions including the 2600-year multi-proxy peat record from the Jebal Barez Mountains in south-eastern Iran (Vaezi et al., 2026), the late-Quaternary synthesis of the central Iranian Plateau focused on the now-vanished Lake Saveh (Nazari et al., 2026), the south-eastern Caspian lagoon-evolution record (Lahijani et al., 2026), and the historical-period syntheses of Vaezi et al. (2019, 2022), Sharifi et al. (2015), Gurjazkaite et al. (2018) and Safaierad et al. (2020).

14.1 The principal paleoclimate archives

Paleoclimate reconstruction is based on a small number of natural archives in which the chemical, isotopic or biological signature of past climate has been preserved over geological time. The archives most relevant to the time scales of archaeological interest fall into four broad categories. Lake sediments accumulate continuously in closed or partly closed basins and preserve, in their

physical structure, their chemistry and their biological content, a near-continuous record of conditions in the lake catchment. Speleothems — the carbonate deposits that form within caves — preserve a high-resolution record of the isotopic composition of drip water, which in turn reflects the isotopic composition of meteoric precipitation in the cave's surface catchment. Marine sediments preserve a global integrated record of sea-surface temperature, oceanic productivity and continental dust delivery. Ice cores preserve records of atmospheric composition and temperature at the latitudes of the polar ice sheets. Each archive has its own resolution, its own dating possibilities and its own particular suite of climate proxies; the most robust paleoclimate reconstructions combine evidence from several archive types.

14.2 Lake sediments and varve chronologies

Lake-sediment cores are among the most directly informative of the paleoclimate archives for archaeological purposes, both because lakes are widely distributed across the continental interiors where most past human populations lived and because their sediments record the climate of the lake catchment with a fidelity that few other archives match. The principal sediment proxies include the proportion of arboreal versus non-arboreal pollen (an indicator of regional vegetation and indirectly of effective moisture), the oxygen-isotope composition of carbonate ostracod shells or authigenic carbonate (an indicator of evaporative concentration and of the isotopic composition of precipitation), the content of organic carbon (an indicator of primary productivity and of erosional inputs from the catchment), the magnetic susceptibility (an indicator of detrital input), and the abundance of specific microfossils such as diatoms and chironomids whose ecological tolerances allow temperature and salinity to be reconstructed quantitatively.

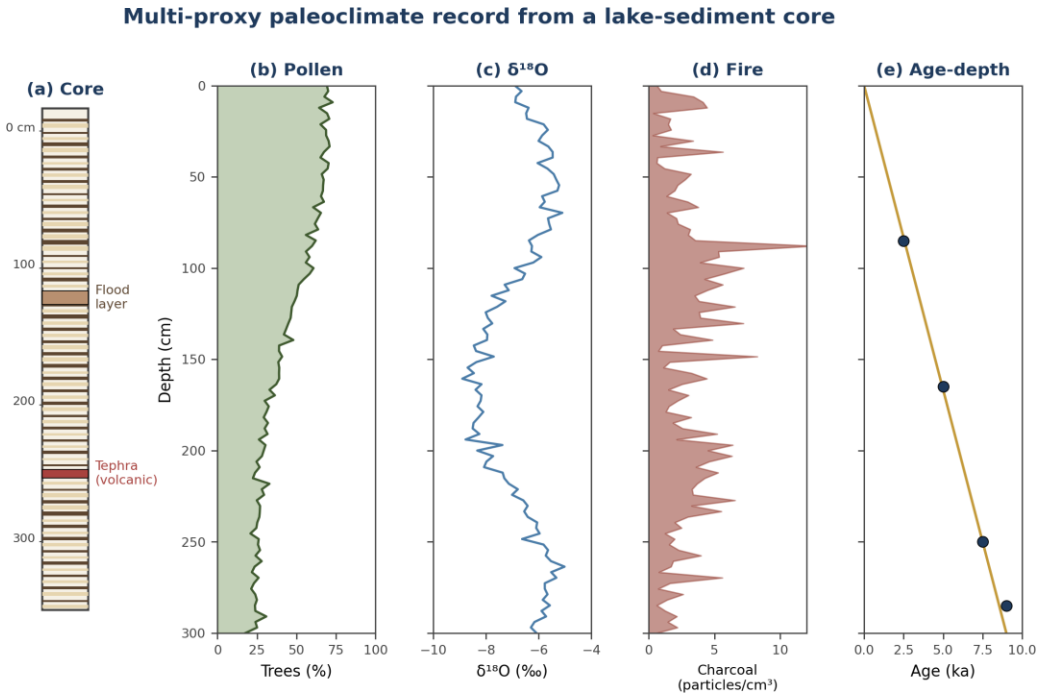

Figure 14.1 · Multi-proxy paleoclimate record from a representative lake-sediment core. Panel (a) shows the schematic core stratigraphy with annual laminae (varves), tephra and flood layers; panels (b)–(d) show three of the principal proxies plotted against depth (pollen as percentage of arboreal taxa, $\delta^{18}O$ of authigenic carbonate, and charcoal abundance); panel (e) shows the age-depth model anchored by ^{14}C dates.

In a small subset of lakes — those whose seasonal stratification and limited bottom-water oxygenation prevent disturbance of the sediment by burrowing organisms — the annual cycle of deposition is preserved as a couplet of distinguishable laminae (typically a light spring–summer layer of carbonate or biogenic silica and a dark autumn–winter layer of fine clastic material). These varved sediments offer the unique advantage of an annual chronology that does not depend on the propagation of radiocarbon uncertainties. Well-known varved sequences include the maar lakes of central Europe, the Lake Suigetsu sequence in Japan (which has been used as a comparison for the IntCal radiocarbon calibration curve), and a small number of lake sequences in the Near East. Where varved sediments are not preserved, age-depth models are constructed from radiocarbon dating of organic macrofossils, supplemented where available by tephrochronology and by paleomagnetic markers.

14.3 Speleothem records

Speleothems — stalagmites, stalactites and flowstones — form within caves through the slow precipitation of calcium carbonate from CO_2-bearing drip water. The oxygen-isotope composition of the precipitated carbonate records, with some fractionation, the oxygen-isotope composition

of the drip water, which in turn integrates the precipitation falling on the cave's surface catchment. The carbon-isotope composition records the contribution of biogenic versus atmospheric CO_2 in the soil overlying the cave, which depends on vegetation productivity and on soil moisture. Trace-element ratios — strontium-to-calcium, magnesium-to-calcium, uranium-to-calcium — record additional aspects of the drip water chemistry that depend on residence time in the karst aquifer and therefore indirectly on effective precipitation.

The principal advantage of speleothem archives is their dating. Speleothems can be dated by uranium-series methods (U-Th) with characteristic uncertainties of one per cent or better over the past several hundred thousand years, which is substantially more precise than the radiocarbon dating that anchors most lake-sediment records. Their principal disadvantages are the relatively small number of caves that contain actively growing, well-stratified speleothems suitable for high-resolution sampling, and the complexity of the karst hydrology that mediates between surface climate and drip water composition. The published archaeological speleothem records have been concentrated in southern Europe, the eastern Mediterranean, the Middle East and East Asia.

14.4 Pollen records and vegetation reconstruction

Pollen analysis — palynology — was among the earliest paleoclimatological methods to be applied at archaeological time scales, and it remains one of the most productive. The principle is simple: pollen grains produced by terrestrial plants are dispersed by wind and water across the landscape and accumulate, in identifiable form, in any sedimentary archive that excludes oxygen and microbial decay. The pollen assemblage from a given stratigraphic level reflects the relative abundance of pollen-producing plants in the regional vegetation at the time of deposition. Reconstructing past vegetation from pollen requires careful attention to the differential pollen production of different taxa (wind-pollinated trees produce vastly more pollen than insect-pollinated herbs), to the differential dispersal of pollen of different sizes, and to the preservation biases that affect particular grain types under particular sedimentary conditions. The mature practice combines counted pollen assemblages with transfer functions calibrated against modern pollen rain to produce quantitative reconstructions of past vegetation composition, climate parameters such as temperature and effective moisture, and biome assignments.

14.5 Holocene climate of southwest Asia

The Holocene climate of southwest Asia — the broad region encompassing the Levant, Anatolia, the Iranian Plateau and the adjacent mountains of the Caucasus and the Hindu Kush — has been reconstructed from a network of lake-sediment, speleothem, peat-bog and marine archives that has expanded substantially over the past twenty years (Stevens et al., 2001; Bar-Matthews et al., 1999, 2003; Sharifi et al., 2015; Gurjazkaite et al., 2018; Safaierad et al., 2020; Vaezi et al., 2019, 2022, 2026). The principal features of the regional climate history may be summarised as follows. The early Holocene (approximately 11.7 to 8.0 ka) was characterized by progressively wetter conditions associated with the strengthening of the Indian Ocean Summer Monsoon (IOSM) and the northward migration of the Intertropical Convergence Zone (Fleitmann et al., 2003; Djamali et al., 2010), and by the development of temperate forest vegetation across much of the region. The mid-Holocene (approximately 8.0 to 4.5 ka), broadly contemporaneous with the so-called Holocene Climate Optimum, was generally the wettest and warmest interval of the entire Holocene in southwest Asia, with high lake levels at Lake Urmia, Lake Mirabad and Lake Zeribar and with the widespread development of Mediterranean and oak–pistachio woodlands in the foothills of the Zagros and the Alborz. The late Holocene (approximately 4.5 ka to the present) has been characterized by progressively drier conditions, by the contraction of forest vegetation toward higher elevations, and by repeated short-term arid excursions of varying intensity, the timing and intensity of which is now resolved at decadal-to-centennial resolution in the most recent multi-proxy peat and lake archives of the Iranian Plateau (Sharifi et al., 2015; Vaezi et al., 2026; Nazari et al., 2024, 2026).

The most recent contribution to this regional synthesis is the 2600-year multi-proxy peat record from the Rayen bog in the Jebal Barez Mountains of southeastern Iran (Vaezi et al., 2026), which resolves the late Holocene hydroclimate of the Jazmurian–Jiroft sector at unprecedented temporal resolution. The record documents a sustained humid phase during the Iron Age Cold Epoch (c. 2570–2200 cal yr BP), a transition to semi-wet conditions during the Roman Warm Period (c. 2200–1550 cal yr BP), a renewed wet interval coincident with the late Sasanian prosperity (c. 1550–1200 cal yr BP), a gradual aridification through the Medieval Warm Period (c. 1200–620 cal yr BP) without the strong monsoon enhancement seen during earlier warm intervals, and the most arid and dustiest phase of the entire late-Holocene record during the Little Ice Age (c. 625–300 cal yr BP), followed by a return toward semi-wet conditions in the modern era. The chronological coincidence between hydroclimatic phases and major Iranian political and cultural transitions — the Achaemenid, Parthian, Sasanian, and post-Mongol periods

— provides a substantially refined empirical basis for the climate–society debate that has shaped this discipline over the past decade, while emphasizing that climate is best understood as an enabler or stressor rather than a deterministic driver of historical change.

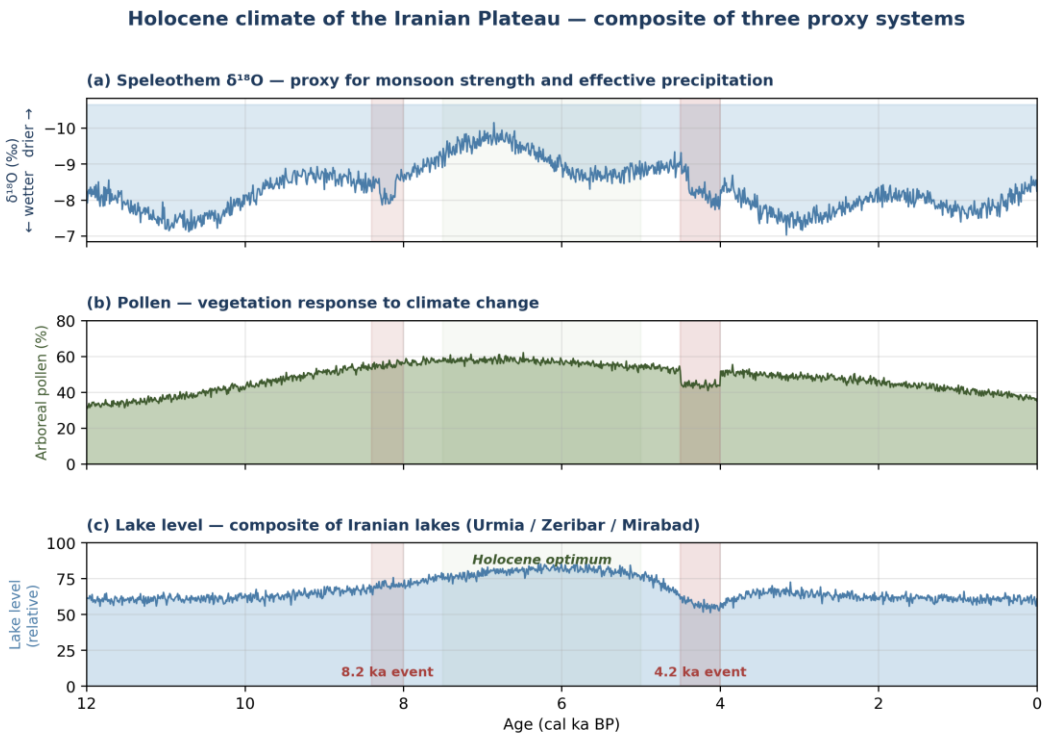

Figure 14.2 · Composite Holocene climate record of the Iranian Plateau, integrating three proxy systems: (a) speleothem $\delta^{18}O$ as a proxy for monsoon strength and effective precipitation, (b) arboreal pollen percentage as a vegetation indicator, and (c) reconstructed lake-level variation from the Iranian lake-sediment network. The Holocene optimum (5–7 ka), the 8.2 ka event, and the 4.2 ka event are highlighted.

14.6 The 4.2 ka event and its archaeological consequences

Among the climatic events of the Holocene that have been most extensively investigated for their archaeological consequences, the so-called 4.2 ka event occupies a particular position. The event, identified initially in marine cores from the Gulf of Oman and now documented in a substantial network of speleothem, lake and ice-core records, consisted of a centennial-scale aridification of the wider Near East and adjacent regions that began approximately 4,200 years ago and lasted between 100 and 300 years depending on the region. The amplitude of the event was substantial: lake levels in several Iranian and Mesopotamian basins dropped by tens of metres, the wooded fraction of regional pollen assemblages dropped by 20 to 40 percentage points, and speleothem $\delta^{18}O$ records show isotopic excursions of one to two per mile toward drier conditions. The cause of the event is debated; the leading hypotheses involve a southward shift of the Intertropical

Convergence Zone, a weakening of the African and Indian summer monsoons, and possibly a contribution from changes in solar irradiance or from explosive volcanism.

The archaeological correlates of the 4.2 ka event have been the subject of substantial debate (Weiss et al., 1993; Cullen et al., 2000; Staubwasser et al., 2003). The event is broadly contemporaneous with the collapse of the Akkadian Empire in Mesopotamia, with the de-urbanization of the Indus Valley civilization, with the end of the Old Kingdom in Egypt, and with substantial reorganizations of settlement in the Mediterranean, in Anatolia and on the Iranian Plateau. The relationship between climatic events and societal change is not straightforward, however, and the modern literature on the 4.2 ka event has moved away from simple climate-determinist explanations toward more nuanced models in which the climatic stress acts as one factor among several, interacting with political, economic and demographic variables that themselves vary substantially between regions (Roberts et al., 2011; Marsh et al., 2018; Vaezi et al., 2022). The 4.2 ka event remains a productive case study for the methodological investigation of climate–society relationships in archaeology, both because the climatic signal is unusually well-documented and because the archaeological evidence for societal response is unusually rich.

An instructive Iranian case study at the longer time scale is that of the now-vanished Lake Saveh on the central Iranian Plateau. The recent synthesis of Nazari et al. (2026), which combines geological mapping, palaeolimnological reconstruction and the critical reading of Persian and Islamic-period historical sources, indicates that a substantial freshwater body existed in the Saveh basin during the late Quaternary and persisted — at progressively reduced extent — into the early historic period before its eventual desiccation. The case is methodologically informative because it brings together the three lines of evidence on which integrated Iranian paleoclimate–archaeology now depends: the geological evidence for the existence and extent of the palaeo-lake, the chronological evidence from dated sedimentary and shoreline deposits, and the documentary record of references to the lake in Persian, Arabic and Islamic-era geographical sources. The disentanglement of the climatic, tectonic, and anthropogenic (irrigation-related) contributions to the disappearance of Lake Saveh remains under investigation, but the broader implication — that substantial late-Quaternary water bodies have been transformed into the arid playas of the present central Plateau within a period that overlaps with the human occupation history — is now firmly established and represents a particularly clear example of climate–society coupling in the Iranian context.

14.7 Iranian paleoclimate records

The Iranian Plateau hosts several of the most informative paleoclimate archives of the wider Near East. Lake Urmia, in the northwest, is the largest endorheic lake of the region and has produced pollen and sedimentological records extending into the late Pleistocene. Lake Zeribar (Stevens et al., 2001), in the western Zagros, and Lake Mirabad, slightly to the south, have been the source of long pollen records that have substantially shaped current understanding of the Holocene vegetation history of southwest Asia. Lake Maharlou and Lake Parishan, in the southern Zagros, have produced shorter but high-resolution Holocene records relevant to the agricultural archaeology of the Persepolis plain. The peat-bog records of Neor Lake in the Talysh Mountains (Sharifi et al., 2015) have produced one of the highest-resolution Holocene multiproxy records of the region, with abrupt climate transitions documented at decadal resolution. Equally important for the southeastern Iranian Plateau are the multi-proxy records from the Jazmurian playa (Vaezi et al., 2019), the Konar Sandal Daryache peat sequence (Gurjazkaite et al., 2018; Vaezi et al., 2022), and the recent 2600-year peat record from the Rayen bog in the Jebal Barez Mountains (Vaezi et al., 2026). Together these archives now permit the reconstruction of hydroclimatic variability in southeastern Iran at a temporal resolution comparable to that of the western Iranian and Mediterranean records, and they explicitly document the interaction between the Mid-Latitude Westerlies and the Indian Ocean Summer Monsoon as the principal control on moisture variability across the late Holocene. Along the southern Caspian margin, the recent synthesis of Lahijani et al. (2026) on the evolution of lagoon formation and desiccation along the south-eastern Caspian coast, and the parallel investigations of the Lake Saveh palaeo-lake on the central Iranian Plateau by Nazari et al. (2026), have substantially extended the Iranian paleoenvironmental record into the coastal and intermontane basin domains that had until recently remained underrepresented.

The growing speleothem network of the Iranian Plateau is a more recent development. Records from Kaboudan Cave in the Zagros, from Katale Khor in northwestern Iran, and from several caves of the central Alborz are now producing high-resolution Holocene records that complement the lake-sediment archives. The integration of these speleothem records with the lake-sediment and pollen archives is producing a regional paleoclimate framework against which the archaeological record of Iran — from the agricultural origins of the Neolithic to the urban systems of the Bronze and Iron Ages and the imperial polities of the Achaemenid, Parthian, Sasanian and Islamic periods — can be interpreted with increasing precision. The current synthesis suggests, among other findings, that the contraction of forested vegetation across the Iranian Plateau during the late

Holocene is partly natural (driven by progressive aridification) and partly anthropogenic (driven by sustained pastoral and agricultural pressure), and that the relative weight of these two contributions varies substantially between regions and between time periods. The disentanglement of natural from anthropogenic vegetation change in the Iranian paleoclimate record remains one of the principal open research questions of the discipline.

14.8 Integration with archaeology

The integration of paleoclimatic reconstruction with archaeological interpretation has matured substantially over the past two decades, partly because of the increasing availability of well-dated regional climate records and partly because of growing methodological sophistication on the archaeological side. The interpretive framework that has gradually emerged is built around three principles. The first is that climate change does not, by itself, cause societal change: it modifies the conditions under which societies operate, and the actual societal outcome depends on the interaction between the climatic stress and the political, economic and demographic structures of the affected society. The second is that the temporal and spatial resolution of the available paleoclimate records is often coarser than the resolution required to test specific hypotheses about climate-society interaction, with the implication that improved paleoclimate data are a precondition for substantive progress on the archaeological side. The third is that the appropriate response to apparent correlations between climatic and societal events is to investigate the mechanistic chain that would connect them — through, for example, agricultural productivity, water availability, herd nutrition, or epidemic disease — rather than to accept the correlation as an explanation in itself.

The Iranian Plateau is a particularly informative laboratory for this integrated work, both because of the richness of its archaeological record and because of the increasing density of its paleoclimate archive. The relationship between the Holocene climate variability documented in the Iranian lakes and speleothems, on the one hand, and the long sequence of Iranian cultural transitions — Neolithic agricultural origins, Chalcolithic settlement expansion, Bronze Age urbanization, the rise and decline of the great imperial polities, the medieval transformations of agriculture and settlement — on the other, is among the most productive research frontiers of contemporary Iranian geo-archaeology. The work is necessarily collaborative, drawing on Earth-science, archaeology, history, and computational modelling, and the integrated framework now emerging is one of the principal contributions of the Iranian research community to the international literature of the discipline.

14.9 Tree-ring climatology and the dendroclimatic network of Iran

Tree-ring analysis, introduced in Chapter 4 as a dating method, is also one of the most informative paleoclimate proxies for the past one to two millennia. The width, the density and the chemistry of the annual rings of trees growing in climatically sensitive sites record the conditions of each growing season at a temporal resolution that no other proxy can match. In semi-arid regions such as the Iranian Plateau, tree-ring width is primarily controlled by water availability during the growing season, and is therefore a sensitive indicator of effective precipitation. The dendroclimatic network of the Iranian Plateau, built up over the past two decades through the work of Pourtahmasi, Esper, Touchan and others, now includes approximately fifty long chronologies extending across the Zagros, the Alborz and the northeast Iranian mountains.

The Iranian dendroclimatic network has produced two principal categories of result. The first is the reconstruction of regional precipitation history for the past several hundred years, with annual resolution and substantially better dating precision than any other available proxy. The reconstruction identifies several documented drought intervals of regional severity: the late seventeenth century drought that contributed to the agricultural difficulties of the late Safavid period, the early nineteenth century drought that affected the Qajar economy, and the late twentieth and early twenty-first century drought that has continued more or less without interruption since approximately 1998. The second is the calibration of older Holocene records against the instrumental and dendroclimatic record, allowing the relative quantitative magnitude of older climate events to be assessed against the directly observed range of more recent variability.

14.10 Speleothem methodology in detail

The interpretation of speleothem oxygen-isotope records as paleoclimate indicators is more subtle than it appears at first glance, and the published Iranian speleothem records have been the occasion for substantial methodological development. The $\delta^{18}O$ of the precipitated carbonate depends on three principal factors: the $\delta^{18}O$ of the drip water entering the cave, the temperature at which precipitation occurs, and the kinetic-fractionation effects that may occur during precipitation if the dripping is rapid or if CO_2 degassing is incomplete. For most Holocene-aged speleothems, the temperature contribution is relatively small (approximately 0.23‰ per °C, working against the dripwater isotopic signal in the typical Northern Hemisphere setting), and the principal interpretive challenge is to relate the dripwater $\delta^{18}O$ to the climate of the cave's surface catchment.

The relationship between meteoric precipitation $\delta^{18}O$ and the climate variables of interest — total annual precipitation, seasonality of precipitation, source-region temperature — has been the subject of substantial study using the present-day observational network of the Global Network of Isotopes in Precipitation. In the Iranian context, the principal control on the long-term mean $\delta^{18}O$ is the so-called amount effect: heavier rainfall events are systematically depleted in ^{18}O relative to lighter events. The principal control on the temporal variation of $\delta^{18}O$ at a given site is the proportion of moisture sourced from the Mediterranean versus from the Indian Ocean and the Persian Gulf, with the latter sources producing systematically heavier precipitation. Periods in which the Iranian climate was relatively more influenced by Mediterranean moisture (typically winter precipitation, often associated with North Atlantic Oscillation variability) are therefore recorded in speleothems as relatively lighter $\delta^{18}O$, while periods of stronger Indian monsoon influence are recorded as heavier $\delta^{18}O$. The interpretation is necessarily complicated by the fact that both source-region contributions and absolute precipitation amount can vary simultaneously, and the disentanglement of these effects requires complementary records from multiple proxies.

14.11 The Iranian speleothem network

The Iranian Plateau hosts a substantial number of caves with active speleothem growth, distributed across the principal carbonate massifs of the Zagros, the Alborz and the Central Iranian Plateau. Systematic survey and sampling of these caves over the past fifteen years has built up a regional speleothem network that is now contributing high-resolution paleoclimate records to the international literature. The principal sites investigated to date include Katale Khor Cave in northwestern Iran, Kaboudan Cave in the central Zagros, Ghar-e Asparid in the southern Zagros, and several caves of the central and eastern Alborz. The records have characteristic temporal resolutions of a few decades at the centennial scale and approach annual resolution at the most recent millennium.

The integration of the speleothem records with the lake-sediment and pollen records has produced a substantially more detailed picture of Holocene climate variability across the Iranian Plateau than was available a generation ago. Three principal results may be highlighted. The first is the documentation of substantial regional gradients across the Plateau: the northern records (Katale Khor, central Alborz) show stronger Mediterranean influence and a more pronounced wet phase during the mid-Holocene optimum, while the southern records (Ghar-e Asparid, southern Zagros) show stronger Indian Ocean monsoon influence and a different timing of mid-

Holocene maxima. The second is the identification of multiple centennial-scale climate events superimposed on the broad Holocene trend, including the 8.2 ka event, the 4.2 ka event already discussed, a 3.2 ka event of regional importance, and the well-documented Late Antique Little Ice Age of approximately 540 to 660 CE. The third is the documentation, at decadal resolution in the most recent millennium, of the climatic conditions associated with the major historical episodes of agricultural difficulty and social stress in the Iranian record, providing an independent benchmark against which the documentary record can be assessed.

14.12 The Late Antique Little Ice Age and Sasanian Iran

Among the most thoroughly documented climate events of the recent Iranian record is the so-called Late Antique Little Ice Age, a cool and arid interval of approximately 540 to 660 CE that has been identified in dendrochronological, speleothem and lacustrine records across Eurasia. The event coincides chronologically with the late Sasanian period in Iran, a time of substantial political and military stress that culminated in the fall of the Sasanian Empire to the Arab conquests of the mid-seventh century. The relationship between the climatic event and the political collapse has been the subject of substantial recent research and is one of the principal case studies for the methodology of climate-society analysis discussed in Section 14.8.

The published evidence indicates that the Late Antique Little Ice Age in Iran was characterized by lower temperatures (perhaps 1 to 1.5°C cooler than the preceding centuries) and by reduced winter precipitation across the Iranian Plateau (Stevens et al., 2001; Sharifi et al., 2015; Vaezi et al., 2022). The Rayen peat record from the Jebal Barez Mountains (Vaezi et al., 2026) brackets this interval within a wider phase of sustained wet conditions over the late Sasanian period (c. 1550–1200 cal yr BP), during which reduced aeolian input and high aquatic productivity at the Rayen and Daryache bogs indicate a regionally coherent humid phase across southeastern Iran, broadly consistent with negative $\delta^{18}O$ excursions in Lake Zeribar and the Soreq Cave stalagmites. The agricultural consequences of the cooling phase would nevertheless have been substantial, particularly for the rain-fed wheat and barley agriculture of the Sasanian core regions; irrigated agriculture, supported by the qanat system that the Sasanians had developed to a high level of refinement, would have been less directly affected. The historical record of the period contains numerous references to agricultural difficulty, to famine, to plague (the so-called Plague of Justinian, which began in 541 CE), and to the political stresses that ultimately weakened the late Sasanian state. The reconstruction of the causal pathway from climate stress through agricultural productivity and pandemic disease to political collapse remains under active investigation, but

the chronological coincidence of the climatic and political events is now sufficiently well-documented that the relationship can no longer be dismissed as coincidence.

14.13 Holocene climate and the agricultural history of Iran

The longer perspective of Iranian Holocene climate provides a framework for understanding the development of agriculture, the rise and fall of urban systems, and the transformations of land use over the past ten thousand years. Several broad patterns are now reasonably well established. The Neolithic emergence of agriculture in the Zagros foothills, documented at sites such as Ganj Dareh, Jarmo and Tepe Asiab during the ninth and eighth millennia BCE, occurred during the gradually warming and wetting conditions of the early Holocene; the climatic setting was favorable, but the agricultural transition was driven by a wider set of factors that climate alone cannot explain. The Chalcolithic expansion of agricultural settlement onto the Iranian Plateau proper, during the sixth and fifth millennia BCE, occurred during the peak of the Holocene optimum, with conditions broadly more favorable than those of the present. The Bronze Age urbanization of the Iranian Plateau, documented at sites such as Shahr-e Sukhteh, Konar Sandal, Tepe Hissar and Tepe Sialk during the fourth and third millennia BCE, occurred during the transition to the drier conditions of the late Holocene; the urban centres developed sophisticated water-management infrastructure in response to the changing conditions, but the long-term aridification trend nevertheless contributed to the eventual contraction of settlement in several of the Bronze Age core regions.

The Iron Age and Achaemenid periods (first millennium BCE) saw the development of the qanat system, the underground gallery technology that taps into the water table at the foot of mountain ranges and transports it by gravity to lowland fields. The qanat allowed the cultivation of land that was beyond the reach of surface irrigation and was a critical enabling technology for the expansion of settlement onto the drier portions of the Iranian Plateau. The recent peat-bog evidence from south-eastern Iran indicates that the Achaemenid expansion of settlement and agriculture in the Jiroft sector coincided with one of the wettest phases of the late Holocene, between approximately 2570 and 2200 cal yr BP (Vaezi et al., 2022, 2026), supporting the hypothesis that hydroclimatic conditions acted as an enabler — rather than as a deterministic driver — of imperial expansion. The Sasanian and early Islamic periods saw the further extension and refinement of qanat technology, the development of qanat-based oasis cities such as Yazd and Kerman, and the establishment of agricultural landscapes that have, in some cases, remained productive into the present; the wet phase between approximately 1550 and 1200 cal yr BP

recorded at Rayen (Vaezi et al., 2026) overlaps with the period of greatest Sasanian territorial extent and provides direct empirical support for the proposed climate–society coupling during this interval. The relationship between Holocene climate, the development of irrigation technology, and the long-term productivity of Iranian agricultural landscapes is one of the more productive interdisciplinary frontiers of the current paleoclimate–archaeology synthesis, and the body of work now being produced by Iranian researchers and their international collaborators — including the recent late-Quaternary syntheses focused on the Lake Saveh basin (Nazari et al., 2026), the south-eastern Caspian coast (Lahijani et al., 2026) and the Jebal Barez sector (Vaezi et al., 2026) — is making a substantial contribution to the international literature on the human–environment relationship in semi-arid regions more broadly.

14.14 Future directions in Iranian paleoclimatology

Several specific research priorities for Iranian paleoclimatology have been identified in the recent literature. The first is the extension of the lake-sediment and speleothem networks to the relatively underrepresented regions of the eastern Iranian Plateau, of Sistan-Baluchistan, and of the Caspian forest belt. The second is the systematic development of high-resolution Holocene records suitable for testing specific archaeological hypotheses about climate-society interaction, with particular emphasis on the transitions between the major periods of Iranian prehistory. The third is the calibration of biological proxies — pollen, ostracod assemblages, diatom assemblages — against the present-day environmental gradients of Iran, to support quantitative paleoenvironmental reconstruction from older sediments. The fourth is the integration of paleoclimate records with archaeological survey data to assess the impact of climate variability on settlement patterns at the regional scale.

The institutional context of this research is also evolving. The Research Institute for Earth Sciences of the Geological Survey of Iran, including the UNESCO Chair on Coastal Geo-Hazard Analysis hosted there since 2021, the Department of Geography of the University of Tehran, the Iranian Centre for Archaeological Research, the National Museum of Iran and a number of universities across the country are now contributing to paleoclimate research alongside international partners. Recent contributions from this network — including the late-Quaternary syntheses of Nazari et al. (2024, 2026), the multi-proxy peat records of Vaezi et al. (2019, 2022, 2026), and the south-Caspian lagoon-evolution synthesis of Lahijani et al. (2026) — illustrate the growing depth of the domestic capacity and its integration with international collaborations. The continuing development of this domestic research capacity, combined with the progressive

expansion of the analytical infrastructure available within the country, is likely to be the principal driver of progress in Iranian paleoclimatology over the next decade. The body of work surveyed in this chapter is, in this sense, both a current research output and the foundation for a more substantial future contribution.

Bibliography

The following bibliography consolidates the references cited in this report together with a selection of additional high-impact works that the interested reader may wish to consult for fuller treatments of specific topics. Entries are organised by topic for ease of consultation, and within each topic by alphabetical order of first author. Citations to journal articles include volume, issue (where applicable) and page range or article identifier; books are cited with publisher and place of publication. Where a work has been particularly influential or has been republished in multiple editions, the most accessible edition is generally preferred.

Foundational works and historical sources

Boucher de Perthes, J. (1847). Antiquités celtiques et antédiluviennes. Treuttel et Wurtz, Paris.

Butzer, K. W. (1971). Environment and Archaeology: An Ecological Approach to Prehistory (2nd ed.). Aldine, Chicago.

Butzer, K. W. (1974). Geoarchaeology in practice. Reviews in Anthropology, 1(1), 130–139.

Butzer, K. W. (1982). Archaeology as Human Ecology: Method and Theory for a Contextual Approach. Cambridge University Press.

Davidson, D. A., & Shackley, M. L. (Eds.) (1976). Geoarchaeology: Earth Science and the Past. Duckworth, London.

Gladfelter, B. G. (1977). Geoarchaeology: The geomorphologist and archaeology. American Antiquity, 42(4), 519–538.

Hassan, F. A. (1979). Geoarchaeology: The geologist and archaeology. American Antiquity, 44(2), 267–270.

Lyell, C. (1863). The Geological Evidences of the Antiquity of Man. John Murray, London.

McDonald, W. A., & Rapp, G. R. (Eds.) (1972). The Minnesota Messenia Expedition: Reconstructing a Bronze Age Regional Environment. University of Minnesota Press, Minneapolis.

Penck, A., & Brückner, E. (1909). Die Alpen im Eiszeitalter. Tauchnitz, Leipzig.

Rapp, G., & Hill, C. L. (2006). Geoarchaeology: The Earth-Science Approach to Archaeological Interpretation (2nd ed.). Yale University Press, New Haven.

Renfrew, C. (1976). Archaeology and the earth sciences. In D. A. Davidson & M. L. Shackley (Eds.), Geoarchaeology: Earth Science and the Past (pp. 1–5). Duckworth, London.

Renfrew, C., & Bahn, P. (2020). Archaeology: Theories, Methods and Practice (8th ed.). Thames & Hudson, London.

Vita-Finzi, C. (1969). The Mediterranean Valleys: Geological Changes in Historical Times. Cambridge University Press.

Waters, M. R. (1992). Principles of Geoarchaeology: A North American Perspective. University of Arizona Press, Tucson.

Sedimentology, soils, micromorphology and stratigraphy

Brown, A. G. (1997). Alluvial Geoarchaeology: Floodplain Archaeology and Environmental Change. Cambridge University Press.

Courty, M. A., Goldberg, P., & Macphail, R. I. (1989). Soils and Micromorphology in Archaeology. Cambridge University Press.

French, C. (2003). Geoarchaeology in Action: Studies in Soil Micromorphology and Landscape Evolution. Routledge, London.

Goldberg, P., & Macphail, R. I. (2006). Practical and Theoretical Geoarchaeology. Blackwell, Oxford.

Harris, E. C. (1989). Principles of Archaeological Stratigraphy (2nd ed.). Academic Press, London.

Holliday, V. T. (2004). Soils in Archaeological Research. Oxford University Press, New York.

Karkanas, P., & Goldberg, P. (2018). Reconstructing Archaeological Sites: Understanding the Geoarchaeological Matrix. Wiley-Blackwell, Oxford.

Macphail, R. I., & Goldberg, P. (2017). Applied Soils and Micromorphology in Archaeology. Cambridge University Press.

Mandel, R. D. (Ed.) (2000). Geoarchaeology in the Great Plains. University of Oklahoma Press, Norman.

Nicosia, C., & Stoops, G. (Eds.) (2017). Archaeological Soil and Sediment Micromorphology. Wiley-Blackwell, Hoboken.

Stein, J. K. (2001). A review of site formation processes and their relevance to geoarchaeology. In P. Goldberg, V. T. Holliday, & C. R. Ferring (Eds.), Earth Sciences and Archaeology (pp. 37–51). Kluwer/Plenum, New York.

Stoops, G. (2003). Guidelines for Analysis and Description of Soil and Regolith Thin Sections. Soil Science Society of America, Madison.

Wentworth, C. K. (1922). A scale of grade and class terms for clastic sediments. Journal of Geology, 30(5), 377–392.

Dating methods

Aitken, M. J. (1985). Thermoluminescence Dating. Academic Press, London.

Aitken, M. J. (1998). An Introduction to Optical Dating: The Dating of Quaternary Sediments by the Use of Photon-Stimulated Luminescence. Oxford University Press.

Baillie, M. G. L. (1995). A Slice through Time: Dendrochronology and Precision Dating. Routledge, London.

Bronk Ramsey, C. (2009). Bayesian analysis of radiocarbon dates. Radiocarbon, 51(1), 337–360.

Bronk Ramsey, C., & Lee, S. (2013). Recent and planned developments of the program OxCal. Radiocarbon, 55(2), 720–730.

Higham, T., Douka, K., Wood, R., Ramsey, C. B., Brock, F., Basell, L., et al. (2014). The timing and spatiotemporal patterning of Neanderthal disappearance. Nature, 512(7514), 306–309.

Libby, W. F. (1955). Radiocarbon Dating (2nd ed.). University of Chicago Press.

Murray, A. S., & Wintle, A. G. (2000). Luminescence dating of quartz using an improved single-aliquot regenerative-dose protocol. Radiation Measurements, 32(1), 57–73.

Reimer, P. J., Austin, W. E. N., Bard, E., Bayliss, A., Blackwell, P. G., Bronk Ramsey, C., et al. (2020). The IntCal20 Northern Hemisphere radiocarbon age calibration curve (0–55 cal kBP). Radiocarbon, 62(4), 725–757.

Rhodes, E. J. (2011). Optically stimulated luminescence dating of sediments over the past 200,000 years. Annual Review of Earth and Planetary Sciences, 39, 461–488.

Walker, M. (2005). Quaternary Dating Methods. Wiley, Chichester.

Geochemistry and stable isotopes

Ambrose, S. H. (1990). Preparation and characterization of bone and tooth collagen for isotopic analysis. Journal of Archaeological Science, 17(4), 431–451.

Bentley, R. A. (2006). Strontium isotopes from the earth to the archaeological skeleton: A review. Journal of Archaeological Method and Theory, 13(3), 135–187.

Frahm, E., & Doonan, R. C. P. (2013). The technological versus methodological revolution of portable XRF in archaeology. Journal of Archaeological Science, 40(2), 1425–1434.

Hedges, R. E. M. (2002). Bone diagenesis: An overview of processes. Archaeometry, 44(3), 319–328.

Lee-Thorp, J. A. (2008). On isotopes and old bones. Archaeometry, 50(6), 925–950.

Pollard, A. M., Heron, C., & Armitage, R. A. (2017). Archaeological Chemistry (3rd ed.). Royal Society of Chemistry, Cambridge.

Sealy, J. (2001). Body tissue chemistry and palaeodiet. In D. R. Brothwell & A. M. Pollard (Eds.), Handbook of Archaeological Sciences (pp. 269–279). Wiley, Chichester.

Shackley, M. S. (Ed.) (2011). X-Ray Fluorescence Spectrometry (XRF) in Geoarchaeology. Springer, New York.

Tykot, R. H. (2004). Scientific methods and applications to archaeological provenance studies. In M. Martini, M. Milazzo, & M. Piacentini (Eds.), Physics Methods in Archaeometry (pp. 407–432). IOS Press, Amsterdam.

Remote sensing, satellite imagery and SAR

Agapiou, A., & Lysandrou, V. (2015). Remote sensing archaeology: Tracking and mapping evolution in European scientific literature from 1999 to 2015. Journal of Archaeological Science: Reports, 4, 192–200.

Casana, J. (2014). Regional-scale archaeological remote sensing in the age of big data: Automated site discovery vs. brute force methods. Advances in Archaeological Practice, 2(3), 222–233.

Casana, J. (2021). Global-scale archaeological prospection using CORONA satellite imagery: Automated, crowd-sourced, and expert-led approaches. Journal of Field Archaeology, 46(2), 60–73.

Hritz, C. (2014). Contributions of GIS and satellite-based remote sensing to landscape archaeology in the Middle East. Journal of Archaeological Research, 22(3), 229–276.

Lasaponara, R., & Masini, N. (2011). Satellite remote sensing in archaeology: Past, present and future perspectives. Journal of Archaeological Science, 38(9), 1995–2002.

Parcak, S. H. (2009). Satellite Remote Sensing for Archaeology. Routledge, London.

Stewart, C. (2017). Detection of archaeological residues in vegetated areas using satellite synthetic aperture radar. Remote Sensing, 9(2), 118.

Tapete, D., & Cigna, F. (2019). Detection of archaeological looting from space: Methods, achievements and challenges. Remote Sensing, 11(20), 2389.

Wiseman, J., & El-Baz, F. (Eds.) (2007). Remote Sensing in Archaeology. Springer, New York.

Airborne LiDAR and topographic visualisation

Canuto, M. A., Estrada-Belli, F., Garrison, T. G., Houston, S. D., Acuña, M. J., Kováč, M., Marken, D., Nondédéo, P., Auld-Thomas, L., Castanet, C., Chatelain, D., Chiriboga, C. R., Drápela, T., Lieskovský, T., Tokovinine, A., Velasquez, A., Fernández-Díaz, J. C., & Shrestha, R. (2018). Ancient lowland Maya complexity as revealed by airborne laser scanning of northern Guatemala. Science, 361(6409), eaau0137.

Chase, A. F., Chase, D. Z., Weishampel, J. F., Drake, J. B., Shrestha, R. L., Slatton, K. C., Awe, J. J., & Carter, W. E. (2011). Airborne LiDAR, archaeology, and the ancient Maya landscape at Caracol, Belize. Journal of Archaeological Science, 38(2), 387–398.

Chase, A. F., Chase, D. Z., Awe, J. J., Weishampel, J. F., Iannone, G., Moyes, H., et al. (2014). Ancient Maya regional settlement and inter-site analysis: The 2013 west-central Belize LiDAR survey. Remote Sensing, 6(9), 8671–8695.

Crutchley, S., & Crow, P. (2018). The Light Fantastic: Using Airborne LiDAR in Archaeological Survey (2nd ed.). Historic England, Swindon.

Devereux, B. J., Amable, G. S., Crow, P., & Cliff, A. D. (2005). The potential of airborne lidar for detection of archaeological features under woodland canopies. Antiquity, 79(305), 648–660.

Doneus, M., & Briese, C. (2011). Airborne laser scanning in forested areas — Potential and limitations of an archaeological prospection technique. In D. C. Cowley (Ed.), Remote Sensing for Archaeological Heritage Management (pp. 59–76). Europae Archaeologiae Consilium, Brussels.

Evans, D. H., Fletcher, R. J., Pottier, C., Chevance, J.-B., Soutif, D., Tan, B. S., et al. (2013). Uncovering archaeological landscapes at Angkor using lidar. Proceedings of the National Academy of Sciences, 110(31), 12595–12600.

Inomata, T., Triadan, D., Vázquez López, V. A., Fernandez-Diaz, J. C., Omori, T., Méndez Bauer, M. B., et al. (2020). Monumental architecture at Aguada Fénix and the rise of Maya civilization. Nature, 582(7813), 530–533.

Kokalj, Ž., & Hesse, R. (2017). Airborne Laser Scanning Raster Data Visualization: A Guide to Good Practice. Založba ZRC, Ljubljana.

Opitz, R. S., & Cowley, D. C. (Eds.) (2013). Interpreting Archaeological Topography: 3D Data, Visualisation and Observation. Oxbow Books, Oxford.

Prümers, H., Betancourt, C. J., Iriarte, J., Robinson, M., & Schaich, M. (2022). Lidar reveals pre-Hispanic low-density urbanism in the Bolivian Amazon. Nature, 606(7913), 325–328.

Štular, B., Kokalj, Ž., Oštir, K., & Nuninger, L. (2012). Visualization of lidar-derived relief models for detection of archaeological features. Journal of Archaeological Science, 39(11), 3354–3360.

UAV photogrammetry, Structure-from-Motion and GIS

Campana, S. (2017). Drones in archaeology: State of the art and future perspectives. Archaeological Prospection, 24(4), 275–296.

Conolly, J., & Lake, M. (2006). Geographical Information Systems in Archaeology. Cambridge University Press.

Hill, A. C., Limp, F., Casana, J., Laugier, E. J., & Williamson, M. (2019). A new era in spatial data recording: Low-cost GIS-tegrated UAVs. Advances in Archaeological Practice, 7(3), 188–198.

Lock, G., & Pouncett, J. (2017). Spatial thinking in archaeology: Is GIS the answer? Journal of Archaeological Science, 84, 129–135.

Verhagen, P., & Whitley, T. G. (2012). Integrating archaeological theory and predictive modeling: A live report from the scene. Journal of Archaeological Method and Theory, 19(1), 49–100.

Verhoeven, G. (2011). Taking computer vision aloft — Archaeological three-dimensional reconstructions from aerial photographs with PhotoScan. Archaeological Prospection, 18(1), 67–73.

Wheatley, D., & Gillings, M. (2002). Spatial Technology and Archaeology: The Archaeological Applications of GIS. Taylor & Francis, London.

Artificial intelligence and machine learning

Bickler, S. H. (2021). Machine learning arrives in archaeology. Advances in Archaeological Practice, 9(2), 186–191.

Caspari, G., & Crespo, P. (2019). Convolutional neural networks for archaeological site detection — Finding 'princely' tombs. Journal of Archaeological Science, 110, 104998.

Davis, D. S. (2019). Object-based image analysis: A review of developments and future directions of automated feature detection in landscape archaeology. Archaeological Prospection, 26(2), 155–163.

Dosovitskiy, A., Beyer, L., Kolesnikov, A., Weissenborn, D., Zhai, X., Unterthiner, T., et al. (2021). An image is worth 16×16 words: Transformers for image recognition at scale. International Conference on Learning Representations (ICLR).

Garcia-Molsosa, A., Orengo, H. A., Lawrence, D., Philip, G., Hopper, K., & Petrie, C. A. (2021). Potential of deep learning segmentation for the extraction of archaeological features from historical map series. Archaeological Prospection, 28(2), 187–199.

LeCun, Y., Bengio, Y., & Hinton, G. (2015). Deep learning. Nature, 521(7553), 436–444.

Lambers, K., Verschoof-van der Vaart, W. B., & Bourgeois, Q. P. J. (2019). Integrating remote sensing, machine learning, and citizen science in Dutch archaeological prospection. Remote Sensing, 11(7), 794.

Orengo, H. A., Conesa, F. C., Garcia-Molsosa, A., Lobo, A., Green, A. S., Madella, M., & Petrie, C. A. (2020). Automated detection of archaeological mounds using machine learning classification of multisensor and multitemporal satellite data. Proceedings of the National Academy of Sciences, 117(31), 18240–18250.

Redmon, J., Divvala, S., Girshick, R., & Farhadi, A. (2016). You only look once: Unified, real-time object detection. Proceedings of the IEEE Conference on Computer Vision and Pattern Recognition (CVPR), 779–788.

Ronneberger, O., Fischer, P., & Brox, T. (2015). U-Net: Convolutional networks for biomedical image segmentation. Medical Image Computing and Computer-Assisted Intervention (MICCAI), LNCS 9351, 234–241.

Trier, Ø. D., Cowley, D. C., & Waldeland, A. U. (2019). Using deep neural networks on airborne laser scanning data: Results from a case study of semi-automatic mapping of archaeological topography on Arran, Scotland. Archaeological Prospection, 26(2), 165–175.

Verschoof-van der Vaart, W. B., & Lambers, K. (2019). Learning to look at LiDAR: The use of R-CNN in the automated detection of archaeological objects in LiDAR data from the Netherlands. Journal of Computer Applications in Archaeology, 2(1), 31–40.

Site formation processes and taphonomy

Behrensmeyer, A. K. (1978). Taphonomic and ecologic information from bone weathering. Paleobiology, 4(2), 150–162.

Karkanas, P. (2018). Geoarchaeological evidence for early human occupation. In M. Henneberg (Ed.), Encyclopedia of Archaeological Sciences. Wiley, Hoboken.

Lyman, R. L. (1994). Vertebrate Taphonomy. Cambridge University Press.

Schiffer, M. B. (1972). Archaeological context and systemic context. American Antiquity, 37(2), 156–165.

Schiffer, M. B. (1983). Toward the identification of formation processes. American Antiquity, 48(4), 675–706.

Schiffer, M. B. (1987). Formation Processes of the Archaeological Record. University of New Mexico Press, Albuquerque.

Wood, W. R., & Johnson, D. L. (1978). A survey of disturbance processes in archaeological site formation. Advances in Archaeological Method and Theory, 1, 315–381.

Case studies and regional applications

Brückner, H., Müllenhoff, M., Gehrels, R., Herda, A., Knipping, M., & Vött, A. (2006). From archipelago to floodplain — Geographical and ecological changes in Miletus and its environs during the past six millennia (Western Anatolia, Turkey). Zeitschrift für Geomorphologie, 142, 63–83.

Helbig, J., Pirson, F., & Schmitt, T. (2017). Geoarchaeological investigations on the harbours of ancient Pergamon. Quaternary International, 425, 51–68.

Marriner, N., & Morhange, C. (2007). Geoscience of ancient Mediterranean harbours. Earth-Science Reviews, 80(3–4), 137–194.

Sadr, K. (2016). The impact of geoarchaeology on Iron Age archaeology in southern Africa: Recent developments. African Archaeological Review, 33(3), 213–225.

Stevens, C. J., & Fuller, D. Q. (2012). Did Neolithic farming fail? The case for a Bronze Age agricultural revolution in the British Isles. Antiquity, 86(333), 707–722.

Wilkinson, T. J. (2003). Archaeological Landscapes of the Near East. University of Arizona Press, Tucson.

Ethics, heritage and the FAIR data movement

Atalay, S. (2012). Community-Based Archaeology: Research with, by, and for Indigenous and Local Communities. University of California Press, Berkeley.

Colwell, C. (2016). Collaborative archaeologies and descendant communities. Annual Review of Anthropology, 45, 113–127.

Cunningham, J. J., & MacEachern, S. (2016). Ethnoarchaeology as slow science. World Archaeology, 48(5), 628–641.

European Association of Archaeologists (2021). EAA Code of Practice. European Association of Archaeologists, Prague.

Fouache, E. (2010). The geoarchaeological approach. In F. Della Casa & B. Berthier (Eds.), Sites of memory: Heritage of yesterday — heritage of tomorrow. CNRS Éditions, Paris.

Fouache, E. (2013). 10,000 ans d'évolution des paysages en Adriatique et en Méditerranée orientale. Maison de l'Orient et de la Méditerranée, Lyon.

Kansa, E. C., & Kansa, S. W. (2013). We all know that a 14 is a sheep: Data publication and professionalism in archaeological communication. Journal of Eastern Mediterranean Archaeology & Heritage Studies, 1(1), 88–97.

Marwick, B. (2017). Computational reproducibility in archaeological research: Basic principles and a case study of their implementation. Journal of Archaeological Method and Theory, 24(2), 424–450.

Smith, L. T. (2012). Decolonizing Methodologies: Research and Indigenous Peoples (2nd ed.). Zed Books, London.

Watkins, J. (2003). Beyond the margin: American Indians, First Nations, and archaeology in North America. American Antiquity, 68(2), 273–285.

Wilkinson, M. D., Dumontier, M., Aalbersberg, I. J., Appleton, G., Axton, M., Baak, A., et al. (2016). The FAIR Guiding Principles for scientific data management and stewardship. Scientific Data, 3, 160018.

Climate change and the archaeological record

Anderson, D. G., Bissett, T. G., Yerka, S. J., Wells, J. J., Kansa, E. C., Kansa, S. W., et al. (2017). Sea-level rise and archaeological site destruction: An example from the southeastern United States using DINAA. PLoS ONE, 12(11), e0188142.

Hambrecht, G., Anderung, C., Brewington, S., Dugmore, A., Edvardsson, R., Feeley, F., et al. (2020). Archaeological sites as distributed long-term observing networks of the past (DISPERSE). Quaternary International, 549, 218–226.

Hollesen, J., Callanan, M., Dawson, T., Fenger-Nielsen, R., Friesen, T. M., Jensen, A. M., et al. (2018). Climate change and the deteriorating archaeological and environmental archives of the Arctic. Antiquity, 92(363), 573–586.

Lahijani, H. A. K., Nazari, H., Nie, J., Xiao, W., Lak, R., Habibi, P., Hosseindoost, M., Amjadi, S., Pourkerman, M., Kabiri, K., Behravesh, M., Garivani, H., Hamzeh, M. A., Abbasi, R., & Naderi Beni, A. (2026). Evolution of lagoon formation and desiccation along the southeast Caspian coast: a historical and modern perspective. Journal of Quaternary Science. https://doi.org/10.1002/jqs.70058.

Markham, A., Osipova, E., Lafrenz Samuels, K., & Caldas, A. (2016). World Heritage and Tourism in a Changing Climate. UNESCO / UNEP, Paris and Nairobi.

Nazari, H., Ritz, J.-F., Fathian, A., Fazeli Nashli, H., Mahan, Sh., Vaezi, A., & Avagyan, A. (2026). Exploring the myth of Lake Saveh on the Iranian Plateau: the effects of climate change and civilizational evolution. The Holocene. https://doi.org/10.1177/09596836251414037.

Sandweiss, D. H., & Kelley, A. R. (2012). Archaeological contributions to climate change research: The archaeological record as a paleoclimatic and paleoenvironmental archive. Annual Review of Anthropology, 41, 371–391.

Paleoseismology and archaeoseismology — general

Ambraseys, N. N., & Melville, C. P. (1982). A History of Persian Earthquakes. Cambridge University Press.

Galadini, F., Hinzen, K.-G., & Stiros, S. (2006). Archaeoseismology: Methodological issues and procedure. Journal of Seismology, 10(4), 395–414.

McCalpin, J. P. (Ed.) (2009). Paleoseismology (2nd ed.). Academic Press, Burlington.

Reicherter, K., Michetti, A. M., & Silva, P. G. (Eds.) (2009). Palaeoseismology: Historical and Prehistorical Records of Earthquake Ground Effects for Seismic Hazard Assessment. Geological Society Special Publication 316. Geological Society of London.

Sieh, K. E. (1978). Pre-historic large earthquakes produced by slip on the San Andreas Fault at Pallett Creek, California. Journal of Geophysical Research, 83(B8), 3907–3939.

Sintubin, M., Stewart, I. S., Niemi, T. M., & Altunel, E. (Eds.) (2010). Ancient Earthquakes. Geological Society of America Special Paper 471. Geological Society of America, Boulder.

Stiros, S. C., & Jones, R. E. (Eds.) (1996). Archaeoseismology. Fitch Laboratory Occasional Paper 7. British School at Athens.

Wallace, R. E. (1981). Active faults, paleoseismology, and earthquake hazards in the Western United States. In D. W. Simpson & P. G. Richards (Eds.), Earthquake Prediction: An International Review (pp. 209–216). American Geophysical Union, Washington DC.

Paleoseismology and active tectonics of Iran

Allen, M. B., Jackson, J., & Walker, R. (2004). Late Cenozoic reorganization of the Arabia–Eurasia collision and the comparison of short-term and long-term deformation rates. Tectonics, 23, TC2008.

Berberian, M. (1995). Master 'blind' thrust faults hidden under the Zagros folds: Active basement tectonics and surface morphotectonics. Tectonophysics, 241(3–4), 193–224.

Berberian, M., & Yeats, R. S. (1999). Patterns of historical earthquake rupture in the Iranian Plateau. Bulletin of the Seismological Society of America, 89(1), 120–139.

Berberian, M., & Yeats, R. S. (2001). Contribution of archaeological data to studies of earthquake history in the Iranian Plateau. Journal of Structural Geology, 23(2–3), 563–584.

Berberian, M. (2014). Earthquakes and Coseismic Surface Faulting on the Iranian Plateau: A Historical, Social and Physical Approach. Developments in Earth Surface Processes 17. Elsevier, Amsterdam.

Hessami, K., Pantosti, D., Tabassi, H., Shabanian, E., Abbassi, M. R., Feghhi, K., & Solaymani, S. (2003). Paleoearthquakes and slip rates of the North Tabriz Fault, NW Iran: Preliminary results. Annals of Geophysics, 46(5), 903–915.

Jackson, J., & McKenzie, D. (1984). Active tectonics of the Alpine-Himalayan Belt between western Turkey and Pakistan. Geophysical Journal of the Royal Astronomical Society, 77(1), 185–264.

Nazari, H. (2006). Analyse de la tectonique récente et active dans l'Alborz Central et la région de Téhéran : Approche morphotectonique et paléoseismologique. PhD thesis, Université Montpellier II.

Nazari, H., Ritz, J.-F., Salamati, R., Shahidi, A., Habibi, H., Ghorashi, M., & Bavandpur, A. K. (2009). Morphological and palaeoseismological analysis along the Taleghan Fault (Central Alborz, Iran). Geophysical Journal International, 178(2), 1028–1041.

Nazari, H., Ritz, J.-F., Salamati, R., Shahidi, A., Habibi, H., Ghorashi, M., & Karimi Bavandpur, A. (2010). Distinguishing between fault scarps and shorelines: the question of the nature of the Kahrizak, North Rey and South Rey features in the Tehran plain (Iran). Terra Nova, 22(3), 227–237. https://doi.org/10.1111/j.1365-3121.2010.00938.x.

Nazari, H., Ritz, J.-F., Walker, R. T., Salamati, R., Rizza, M., Patnaik, R., Hollingsworth, J., Alimohammadian, H., Jalali, A., Kaveh Firouz, A., & Shahidi, A. (2014). Palaeoseismic evidence for a medieval earthquake, and preliminary estimate of late Pleistocene slip-rate, on the Firouzkuh

Strike-slip fault in the Central Alborz Region of Iran. Journal of Asian Earth Sciences, 82, 124–135.

Nazari, H., Ritz, J.-F., Burg, J.-P., Shokri, M., Haghipour, N., Mohammadi Vizhehd, M., Avagyan, A., Fazeli Nashli, H., & Ensani, M. (2021). Active tectonics along the Khazar fault (Alborz, Iran). Journal of Asian Earth Sciences, 219, 104893. https://doi.org/10.1016/j.jseaes.2021.104893.

Ritz, J.-F., Nazari, H., Ghassemi, A., Salamati, R., Shafei, A., Solaymani, S., & Vernant, P. (2006). Active transtension inside Central Alborz: A new insight into northern Iran–southern Caspian geodynamics. Geology, 34(6), 477–480.

Solaymani Azad, S., Nemati, M., Foroutan, M., Hessami, K., Dominguez, S., Bolourchi, M. J., Talebian, M., & Shahpasandzadeh, M. (2015). Active strike-slip faulting and earthquake hazard analyses in the central part of the Doruneh Fault, NE Iran. Journal of Asian Earth Sciences, 106, 14–25.

Talebian, M., & Jackson, J. (2004). A reappraisal of earthquake focal mechanisms and active shortening in the Zagros Mountains of Iran. Geophysical Journal International, 156(3), 506–526.

Vernant, P., Nilforoushan, F., Hatzfeld, D., Abbassi, M. R., Vigny, C., Masson, F., Nankali, H., Martinod, J., Ashtiani, A., Bayer, R., Tavakoli, F., & Chéry, J. (2004). Present-day crustal deformation and plate kinematics in the Middle East constrained by GPS measurements in Iran and northern Oman. Geophysical Journal International, 157(1), 381–398.

Walker, R., & Jackson, J. (2004). Active tectonics and Late Cenozoic strain distribution in central and eastern Iran. Tectonics, 23, TC5010.

Ritz, J.-F., Nazari, H., Balescu, S., Lamothe, M., Salamati, R., Ghassemi, A., Shafei, A., Ghorashi, M., & Saidi, A. (2012). Paleoearthquakes of the past 30 000 years along the North Tehran Fault, Iran. Journal of Geophysical Research, 117, B06305. https://doi.org/10.1029/2012JB009147.

Rizza, M., Vernant, P., Ritz, J.-F., Peyret, M., Nankali, H., Nazari, H., Djamour, Y., Salamati, R., Tavakoli, F., Chéry, J., Mahan, S. A., & Masson, F. (2013). Morphotectonic and geodetic evidence for a constant slip-rate over the last 45 kyr along the Tabriz fault (Iran). Geophysical Journal International, 193(3), 1083–1094. https://doi.org/10.1093/gji/ggt041.

Hollingsworth, J., Nazari, H., Ritz, J.-F., Salamati, R., Talebian, M., Bahroudi, A., Walker, R., Rizza, M., & Jackson, J. (2010). Active tectonics of the East Alborz mountains, NE Iran; rupture of the left-lateral Astaneh fault system during the great 856 AD Qumis earthquake. Journal of Geophysical Research, 115, B12313. https://doi.org/10.1029/2009JB007185.

Nazari, H., Fattahi, M., Meyer, B., Sebrier, M., Talebian, M., Forootan, M., Le Dortz, K., Bateman, M. D., & Ghorashi, M. (2009). First evidence for large earthquakes on the Deshir Fault, Central Iran Plateau. Terra Nova, 21(6), 417–426. https://doi.org/10.1111/j.1365-3121.2009.00892.x.

Foroutan, M., Meyer, B., Sébrier, M., Nazari, H., Murray, A. S., Le Dortz, K., Shokri, M. A., Arnold, M., Aumaitre, G., Bourlès, D., Keddadouche, K., Solaymani Azad, S., & Bolourchi, M. J. (2014). Late Pleistocene–Holocene right-slip rate and paleoseismology of the Nayband fault, western margin of the Lut block, Iran. Journal of Geophysical Research: Solid Earth, 119, 3517–3560. https://doi.org/10.1002/2013JB010746.

Foroutan, M., Sébrier, M., Nazari, H., Meyer, B., Fattahi, M., Rashidi, A., Le Dortz, K., & Bateman, M. D. (2012). New evidence for large earthquakes on the Central Iran plateau: palaeoseismology of the Anar fault. Geophysical Journal International, 189(1), 6–18. https://doi.org/10.1111/j.1365-246X.2012.05365.x.

Fathian, A., Atzori, S., Nazari, H., Reicherter, K., Salvi, S., Svigkas, N., Tatar, M., Tolomei, C., & Yaminifard, F. (2021). Complex co- and postseismic faulting of the 2017–2018 seismic sequence in western Iran revealed by InSAR and seismic data. Remote Sensing of Environment, 253, 112224.

Fathian, A., Koyi, H., Back, S., Nazari, H., Shugar, D. H., Shokri, M. A., & Reicherter, K. (2026). Onshore–offshore evidence for active tectonics and the propagation of the Zagros deformation front into the Persian Gulf. Quaternary Science Reviews. https://doi.org/10.1016/j.quascirev.2025.109752.

Faridi, M., Nazari, H., Burg, J.-P., Haghipour, N., Talebian, M., Ghorashi, M., Shokri, M. A., Ahmadzadeh, E., & Sahebari, S. S. (2019). Structural characteristics, paleoseismology and slip rate of the Qoshadagh Fault, northwest of Iran. Geotectonics, 53(2), 280–297.

Faridi, M., Burg, J.-P., Nazari, H., Haghipour, N., & Faridi, M. (2023). Neotectonics and paleoseismology of the North Tabriz Fault, Azerbaijan Region, northwest Iran. Journal of Asian Earth Sciences, 254, 105727. https://doi.org/10.1016/j.jseaes.2023.105727.

Kamali, Z., Nazari, H., Rashidi, A., Heyhat, M. R., Khatib, M. M., & Derakhshani, R. (2023). Seismotectonics, geomorphology and paleoseismology of the Doroud Fault, a source of seismic hazard in Zagros. Applied Sciences, 13(6), 3747. https://doi.org/10.3390/app13063747.

Talebian, M., Copley, A. C., Fattahi, M., Ghorashi, M., Jackson, J. A., Nazari, H., Sloan, R. A., & Walker, R. T. (2016). Active faulting within a megacity: the geometry and slip rate of the Pardisan thrust in central Tehran, Iran. Geophysical Journal International, 207(3), 1688–1699.

Copley, A., Faridi, M., Ghorashi, M., Hollingsworth, J., Jackson, J., Nazari, H., Oveisi, B., & Talebian, M. (2013). The 2012 August 11 Ahar earthquakes: consequences for tectonics and earthquake hazard in the Turkish–Iranian plateau. Geophysical Journal International, 196(1), 15–21. https://doi.org/10.1093/gji/ggs379.

Walker, R. T., Bergman, E. A., Elliott, J. R., Fielding, E. J., Ghods, A.-R., Ghoraishi, M., Jackson, J., Nazari, H., Nemati, M., Oveisi, B., Talebian, M., & Walters, R. J. (2013). The 2010–2011 South Rigan (Baluchestan) earthquake sequence and its implications for distributed deformation and earthquake hazard in southeast Iran. Geophysical Journal International, 193(1), 349–374. https://doi.org/10.1093/gji/ggs109.

Jackson, J., Bouchon, M., Fielding, E., Funning, G., Ghorashi, M., Hatzfeld, D., Nazari, H., Parsons, B., Priestley, K., Talebian, M., Tatar, M., Walker, R., & Wright, T. (2006). Seismotectonic, rupture process, and earthquake-hazard aspects of the 2003 December 26 Bam, Iran, earthquake. Geophysical Journal International, 166(3), 1270–1292. https://doi.org/10.1111/j.1365-246X.2006.03056.x.

Talebian, M., Fielding, E. J., Funning, G. J., Ghorashi, M., Jackson, J., Nazari, H., Parsons, B., Priestley, K., & Rosen, P. A. (2004). The 2003 Bam (Iran) earthquake: rupture of a blind strike-slip fault. Geophysical Research Letters, 31, L11611.

Fielding, E. J., Talebian, M., Rosen, P. A., Nazari, H., Jackson, J. A., Ghorashi, M., & Walker, R. (2005). Surface ruptures and building damage of the 2003 Bam, Iran, earthquake mapped by satellite synthetic aperture radar interferometric correlation. Journal of Geophysical Research, 110, B03302.

Faridi, M., Burg, J.-P., Nazari, H., Talebian, M., & Ghorashi, M. (2017). Active faults pattern and interplay in the Azerbaijan region (NW Iran). Geotectonics, 51(4), 428–437.

Rizza, M., Mahan, S., Ritz, J.-F., Nazari, H., Hollingsworth, J., & Salamati, R. (2011). Using luminescence dating from coarse matrix material to estimate fault slip-rate in arid domain: example of the Astaneh Fault (Iran). Quaternary Geochronology, 6(3–4), 390–406. https://doi.org/10.1016/j.quageo.2011.03.001.

Hollingsworth, J., Jackson, J., Walker, R., & Nazari, H. (2008). Extrusion tectonics and subduction in the eastern South Caspian region since 10 Ma. Geology, 36(10), 763–766.

Fattahi, M., Walker, R., Hollingsworth, J., Bahroudi, A., Nazari, H., Talebian, M., Armitage, S., & Stokes, S. (2006). Holocene slip-rate on the Sabzevar thrust fault, NE Iran, determined using

optically stimulated luminescence (OSL). Earth and Planetary Science Letters, 245(3–4), 673–684.

Le Dortz, K., Meyer, B., Sébrier, M., Braucher, R., Bourlès, D., Benedetti, L., Nazari, H., & Foroutan, M. (2012). Interpreting scattered in-situ produced cosmogenic nuclide depth-profile data. Quaternary Geochronology, 11, 98–115. https://doi.org/10.1016/j.quageo.2012.02.020.

Nazari, H., & Ghorashi, M. (2021). Paleoseismology (Persian translation of McCalpin, 2009, 2nd ed.). Avand Danesh / Research Institute for Earth Sciences, Geological Survey of Iran, 790 pp. ISBN 978-622-627109-7. (Selected Book of the Year 2023, Islamic Republic of Iran.)

Fazeli Nashli, H., Theodorakopoulou, K., Stamoulis, K., Athanassas, C., Nazari, H., Nokandeh, J., Jamshidi Yeganeh, S., & Shokri, M. (2023). Deciphering the chronology of Tepe Sialk (South) "Ziggurat", North-Central Iranian Plateau, through optically stimulated luminescence (OSL) dating. Journal of Archaeological Science: Reports, 48, 103860.

Bakhtiarizadeh, Z., Nazari, H., Shokri, M., Mahfroozi, A., & Kaveh-Firooz, A. (2018). Archaeoseismological investigation along the Khazar fault system, based on the paleoseismology of the Gohar Tappeh proto-historic site, Behshahr–Mazandaran. Scientific Quarterly Journal of Geosciences, 28(110), 209–220.

Pirazzoli, P. A., Reyss, J.-L., Fontugne, M., Haghipour, A., Hilgers, A., Kasper, H. U., Nazari, H., Preusser, F., & Radtke, U. (2004). Quaternary coral-reef terraces from Kish and Qeshm Islands, Persian Gulf: new radiometric ages and tectonic implications. Quaternary International, 120, 15–27.

Preusser, F., Radtke, U., Fontugne, M., Haghipour, A., Hilgers, A., Kasper, H. U., Nazari, H., & Pirazzoli, P. A. (2003). ESR dating of raised coral reefs from Kish Island, Persian Gulf. Quaternary Science Reviews, 22, 1317–1322.

Fathian, A., Nazari, H., Shokri, M. A., Talebian, M., Ghorashi, M., & Reicherter, K. (2022). Morphological and paleoseismic evidence of surface faulting in the coastal Zagros, southwestern Iran. EGU General Assembly Conference Abstracts, EGU22-6407.

Nazari, H. (2017). Earthquakes and Coseismic Surface Faulting on the Iranian Plateau (Persian translation of Berberian, 2014). Avand Danesh / Geological Survey of Iran, 680 pp. ISBN 978-600-9136-29-2.

Paleoclimatology — general

Bradley, R. S. (2014). Paleoclimatology: Reconstructing Climates of the Quaternary (3rd ed.). Academic Press, San Diego.

Cheng, H., Edwards, R. L., Sinha, A., Spötl, C., Yi, L., Chen, S., et al. (2016). The Asian monsoon over the past 640,000 years and ice age terminations. Nature, 534(7609), 640–646.

Lowe, J. J., & Walker, M. J. C. (2014). Reconstructing Quaternary Environments (3rd ed.). Routledge, London.

Mayewski, P. A., Rohling, E. E., Stager, J. C., Karlén, W., Maasch, K. A., Meeker, L. D., et al. (2004). Holocene climate variability. Quaternary Research, 62(3), 243–255.

Wanner, H., Beer, J., Bütikofer, J., Crowley, T. J., Cubasch, U., Flückiger, J., et al. (2008). Mid- to late Holocene climate change: An overview. Quaternary Science Reviews, 27(19–20), 1791–1828.

Wanner, H., Solomina, O., Grosjean, M., Ritz, S. P., & Jetel, M. (2011). Structure and origin of Holocene cold events. Quaternary Science Reviews, 30(21–22), 3109–3123.

Paleoclimate of southwest Asia and the Iranian Plateau

Bar-Matthews, M., Ayalon, A., Gilmour, M., Matthews, A., & Hawkesworth, C. J. (2003). Sea-land oxygen isotopic relationships from planktonic foraminifera and speleothems in the Eastern Mediterranean region and their implication for paleorainfall during interglacial intervals. Geochimica et Cosmochimica Acta, 67(17), 3181–3199.

Cullen, H. M., deMenocal, P. B., Hemming, S., Hemming, G., Brown, F. H., Guilderson, T., & Sirocko, F. (2000). Climate change and the collapse of the Akkadian empire: Evidence from the deep sea. Geology, 28(4), 379–382.

Djamali, M., de Beaulieu, J. L., Shah-Hosseini, M., Andrieu-Ponel, V., Ponel, P., Amini, A., et al. (2008). A late Pleistocene long pollen record from Lake Urmia, NW Iran. Quaternary Research, 69(3), 413–420.

Djamali, M., Akhani, H., Khoshravesh, R., Andrieu-Ponel, V., Ponel, P., & Brewer, S. (2011). Application of the global bioclimatic classification to Iran: Implications for understanding the modern vegetation and biogeography. Ecologia Mediterranea, 37(1), 91–114.

Jones, M. D., Roberts, C. N., Leng, M. J., & Türkeş, M. (2006). A high-resolution late Holocene lake isotope record from Turkey and links to North Atlantic and monsoon climate. Geology, 34(5), 361–364.

Roberts, N., Eastwood, W. J., Kuzucuoğlu, C., Fiorentino, G., & Caracuta, V. (2011). Climatic, vegetation and cultural change in the eastern Mediterranean during the mid-Holocene environmental transition. The Holocene, 21(1), 147–162.

Sharifi, A., Pourmand, A., Canuel, E. A., Ferer-Tyler, E., Peterson, L. C., Aichner, B., et al. (2015). Abrupt climate variability since the last deglaciation based on a high-resolution, multi-proxy peat record from NW Iran: The hand that rocked the Cradle of Civilization? Quaternary Science Reviews, 123, 215–230.

Stevens, L. R., Wright, H. E., & Ito, E. (2001). Proposed changes in seasonality of climate during the Lateglacial and Holocene at Lake Zeribar, Iran. The Holocene, 11(6), 747–755.

Stevens, L. R., Ito, E., Schwalb, A., & Wright, H. E. (2006). Timing of atmospheric precipitation in the Zagros Mountains inferred from a multi-proxy record from Lake Mirabad, Iran. Quaternary Research, 66(3), 494–500.

Van Zeist, W., & Bottema, S. (1991). Late Quaternary Vegetation of the Near East. Beihefte zum Tübinger Atlas des Vorderen Orients, Reihe A 18. Reichert, Wiesbaden.

Weiss, H., Courty, M.-A., Wetterstrom, W., Guichard, F., Senior, L., Meadow, R., & Curnow, A. (1993). The genesis and collapse of third millennium north Mesopotamian civilization. Science, 261(5124), 995–1004.

Wright, H. E., McAndrews, J. H., & van Zeist, W. (1967). Modern pollen rain in western Iran, and its relation to plant geography and Quaternary vegetational history. Journal of Ecology, 55(2), 415–443.

Vaezi, A., Routh, J., Naderi Beni, A., & Tavakoli, V. (2026). A 2600-year multi-proxy peat record from the Jebal Barez Mountains, south-eastern Iran: hydroclimatic oscillations and cultural context. Palaeogeography, Palaeoclimatology, Palaeoecology, 696, 113883. https://doi.org/10.1016/j.palaeo.2026.113883.

Vaezi, A., Routh, J., Djamali, M., Gurjazkaite, K., Tavakoli, V., Naderi Beni, A., & Roberts, P. (2022). New multi-proxy record shows potential impacts of precipitation on the rise and ebb of Bronze Age and imperial Persian societies in southeastern Iran. Quaternary Science Reviews, 298, 107855. https://doi.org/10.1016/j.quascirev.2022.107855.

Vaezi, A., Ghazban, F., Tavakoli, V., Routh, J., Naderi Beni, A., Bianchi, T. S., Curtis, J. H., & Kylin, H. (2019). A late Pleistocene–Holocene multi-proxy record of climate variability in the Jazmurian playa, southeastern Iran. Palaeogeography, Palaeoclimatology, Palaeoecology, 514, 754–767. https://doi.org/10.1016/j.palaeo.2018.09.026.

Gurjazkaite, K., Routh, J., Djamali, M., Vaezi, A., Poher, Y., Naderi Beni, A., Tavakoli, V., & Kylin, H. (2018). Vegetation history and human–environment interactions through the late Holocene in Konar Sandal, SE Iran. Quaternary Science Reviews, 194, 143–155. https://doi.org/10.1016/j.quascirev.2018.06.026.

Safaierad, R., Mohtadi, M., Zolitschka, B., Yokoyama, Y., Vogt, C., & Schefuß, E. (2020). Elevated dust depositions in West Asia linked to ocean–atmosphere shifts during North Atlantic cold events. Proceedings of the National Academy of Sciences, 117(31), 18272–18277. https://doi.org/10.1073/pnas.2004071117.

Hamzeh, M. A., Mahmudy Gharaie, M. H., Alizadeh Ketek Lahijani, H., Djamali, M., Moussavi Harami, R., & Naderi Beni, A. (2016). Holocene hydrological changes in SE Iran, a key region between Indian Summer Monsoon and Mediterranean winter precipitation zones, as revealed from a lacustrine sequence from Lake Hamoun. Quaternary International, 408, 25–39.

Fleitmann, D., Burns, S. J., Mudelsee, M., Neff, U., Kramers, J., Mangini, A., & Matter, A. (2003). Holocene forcing of the Indian Monsoon recorded in a stalagmite from southern Oman. Science, 300(5626), 1737–1739.

Bar-Matthews, M., Ayalon, A., Kaufman, A., & Wasserburg, G. J. (1999). The Eastern Mediterranean paleoclimate as a reflection of regional events: Soreq Cave, Israel. Earth and Planetary Science Letters, 166, 85–95.

Djamali, M., Akhani, H., Andrieu-Ponel, V., Braconnot, P., Brewer, S., de Beaulieu, J.-L., Fleitmann, D., Fleury, J., Gasse, F., Guibal, F., Jackson, S., Lézine, A.-M., Médail, F., Ponel, P., Roberts, N., & Stevens, L. (2010). Indian Summer Monsoon variations could have affected the early-Holocene woodland expansion in the Near East. The Holocene, 20(5), 813–820.

Nazari, H., Ritz, J.-F., Najar, E., Fathian, A., Fazeli Nashli, H., Mahan, Sh., Vaezi, A., & Avagyan, A. (2024). Iranian Plateau in the Late Quaternary: a time when Iran was green! UCCGHA 029, Khazeh Publishers, 130 pp. ISBN 978-622-8423-23-4.

Nazari, H., Ritz, J.-F., Burg, J.-P., Haghipour, N., Shokri, M., Ensani, M. R., Mohammadi Vizheh, M., Avagyan, A., & Fazeli Nashli, H. (2025). Geometry, kinematics and archaeoseismology of the Khazar Fault System in northern Iran, the south Caspian Sea. UCCGHA 025, Khazeh Publishers, 88 pp. ISBN 978-622-8423-19-7.

Appendix A - Glossary of Technical Terms

The following glossary defines the technical terms used throughout the report. Definitions are intended for the general reader and are not exhaustive; for fuller treatments the reader is referred to the relevant chapter and to the literature cited in the bibliography.

Table A.1 · Glossary of technical terms used in the report.

Term	Definition
Alluvium	Sediment deposited by flowing water in a river, stream or floodplain context.
Anthrosol	Soil whose properties have been substantially altered by sustained human activity over long periods of occupation.
Bioturbation	Mixing of sediments by the activities of plants and animals, particularly burrowing fauna and root systems.
Bundle adjustment	Joint estimation of camera positions, orientations, and three-dimensional point coordinates from overlapping photographs.
Calibration (14C)	Conversion of a conventional radiocarbon age into a calendar age using a calibration curve such as IntCal20.
CNN	Convolutional neural network — a deep learning model designed for grid-structured data such as images.
Colluvium	Sediment transported and deposited by gravity-driven processes such as soil creep and slope wash.
DEM / DTM / DSM	Digital Elevation Model / Digital Terrain Model (bare earth) / Digital Surface Model (including vegetation and buildings).
Dendrochronology	Dating method based on the matching of tree-ring sequences across overlapping samples.
Diagenesis	Physical, chemical and biological alteration of sediments after deposition but before metamorphism.
FAIR data	Findable, Accessible, Interoperable, Reusable — principles for the curation of scientific data.
GCP	Ground Control Point — a surveyed marker used to georeference photogrammetric or remote-sensing products.
GSD	Ground Sample Distance — the linear ground dimension represented by one pixel of an image.
Harris matrix	Graphical representation of the stratigraphic relationships between archaeological contexts.
IoU	Intersection over Union — overlap metric used to evaluate object detection and segmentation models.

Term	Definition
LiDAR	Light Detection and Ranging — active remote-sensing method using laser pulses to measure distance.
mAP	Mean Average Precision — standard summary metric for object-detection models.
Micromorphology	Microscopic study of undisturbed soil and sediment thin sections.
NDVI	Normalized Difference Vegetation Index — a ratio of red and near-infrared reflectance that quantifies vegetation vigour.
OSL	Optically Stimulated Luminescence — a dating method based on accumulated radiation dose in mineral grains.
Palynology	Microscopic study of pollen grains preserved in sediments, used for vegetation reconstruction.
Pedogenesis	The formation and development of soils from parent material.
RTK	Real-Time Kinematic — GNSS positioning technique providing centimeter-level accuracy in real time.
Sacbe	Maya term for a paved or raised causeway connecting major sites or precincts within a site.
SAR	Synthetic Aperture Radar — active microwave remote-sensing technique that operates in all weathers.
SfM	Structure-from-Motion — algorithmic framework for three-dimensional reconstruction from overlapping photographs.
Stratigraphy	Study of the spatial and temporal relationships of layered deposits.
Taphonomy	Systematic study of the processes affecting organic remains after death and before recovery.
Tell	Artificial mound formed by accumulated debris of successive habitation phases, characteristic of the Near East.
Terra preta	Anthropogenic dark earth of the Amazon basin, formed by long-term human habitation.
U-Net	Convolutional neural network architecture for semantic segmentation, with paired down sampling and up sampling paths.
UAV	Unmanned Aerial Vehicle — small autonomous aircraft used for remote sensing and photogrammetry.
Varves	Annually laminated couplets of light and dark sediment, used as a chronological tool in lake deposits.
XRF	X-Ray Fluorescence — non-destructive analytical technique for elemental composition.

Table A.1 · Glossary of technical terms used in the report.

Appendix B - Common Software and Tools

The following list summarizes the software packages most frequently encountered in contemporary geo-archaeological practice. The list is not exhaustive and is provided for orientation; equivalents and successors exist in most categories, and the field is evolving rapidly.

Table B.1 · Common software packages in geo-archaeological practice

Category	Software	Typical use
GIS — desktop	QGIS, ArcGIS Pro	Spatial analysis, predictive modelling, cartography
GIS — server / web	GeoServer, MapServer	Publishing spatial data on the web
Photogrammetry	Agisoft Metashape, RealityCapture, OpenDroneMap	SfM-MVS reconstruction from photographs
Point-cloud processing	CloudCompare, LASTools, PDAL	Filtering and analysis of LiDAR and photogrammetric point clouds
LiDAR visualisation	Relief Visualization Toolbox, LiVT	Hillshade, sky-view factor, openness visualisations
Image processing	SAGA GIS, GDAL, ENVI	Raster processing, spectral indices, classification
Machine learning	TensorFlow, PyTorch, scikit-learn	Training and inference of statistical and deep models
Object detection	YOLOv8, Detectron2, MMDetection	Specific frameworks for detection tasks
Statistics	R, Python (NumPy, SciPy)	General statistical analysis and visualisation
Dating calibration	OxCal, CALIB, Bacon	Radiocarbon calibration and age-depth modelling
3-D modelling / VR	Blender, Unreal Engine	Reconstruction visualisation and interactive presentation
Database	PostgreSQL + PostGIS	Spatial database for site inventories and survey data

Table B.1 · Common software packages in geo-archaeological practice, grouped by category.

Appendix C - Selected Online Resources

The following list points to selected online resources that may be of practical use to researchers entering the field. All entries were verified as accessible at the time of writing, but URLs are subject to change.

C.1 Open imagery and elevation data

Copernicus Open Access Hub (Sentinel-1 and Sentinel-2 imagery): scihub.copernicus.eu — administered by the European Space Agency, providing free access to Sentinel mission products under an open data license.

USGS EarthExplorer (Landsat archive, SRTM elevation, declassified imagery): earthexplorer.usgs.gov — administered by the United States Geological Survey, providing free access to a wide range of satellite and airborne imagery.

OpenTopography (LiDAR data, global elevation models): opentopography.org — a community resource for high-resolution topographic data, including community-contributed archaeological datasets.

C.2 Software and code repositories

QGIS Project: qgis.org — the principal open-source GIS package, with an active developer community and extensive plugin ecosystem.

PDAL (Point Data Abstraction Library): pdal.io — open-source library for processing point-cloud data, particularly LiDAR.

PyTorch and TensorFlow: pytorch.org, tensorflow.org — the two principal open-source deep-learning frameworks, with documentation, tutorials, and pre-trained model zoos.

C.3 Reference databases and gazetteers

Pleiades (gazetteer of the ancient Mediterranean): pleiades.stoa.org — a community-curated database of places known from Greek and Latin sources, with stable identifiers and geographical coordinates.

ChronoLog and Chrono Models project (radiocarbon database): a community archive of published radiocarbon dates with metadata supporting Bayesian re-analysis.

ArchaeoPlot: open-access platform for the publication and re-analysis of archaeological survey data.

Appendix D - Data Formats and Metadata Standards

The interoperability of digital geo-archaeological data depends on a small number of widely adopted file formats and metadata standards. The following table summarises the principal formats encountered in contemporary practice, together with their typical use and their principal alternatives. The list is not exhaustive but covers the formats most likely to be encountered by a researcher entering the field.

Table D.1 · Principal data formats in contemporary digital geo-archaeology

Format	Type	Typical use	Notes / alternatives
GeoTIFF	Raster	Satellite imagery, DEMs, raster GIS layers	De facto standard; supports embedded metadata
JPEG 2000	Raster (compressed)	Large satellite mosaics, archival imagery	Wavelet compression; supports tiling
NetCDF	Multi-dimensional raster	Climate data, multi-temporal stacks	Self-describing; CF metadata convention
LAS / LAZ	Point cloud	LiDAR returns and dense photogrammetric clouds	LAZ is compressed; supports per-point attributes
E57	Point cloud	Terrestrial laser scanning	ASTM standard; supports imagery alongside points
GeoJSON	Vector	Web mapping, lightweight vector exchange	Plain text; simple but limited attribute support
ESRI Shapefile	Vector	Legacy GIS exchange	Limited (10 char names); being replaced by GeoPackage
GeoPackage	Vector + raster	Modern container for spatial data	SQLite-based; OGC standard
OBJ / PLY	3-D mesh	Textured meshes from photogrammetry	OBJ widely supported; PLY supports vertex color
glTF	3-D mesh	Web-based 3-D visualization	Compact binary; designed for streaming
COG	Cloud-optimized raster	Web-accessible large rasters	Tiled and pyramidalised GeoTIFF variant
STAC	Catalogue specification	Indexing remote-sensing archives	JSON-based; widely adopted by space agencies

Table D.1 · Principal data formats in contemporary digital geo-archaeology.

D.1 Metadata standards

Beyond the file formats themselves, a small number of metadata standards govern the description and indexing of geo-archaeological datasets. The Dublin Core element set provides the minimal metadata vocabulary (title, creator, date, identifier, and so on) that is used as a baseline by most repositories. The ISO 19115 standard for geographic information provides a more detailed vocabulary specifically for spatial datasets, and is the basis of the metadata profiles used by most national mapping agencies. The Open Archives Initiative Protocol for Metadata Harvesting (OAI-PMH) provides a mechanism for the systematic discovery of distributed metadata across institutional repositories. Recent archaeological-community work has produced extensions of these general standards for archaeological purposes, including the CIDOC Conceptual Reference Model and its derivatives for the description of cultural-heritage data.

The cumulative effect of these formats and standards, properly used, is to make geo-archaeological data discoverable, accessible and reusable beyond the immediate context of the original research project. The cumulative effect of their improper use — or, more commonly, of their non-use — is to render datasets effectively inaccessible to anyone other than their original producers, which is the principal cause of the so-called dark-data problem that the FAIR-data movement is attempting to address. A modest investment in the proper handling of formats and metadata at the time of data production yields a substantial dividend in the long-term value of the resulting datasets.

D.2 Persistent identifiers

A complementary mechanism for the long-term accessibility of digital data is the assignment of persistent identifiers to datasets, publications, samples, and the institutions and individuals that produce them. The Digital Object Identifier (DOI) is the most widely used persistent-identifier scheme and is the basis on which most scholarly publications and an increasing number of datasets are now indexed. The International Generic Sample Number (IGSN) provides a comparable scheme specifically for physical samples, and is increasingly required by geological and palaeontological journals for the publication of sample-based research. The Open Researcher and Contributor Identifier (ORCID) provide persistent identification for individual researchers and is now required by many funding bodies and journals. The systematic use of persistent identifiers in geo-archaeological practice is one of the simplest and most effective contributions that an individual researcher can make to the long-term integrity of the digital record.

Appendix E - Field Protocols and Good Practice

The technical methods surveyed in the main body of this report acquire their evidential value only when they are deployed in the field according to disciplined, replicable protocols. The present appendix summarises the principal protocols associated with the most common geo-archaeological field operations. The protocols are necessarily simplified for a synthetic treatment of this kind; in operational practice, each is accompanied by detailed standards specific to the project, the regional regulatory environment, and the analytical pipeline that will subsequently process the samples.

E.1 Sediment sampling for laboratory analysis

Sediment samples for laboratory analysis are taken from cleaned excavation sections or from dedicated core holes. The principal requirements are that the sample is identified unambiguously, that its three-dimensional position is recorded with appropriate precision, and that it is protected from contamination during collection, transport and storage. Each sample is assigned a unique alphanumeric identifier, typically combining the site code, the year, the trench number, the context number and a within-context serial number. The sample volume depends on the planned analyses: a typical multi-purpose sample is approximately 500 grams, which is sufficient for grain-size determination, geochemistry, micromorphology and a portion of insurance reserve. Samples for organic and isotopic analysis require greater care to avoid contamination by modern handling, and are normally collected using gloved and tool-cleaned procedures.

E.2 Dating samples

Samples for radiocarbon dating are subject to particularly stringent contamination controls. The principal risks are the introduction of younger carbon from modern handling (skin oils, packaging materials) and the redistribution of carbon between the sample and the surrounding sediment. The standard procedure is to identify the sample in situ, to clean the surrounding sediment from any visible adherent material, to extract the sample using clean stainless-steel tools, and to wrap it in aluminium foil with the sample identifier marked on the outside. Plastic and paper packaging are avoided because of their potential to introduce carbon contaminants. Samples for OSL dating require the additional precaution that they must be extracted in light-tight conditions; the standard procedure is to extract the sample at night, by red-filter light, or through a light-tight extraction tube that protects the sample from any light exposure during collection.

E.3 Photogrammetric documentation

Photogrammetric documentation of excavated surfaces requires that the surface be cleaned, that scale bars and at least three targets of known position be placed within the frame, and that overlapping photographs be acquired from a sufficient variety of viewpoints to ensure complete coverage. The standard practice is to acquire approximately 100 photographs of a typical excavation surface, distributed in a rough circle around the surface at a viewing angle of approximately 45 degrees, supplemented by nadir photographs from directly above. Camera settings are fixed manually (focus, aperture, shutter speed and ISO) to avoid the variations that auto-exposure introduces between successive frames. The resulting model is post-processed against the surveyed targets to produce a georeferenced output.

E.4 General principles

Underlying these specific protocols is a small number of general principles that recur in every field operation. The first is the principle of explicit identification: every sample, every photograph, every measurement, and every observation must be unambiguously identified at the moment of collection. The second is the principle of redundant documentation: each key piece of information is recorded in at least two independent ways (a written field notebook, a digital tablet, a photograph of the section, a GNSS reading), so that the failure of any single recording medium does not compromise the dataset. The third is the principle of replicability: a competent colleague, given the field documentation, should be able to reconstruct the procedure followed in the field and to assess its appropriateness. The fourth is the principle of conservatism: where the appropriate procedure is unclear, the most cautious available option is followed. These principles are not, in any meaningful sense, advanced practice; they are the elementary discipline of field-based science, and their consistent application is the principal practical difference between datasets that retain their value over decades and datasets whose value is exhausted within months of their production.

Appendix F - Sample Documentation Templates

The disciplined documentation of field operations depends on a small number of standard forms and templates that capture the same categories of information in a consistent way across operations, projects and decades. The present appendix reproduces in compact form the principal templates that the contemporary geo-archaeologist is likely to encounter or to develop. The templates are not normative — every well-managed project develops its own variants — but they capture the categories of information that any competent documentation system must record.

F.1 Context sheet

The context sheet is the foundational document of a stratigraphic excavation. One sheet is filled out for every distinguishable depositional unit (deposit, cut, fill, structure, surface). The principal categories of information are: the context identifier, the unit type (deposit, cut, fill, structure, surface, find), the date of excavation, the names of the excavators, the dimensions of the unit, its three-dimensional position (top and bottom elevations, plan extent), the sedimentological description (color, texture, structure, compaction, inclusions), the stratigraphic relationships to other contexts (above, below, equal to, cut by, fills), the interpretation of the depositional event, the finds recovered, the samples taken, and any photographs and drawings made. The full context sheet is typically two to four pages in length and is normally completed before the unit is fully excavated.

F.2 Sample log

The sample log records every sample taken from the site, regardless of its destination. The principal categories of information are: the sample identifier, the date taken, the context from which it was taken, the three-dimensional position of the sample within the context, the sample type (bulk sediment, oriented monolith, charcoal, bone, OSL tube, micromorphology block, isotope sample, ancient-DNA sample), the volume or mass of the sample, the storage conditions required, the planned analyses, the name of the collector, and the current location of the sample. The sample log is normally maintained as a single document for the entire site, with each sample assigned a serial number on collection.

F.3 Photographic register

The photographic register records every photograph taken at the site. The principal categories of information are: the photograph identifier (which is normally the file name produced by the

camera), the date and time of capture, the camera and lens used, the subject of the photograph, the context or contexts visible, the orientation of the photograph (the azimuth of the camera's view direction), the name of the photographer, and any technical notes (lighting conditions, special purposes, the inclusion of scale bars or annotation boards). The photographic register is essential for the long-term value of the photographic archive, since photographs without metadata rapidly become uninterpretable as institutional memory of the project fades.

F.4 Daily log

The daily log is the principal narrative document of the excavation. One entry is made each working day and records, in chronological order, the principal events of the day. The categories of information include: the date and weather conditions, the personnel present, the contexts excavated, the principal finds and observations, any methodological decisions made, any unexpected events (collapses, visitors, equipment failures), and a brief synthesis of what was achieved and what remains to be done. The daily log is the document most often consulted decades after the original excavation when questions arise about the conduct of the work; its careful maintenance is one of the principal practical responsibilities of the project director.

Appendix G - Worked Numerical Examples

The present appendix presents three short worked examples that illustrate the routine numerical operations of contemporary geo-archaeology. Each example is presented in self-contained form and uses values typical of the situations described in the main body of the report. The examples are intended for the reader who wishes to see explicitly how the methods discussed elsewhere are translated into specific numerical outputs.

G.1 Radiocarbon calibration

A charcoal sample from a hearth at a Late Bronze Age site yields a conventional radiocarbon age of 3120 ± 30 14C years BP. The corresponding calendar age range is obtained by calibration against the IntCal20 calibration curve. The calibration procedure, performed routinely in software packages such as OxCal, identifies the portion of the calibration curve whose 14C ages overlap the measured range and reports the corresponding calendar-age intervals at the chosen confidence level. For the sample in question, the calibrated age range at 95.4 % probability is approximately 1452 to 1313 cal BCE, with the highest-probability concentration in the period 1430 to 1370 cal BCE. The reported calibrated age is conventionally written in the form '1452–1313 cal BCE (95.4 %)', and it is this calibrated range, not the raw 14C age, that is compared with chronologies derived from other evidence.

G.2 Slope from a digital elevation model

A 1-metre-resolution digital elevation model is being analysed to identify candidate locations for archaeological survey. The slope at each pixel is computed from the elevation differences between the pixel and its eight neighbours. For a pixel at elevation 245.3 m, with eastward neighbour at 245.8 m, westward at 244.9 m, northward at 245.5 m and southward at 245.1 m, the horizontal gradient components are approximately (245.8 − 244.9) / 2 = 0.45 m per metre eastward and (245.5 − 245.1) / 2 = 0.20 m per meter northward. The combined gradient magnitude is $\sqrt{(0.45^2 + 0.20^2)} \approx 0.49$ m per meter, corresponding to a slope angle of arctan (0.49) ≈ 26°. Slopes of this magnitude exceed the typical threshold for sustained agricultural use (15–20°) and would mark this pixel as a low-probability location for an agricultural settlement, although they would not preclude other land uses.

G.3 Confusion matrix for a binary classifier

A convolutional neural network has been trained to detect burial mounds in airborne LiDAR-derived hillshades. Applied to a held-out validation set of 400 image tiles, the model produces 80

true positives (correctly predicted mounds), 12 false positives (predicted mounds that are not real), 8 false negatives (real mounds missed), and 300 true negatives (correctly identified empty tiles). The precision is 80 / (80 + 12) ≈ 0.870, indicating that 87 % of predicted mounds are real. The recall is 80 / (80 + 8) ≈ 0.909, indicating that 91 % of real mounds are detected. The F1 score is the harmonic mean of these two, 2 × (0.870 × 0.909) / (0.870 + 0.909) ≈ 0.889. These figures would be considered good but not exceptional performance, and the principal limitation of the model is the residual false-positive rate; field verification of the predicted mounds would in this case identify the 12 incorrect detections at the cost of a modest field campaign.

Postface

The discipline of geo-archaeology, as it stands at the close of the second decade of the twenty-first century, occupies a position that few of its early-twentieth-century antecedents would have predicted. The slow geological excavations of the Somme valley in the nineteenth century, the painstaking sedimentological work of the Cambridge school in the mid twentieth century, and the integrative Mediterranean syntheses of the late twentieth century have all contributed to the discipline as currently practiced, but none of them anticipated the speed and the scale at which digital methods would come to dominate the analytical landscape. The geo-archaeologist of the present decade routinely processes datasets that would have been technically impossible to acquire a generation ago, with consequences for the spatial and temporal scope of the discipline that are still being absorbed.

The present report has attempted to survey this transformed landscape from a single coherent viewpoint, integrating the long-standing principles of stratigraphy and sedimentology with the visual concepts that distinguish current practice. It is offered both as an introduction for readers new to the discipline and as a reference for working researchers who wish to assess where individual methods stand at the time of writing. The pace of methodological change is sufficient that any such synthesis is, by the time it appears in print, already slightly out of date; the responsibility of the reader is to use the synthesis as a baseline against which subsequent developments can be assessed, rather than as a final word on any specific topic.

Several methodological priorities are likely to dominate the next decade of geo-archaeological research. The integration of multi-sensor remote sensing into routine workflows will continue to mature, and the analytical pipelines that exploit the combined information content of LiDAR, hyperspectral imagery, SAR and UAV photogrammetry are likely to reach genuine operational stability within a few years. The application of deep-learning models will continue to expand, accompanied by the necessary methodological work on bias, interpretability, and ethical deployment. The integration of geo-archaeological reconstruction with palaeogenomic and palaeoproteomic evidence is likely to produce one of the most productive interdisciplinary frontiers of the decade. And the response of the discipline to climate-driven loss of archaeological heritage will become an increasingly central preoccupation, both as a research priority and as a contribution to the broader public discussion of climate-change consequences.

Across all of these developments, the foundational responsibility of the geo-archaeologist remains what it has always been: the careful reading of the depositional record, the disciplined

integration of multiple lines of evidence, the patient construction of chronologies that survive critical scrutiny, and the honest communication of the results to colleagues, to descendant communities, and to the broader public. The methods change; the responsibility does not.

A note on the limits of the present synthesis

A synthesis of the kind attempted in this report is necessarily a compromise between coverage and depth. Each of the twelve chapters could have been expanded to a monograph in its own right, and several of them already are: monographs on radiocarbon calibration, on airborne LiDAR, on archaeological GIS, on machine-learning approaches to remote sensing, and on-site formation theory has appeared in the past decade and are essential reading for any serious practitioner. The function of the present report is not to replace those monographs but to provide the orientation that allows them to be approached usefully. Readers who have followed the report this far are well placed to identify the specific topics that are most relevant to their own work and to engage with the more detailed literature on those topics.

Several topics that fall within the broader compass of geo-archaeology have been omitted entirely from the present treatment, and the reader should be aware of these gaps. The geo-archaeology of underwater contexts — submerged settlements, ancient shipwrecks, prehistoric coastal occupations now beneath the sea — has been touched on only briefly in the case-study chapter, and the specialized methods of underwater archaeology have not been addressed at all. The geo-archaeology of cave and rockshelter sites, with its distinctive stratigraphic and taphonomic challenges, has likewise received only passing mention. The geo-archaeology of urban contexts, in which the depositional history is conditioned by sustained intensive human activity over centuries or millennia, has been touched on through the discussion of anthrosols but not treated systematically. Each of these subfields would deserve a chapter of its own in a fuller synthesis.

The report has also been written from a particular perspective — that of a researcher trained in the Earth sciences and reading the archaeological record through that lens. A complementary perspective, in which the archaeological questions are primary and the Earth-science methods are deployed in their service, would have produced a different organisation and a different selection of topics. The mature practice of the discipline depends on both perspectives in roughly equal measure, and the most productive working groups in contemporary geo-archaeology are those in which both traditions are represented.

Acknowledgements

This synthesis was prepared during 2026 at the UNESCO Chair on Coastal Geo-Hazard Analysis, Research Institute for Earth Sciences, Geological Survey of Iran. It draws on the published literature of the past two decades and on the working knowledge of a wide community of colleagues whose contributions, both direct and indirect, are gratefully acknowledged. Author appreciates deeply to F. Nazari from Universidad Carlos III de Madrid (uc3m) for her cooperation and fruitful assistance in the AI processing; G. Farahani and B. Akbarpour from IGM for their contribution in layout pages and Z. Kazeminia as well as H. Alibeigi from RIES for the publishing. The book is offered to the geo-archaeological community in the hope that it will be useful to graduate students entering the field, to working archaeologists seeking to integrate digital methods into their practice, and to colleagues in adjacent disciplines who wish to understand what geo-archaeology has become in the present decade.

A particular debt is owed to the colleagues whose patient discussion shaped the structure of this synthesis, and to the international research community whose published work is its principal source of material. The treatment of the Iranian Bronze Age tells in Chapter 11, in particular, draws on a long tradition of regional research that has been conducted, often under difficult circumstances, by Iranian and international colleagues over many decades. Their accumulated body of work is one of the principal demonstrations that productive geo-archaeology depends not on the latest technical innovation but on the patient, sustained engagement of competent researchers with the material record of specific places and specific times. The technical methods surveyed in this book acquire their full evidential value only when they are deployed in that sustained, place-specific way.

Hamid Nazari

UNESCO Chair on Coastal Geo-Hazard Analysis

Research Institute for Earth Sciences

Tehran 2026

Visual Atlas · Index of Figures

The following index lists all twenty-six figures of the report, grouped by chapter. Each entry gives the figure number, the short title, and the principal subject of the figure. The atlas is intended as a quick reference for readers seeking a particular illustration or wishing to locate the visual content associated with a given topic.

Chapter 1 · Foundations

Figure 1.1 · Geo-archaeology at the intersection of three scientific domains.

Figure 1.2 · A condensed timeline of geo-archaeological milestones (1837–2025).

Chapter 2 · Earth Science Principles

Figure 2.1 · Idealized stratigraphic column showing the principle of superposition.

Figure 2.2 · Idealized soil profile with O, A, E, B, C and R horizons.

Figure 2.3 · Principal palaeoenvironmental proxies used in geo-archaeology.

Chapter 3 · Field and Laboratory Techniques

Figure 3.1 · Three common sampling strategies: random, systematic and targeted.

Figure 3.2 · Wentworth (1922) grain-size classification.

Chapter 4 · Dating Methods

Figure 4.1 · Exponential decay of 14C and the practical dating range.

Figure 4.2 · The three principal stages of optically stimulated luminescence dating.

Figure 4.3 · Cross-dating principle of dendrochronology.

Chapter 5 · Geochemistry and Isotopes

Figure 5.1 · Atomic principle of X-ray fluorescence spectrometry.

Figure 5.2 · δ13C vs δ15N space for the principal dietary regimes.

Chapter 6 · Remote Sensing

Figure 6.1 · Regions of the electromagnetic spectrum and operational sensors.

Figure 6.2 · Spectral reflectance curves and NDVI transect with buried-feature anomaly.

Chapter 7 · Airborne Laser Scanning

Figure 7.1 · LiDAR-derived Digital Surface Model versus Digital Terrain Model.

Geo-archaeology and Visual Concept — A Scientific Synthesis

Hamid Nazari · Spring 2026

ABOUT THE BOOK

Geo-archaeology and *Visual Concept — A Scientific Synthesis* presents an integrated view of the interdisciplinary field that connects earth sciences, archaeology and advanced visual technologies to reconstruct the physical settings of the human past. From foundational methods to cutting-edge tools such as remote sensing, LiDAR, UAV photogrammetry, GIS and artificial intelligence, the book provides a coherent framework for investigating how past societies lived with, adapted to, and shaped their environments.

With a global perspective and a strong focus on the Iranian Plateau, the book offers methods, concepts and case studies that are essential for researchers, students and heritage managers working in an era of rapid technological change.

KEY FEATURES

Comprehensive coverage of geo-archaeological methods

State-of-the-art visual technologies and digital workflows

Artificial intelligence and machine learning in archaeology

Strong emphasis on site formation and landscape context

Case studies from around the world and Iran

Ethics, heritage management and future directions

This work is a documentary synthesis prepared as part of the six-month research proposal "Geo-archaeology and Visual Concepts: A Documentary and Office-Based Approach". It compiles, organises and reformulates existing scientific knowledge to produce a coherent reference for research and education.

UNESCO Chair on Coastal Geo-Hazard Analysis
Research Institute for Earth Sciences
Geological Survey of Iran

unesco Chair

هوش زمین کانسار
Intelligent Geo-Mine
I G M

ISBN 978-622-1582-14-3